

# NASA Technical Memorandum 74043

(NASA-TM-74043) LOW-SPEED WIND TUNNEL  
INVESTIGATION OF AN ADVANCED SUPERSONIC  
CRUISE ARROW-WING CONFIGURATION (NASA) 85 P  
HC A05/MF A01 CSCL 01A

N77-29096  
Unclassified  
G3/02 40856

## Low-Speed Wind Tunnel Investigation of an Advanced Supersonic Cruise Arrow-Wing Configuration

Paul L. Coe, Jr., Paul M. Smith, and Lysle P. Parlett

JULY 1977



NASA

National Aeronautics and  
Space Administration

LOW-SPEED WIND TUNNEL  
INVESTIGATION OF AN ADVANCED  
SUPERSONIC CRUISE ARROW-WING CONFIGURATION

By Paul L. Coe, Jr., Paul M. Smith  
and Lysle P. Parlett  
Langley Research Center

SUMMARY

Tests have been conducted in the Langley V/STOL tunnel to provide a preliminary assessment of possible means for improving the low-speed aerodynamic characteristics of advanced supersonic cruise arrow-wing configurations and to extend the existing data base of such configurations. Principle configuration variables included; wind leading-and trailing-edge flap deflection, fuselage nose strakes, and engine exhaust nozzle deflection.

The results of the investigation showed that deflecting the wing leading-edge apex flaps downward to suppress the wing apex vortices provided improved longitudinal stability but resulted in reduced directional stability. The model exhibited relatively low values of directional stability over the operational angle of attack range and experienced large asymmetric yawing moments at high angles of attack. The use of nose strakes was found to be effective in increasing the directional stability and eliminating the asymmetric yawing moment.

The results of the investigation also showed that deflecting the plain trailing edge flaps for increased lift resulted in some desirable reductions in effective dihedral. However, the level of effective dihedral was still

relatively high, and when coupled with inadequate lateral control, resulted in a crosswind landing constraint which limited the approach lift coefficient of the configuration. The use of symmetric and differential thrust vectoring increased the lateral control capability, which resulted in relaxed crosswind landing constraints and increased approach lift coefficients.

#### INTRODUCTION

The National Aeronautics and Space Administration is currently investigating the aerodynamic characteristics of advanced supersonic cruise aircraft concepts. These conceptual designs typically incorporate a low aspect ratio highly swept arrow-wing. Although wind tunnel tests of such configurations indicate that high levels of aerodynamic efficiency may be obtained at transonic and supersonic speeds (see references 1 and 2), recent low-speed wind tunnel studies (see, for example, reference 3) have identified several deficiencies in the areas of low-speed performance, stability and control.

The present investigation is part of a broad research program which is intended to provide detailed information on the static and dynamic stability and control characteristics of advanced supersonic cruise arrow-wing configurations at low speeds. The model used in the present static force tests was a light-weight, dynamically-scaled model which will be subsequently free flight tested in the Langley full-scale tunnel to provide a qualitative evaluation of low-speed handling qualities. The model will also be used in forced oscillation tests to determine the dynamic stability derivatives for use in analytical stability and control studies.

Previous low-speed studies conducted with a geometrically similar large-scale model of the present configuration have been reported in reference 3. The present investigation was specifically intended to provide a preliminary assessment of: (1) revised leading-edge devices for improved longitudinal stability; (2) trailing-edge flap effectiveness and the effect of trailing-edge flap deflection on effective dihedral; (3) thrust vectoring of conventional underslung engines for improved low-speed performance; (4) the effect of various airframe components on lateral-directional stability and (5) differential thrust vectoring concepts used in conjunction with differential trailing-edge flap deflection for increased lateral control.

The tests were conducted in the Langley V/STOL tunnel over an angle of attack range from about  $-5^\circ$  to  $25^\circ$  for sideslip angles of  $0^\circ$  and  $\pm 5^\circ$ . The tests were conducted at a Reynolds number (based on the mean aerodynamic chord) of about  $2.5 \times 10^6$ .

#### SYMBOLS

The longitudinal data are referred to the wind system of axes, and the lateral-directional data are referred to the body system of axes as illustrated in figure 1. The moment reference center for the tests was located at 53.8 percent of the wing mean aerodynamic chord.

The dimensional quantities herein are given in both the International System of Units (SI) and the U.S. Customary Units.

b	wing span, m (ft)
$C_D$	drag coefficient, $\frac{\text{Drag}}{qS}$
$C_L$	lift coefficient, $\frac{\text{Lift}}{qS}$

$C_{L,\Gamma}$	additional circulation lift, $\frac{\text{lift due to additional flow circulation}}{qS}$
$C_l$	rolling-moment coefficient, $\frac{\text{Rolling moment}}{qSb}$
$C_m$	pitching-moment coefficient, $\frac{\text{Pitching moment}}{qSc}$
$C_n$	yawing-moment coefficient, $\frac{\text{Yawing moment}}{qSb}$
$C_T$	thrust coefficient, $\frac{\text{Thrust}}{qS}$
$C_Y$	side-force coefficient, $\frac{\text{Side force}}{qS}$
$\bar{c}$	mean aerodynamic chord, m (ft)
$i_t$	horizontal-tail incidence, positive when leading-edge is up, deg
$q$	free-stream dynamic pressure, Pa ( $1\text{bf}/\text{ft}^2$ )
$S$	wing area, $\text{m}^2(\text{ft}^2)$
$X, Y, Z$	body-axis coordinates
$\alpha$	angle of attack, deg
$\beta$	angle of sideslip, deg
$\delta_f$	trailing-edge flap deflection, positive when trailing is edge down, deg
$\delta_N$	exhaust nozzle deflection (positive downward), deg
$C_{l\beta} = \frac{\partial C_l}{\partial \beta}$	
$C_{n\beta} = \frac{\partial C_n}{\partial \beta}$	
$C_{Y\beta} = \frac{\partial C_Y}{\partial \beta}$	
Model Component Designations	
H	horizontal tail
$L_1$	wing leading-edge apex flap (see figure 2(a))
$L_2$	leading-edge flap on outboard wing panel (see figure 2(a))

$t_1, t_3, t_5, t_6$  wing trailing-edge flap segments (see figure 2(a))

$V_{1,2}$  outboard vertical fins

$V_3$  centerline vertical tail

$V_4$  centerline ventral fin

WB wing-body combination

## MODEL

The model used in the present investigation was a lightweight dynamically scaled model which will be used in subsequent wind tunnel free-flight tests and in forced oscillation tests. The dimensional characteristics of the 0.045 scale model are listed in table I and shown in figure 2. A photograph of the model mounted for tests in the Langley V/STOL tunnel is presented in figure 3.

Previous studies with a geometrically similar, large-scale model are reported in reference 3. The model of the present investigation differed slightly from the large-scale model. In particular, the present model incorporated revised leading-edge flaps (see figure 2(c) and 2(d) for comparison) intended to provide improved longitudinal stability characteristics. The present model also incorporated a forward shift in lower surface engine location (see figure 2(b) for comparison). The forward shift in engine location resulted in approximate alignment of the nozzle exhaust with the trailing-edge flap system, and was intended to determine if such an arrangement would be effective for developing additional circulation lift.

The model wing consisted of an arrow planform with an inboard leading-edge sweep angle of  $74^\circ$ , a midspan sweep angle of  $70.5^\circ$ , and an outboard sweep of  $60^\circ$ . The leading-edge apex flaps could be deflected from  $0^\circ$  to  $30^\circ$  and the

leading-edge of the outboard wing panel could be deflected from  $0^\circ$  to  $45^\circ$ , or replaced with a Krueger flap arrangement (see figures 2(c) and 2(d)).

The model was equipped with four engine simulators which consisted of tip driven fans powered by externally supplied compressed air. The nozzle exhaust could be deflected using  $20^\circ$  elbow segments (see figure 2(b)), and the trailing-edge flap system shown in figure 2(a) permitted deflection of the individual segments.

#### TESTS

Static force tests were conducted over an angle of attack range of  $-5^\circ$  to  $25^\circ$  for an angle of sideslip range  $-5^\circ$  to  $+5^\circ$ . The configuration variables associated with the wing-body-outboard vertical fin combination included; wing-apex leading-edge flaps, outboard wing-panel leading-edge flaps, and wing trailing-edge flaps. Tests were also conducted to include the effects of; various airframe component combinations, control surface deflections, engine thrust coefficient, and engine exhaust nozzle deflection.

Engine thrust coefficient was obtained from static calibration of engine thrust versus engine rotational speed. Power-on tests were performed for the model with a nominal value of thrust coefficient of 0.13, obtained by maintaining constant values of RPM. Power-off tests ( $C_T = 0$ ) were performed with the engine simulators allowed to windmill. The unpowered tests were conducted at a Reynolds number (based on the mean aerodynamic chord) of approximately  $2.5 \times 10^6$ . Due to engine-simulator thrust restrictions, power on tests ( $C_T = 0.13$ ) were conducted at a Reynolds number of about  $2.0 \times 10^6$ .

In addition to the forgoing tests, a limited number of smoke flow visualization tests were conducted to aid in the interpretation of the results.

## PRESENTATION OF RESULTS

A run schedule and a tabular listing of data are presented in the appendix. The results and discussion are presented in accordance with the following outline.

	Page	Figures
<b>Longitudinal Aerodynamic Characteristics</b>		
Effect of wing leading-edge devices. . . . .	7	4
Effect of trailing-edge flap deflection. . . . .	9	6,7
Effect of thrust vectoring. . . . .	10	8
Horizontal tail effectiveness. . . . .	11	9,10
<b>Lateral-Directional Characteristics</b>		
Effect of wing leading-edge devices. . . . .	12	11
Effect of trailing-edge flap deflection. . . . .	13	12
Airframe component build-up studies. . . . .	14	13,14
Effect of fuselage forebody strakes. . . . .	15	15,16,17,18
<b>Lateral Control Characteristics</b>		
Aerodynamic lateral control effectiveness. . . . .	18	19,20,21,22, 23,24
Effect of thrust vectoring . . . . .	21	25,26,27

## RESULTS AND DISCUSSION

### Longitudinal Aerodynamic Characteristics

Effect of wing leading-edge devices. - The longitudinal aerodynamic characteristics of the basic wing-body-outboard vertical fin combination ( $L_1=L_2 = 0$ ) and the wing-body-outboard vertical fin combination with wing-leading edge devices def' ed are presented in figure 4. The data show that for  $\alpha < 5^\circ$  the leading-edge devices tested had no effect on the longitudinal aerodynamic characteristics; and that for the moment reference center tested,

the wing-body-outboard vertical fin combination was about 4-percent unstable (i.e.,  $\partial C_m / \partial C_L = 0.04$ ). However, for  $\alpha > 5^\circ$  the instability of the basic wing-body-outboard vertical fin combination ( $L_1 = L_2 = 0$ ) increased markedly with increasing angle of attack. Past investigations (see, for example, references 3 and 4) have shown that such marked increases in the level of longitudinal instability are attributable to the formation of wing apex vortices and also to the stall of the outboard wing panels. References 3 and 4 have also shown that deflection of the wing apex, and deflection of the leading-edge of the outboard wing panels, is effective in both reducing the magnitude of the instability and in delaying the angle of attack at which the instability occurs. The data of figure 4 show that deflecting the single segment apex flap  $30^\circ$  substantially reduces the marked non-linear variation of  $C_m$  with  $C_L$  and thus provides a stabilizing effect for angles of attack above  $5^\circ$ . During this phase of the investigation a limited number of smoke flow visualization tests were conducted. The smoke flow studies indicated that deflection of the apex flap was effective in reducing the intensity of the apex vortices; however, some vortex formation could still be observed. This result correlates well with measured data presented in figure 4, in that some increase in the level of instability is still present for the model with the apex flaps deflected.

Figure 4 also shows the effect of deflecting the plain leading-edge flap of the outboard wing panel, and replacing this outboard leading-edge flap segment with a Krueger flap. (see figure 2(d) for details). The data of figure 4 indicate that both the plain leading-edge flap and the leading-edge Krueger flap provided a small favorable contribution to longitudinal stability at high angles of attack, and that the contribution of the leading-edge

Krueger flap was slightly greater than that of the plain leading edge flap. This result is attributable to the improvement in the flow conditions over the outboard wing panels.

Figure 5 presents a comparison of longitudinal data obtained for the present model, with data obtained for the larger model reported in reference 3. The model of reference 3 had a deflectable leading-edge apex flap system and a plain, permanently deflected, leading-edge flap on the outboard wing panel. As can be seen from figure 5, the data for the models are in relatively good agreement. The small differences shown are probably due to the slight differences in model geometry, and also to the difference in test conditions (i.e.,  $R_N = 2.5 \times 10^6$  versus  $R_N = 5.17 \times 10^6$ ).

Effect of trailing-edge flap deflection. - The segmented trailing-edge flap system is sketched in figure 2(a). The angular deflection of the individual segments is described normal to the respective flap hinge lines. A trailing-edge flap setting indicated as  $\delta_f = 40^\circ/30^\circ/20^\circ$  corresponds to a condition wherein the inboard trailing edge flap segments ( $t_1$ ) are deflected  $40^\circ$ , the mid-span segments ( $t_3$ ) are deflected to  $30^\circ$ , and the outer flap segments ( $t_5$ ) are deflected to  $20^\circ$ .

Figure 5 presents the longitudinal aerodynamic characteristics of the wing-body-outboard vertical fin combination for various trailing-edge flap deflections. The data of figure 6 indicate that for  $\alpha < 10^\circ$ , deflecting the plain trailing-edge flap from  $0^\circ$  to  $30^\circ$  results in essentially a linear increase in  $C_L$  with increasing  $\delta_f$ . However, at higher angles of attack, or higher flap deflections, the effectiveness of the trailing-edge flap system is reduced. The reduction in trailing-edge flap effectiveness, which occurs at

high flap deflections and high angles of attack, is attributed to the separation of flow over the trailing-edge flap system.

In order to provide some insight into the effectiveness of the individual trailing-edge flap segments, tests were conducted in which the segments were deflected individually. Figure 7 summarizes the resulting increment in lift coefficient as a function of flap deflection for individual segments  $t_1$ ,  $t_3$ , and  $t_5$ . From figure 7 it can be seen that the inboard trailing-edge flap segment ( $t_1$ ) is most effective in producing lift, and that the outboard trailing-edge flap segment ( $t_5$ ) is relatively ineffective. At present, the high sweep of the hinge line of segment  $t_5$  is thought to be responsible for its relatively poor lifting characteristics. It is of course recognized that the incremental values of lift coefficient presented in figure 7, will not necessarily sum to the total obtained by deflection of the entire trailing-edge flap system. However, the data of figure 7 are in qualitative agreement with the data of figure 6 and therefore are thought to be indicative of the relative effectiveness of the individual trailing-edge flap segments.

Effect of thrust vectoring.- The discussion of reference 5 has indicated that the overall efficiency of the present configuration may be significantly improved by the application of propulsive-lift concepts which provide improved low-speed performance. Previous low-speed investigations (see reference 3) have included the use of a simple thrust vectoring arrangement wherein the exhaust flow of the conventional lower surface engines was deflected downward. The results of reference 3 indicate that due to the relatively far aft location of the exhaust nozzles, the increment in lift due to the thrust vectoring concept was limited to the vector component of the thrust force, and that no

additional circulation lift was developed. Therefore, to more nearly align the nozzle exits with the trailing-edge flap system, and thereby determine if such an arrangement would develop additional circulation lift, the underslung engines were moved forward of the location tested in reference 3 (see figure 2(b) for comparison of engine locations).

The longitudinal aerodynamic characteristics of the present configuration with the exhaust nozzles undeflected ( $\delta_N = 0^\circ$ ) and with the exhaust nozzles deflected ( $\delta_N = 20^\circ$ ) are presented in figure 8. Analysis of the data of figure 8(a) indicates that for the undeflected exhaust nozzles, the increment in lift coefficient due to thrust effects is simply the vector component of the thrust force given by the expression

$$\Delta C_L = C_T \sin \alpha \quad (1)$$

With the deflected exhaust nozzles, static calibration tests showed that the jet exhaust was deflected through the geometric nozzle angle. Analysis of the data of figure 8(b) indicates that very small values of additional circulation lift ( $C_{L,T}$ ) are obtained.

$$C_{L,T} = C_L \left[ \frac{\text{power on}}{\text{power off}} - C_T \sin (\alpha + \delta_N) \right] \quad (2)$$

For example, at  $\alpha = 10^\circ$   $C_{L,T}$  is computed to be about only 2-percent of the total lift.

Horizontal tail effectiveness. - Figure 9 presents a comparison of the data obtained for the model with the horizontal tail off and on. From these data it can be seen that for angles of attack less than  $10^\circ$ , the horizontal tail provides only a small contribution to longitudinal stability. However, at higher angles of attack the horizontal tail does provide a somewhat greater stabilizing contribution. Figure 9 also shows that, as expected, thrust

affected the level of the tail-off pitching moment; however, it did not alter the horizontal tail effectiveness.

The longitudinal control effectiveness, provided by deflecting the all movable horizontal tail through a range of tail incidences corresponding to  $\pm 15^\circ$ , is shown in figure 10. Although the horizontal tail tested was ineffective for providing longitudinal stability at low angles of attack, the data of figure 10 show that the horizontal tail does provide longitudinal control. Furthermore, the data indicated that the longitudinal control effectiveness remains fairly constant over the angle of attack range tested, and that the control effectiveness was not altered by thrust effects. It should be noted that the horizontal tail apparently did not stall over the range of conditions investigated, and therefore, even higher levels of longitudinal control may be obtained by increasing the horizontal tail incidence above the values considered herein.

#### Lateral-Directional Characteristics

Effect of wing leading-edge devices. - As mentioned in a previous section, deflection of the wing leading-edge apex flap,  $L_1$ , and deflection of the leading-edge flap of the outboard wing panel,  $L_2$ , resulted in a beneficial contribution to longitudinal stability.

Figure 11 shows the effect on the lateral-directional stability characteristics of deflecting the leading-edge apex flap,  $L_1$ , and the outboard panel leading-edge flap,  $L_2$ . The data of figure 11 show that the basic wing-body-outboard vertical fin combination ( $L_1 = L_2 = 0$ ) exhibits stable values of the directional stability derivative,  $C_{n\beta}$ , and that  $C_{n\beta}$  increased with increasing angle of attack. Consideration of the side force derivative,  $C_{y\beta}$  indicates

that the increase in directional stability (i.e., increased values of  $C_{n\beta}$ ) with increasing angle of attack, originates from a body station forward of the moment reference center. This result has been observed for other highly swept arrow-wing configurations (see, for example, reference 4) and has been associated with the interaction of the wing apex vortices on the forward portion of the configuration. As can be seen from the data of figure 11, deflecting the wing apex flaps downward in order to suppress the wing apex vortices, and hence provide improved longitudinal stability, results in a reduction in directional stability. The data of figure 11 also show that deflecting the outboard panel leading-edge flap had no significant effect on directional stability, and that deflection of either the leading-edge apex flap or the outboard panel leading-edge flap had only slight effects on the effective dihedral derivative,  $C_{l\beta}$ , for  $\alpha < 15^\circ$ . It should be noted that although the leading edge devices tested had only a slight effect on  $C_{l\beta}$ , the level of  $C_{l\beta}$  at the higher angles of attack is relatively high. Previous simulation studies of similar arrow-wing concepts have indicated that such high levels of  $-C_{l\beta}$  result in poor handling qualities and lateral control characteristics.

Effect of trailing-edge flap deflection. - As pointed out in a previous section, the relatively high levels of  $-C_{l\beta}$  exhibited by the model may lead to handling qualities and lateral control problems. However, the results of reference 6 have indicated that reductions in  $-C_{l\beta}$  may accompany increased trailing-edge flap deflections.

Figure 12 presents the variation of the effective dihedral derivative, with lift coefficient, for various trailing-edge flap deflections. As can be seen from figure 12(a), increasing the trailing-edge flap deflection results in reduced levels of  $-C_{l\beta}$  at a given lift coefficient. In order to determine if

the above result could be attributed to an increased loading on the inboard portion of the wing, tests were conducted for nonuniform trailing edge flap deflections of  $30^\circ/0^\circ/0^\circ$  and  $0^\circ/40^\circ/20^\circ$ . These conditions were selected in an attempt to achieve as much variation of spanwise load distribution as possible. Figure 12(b) presents a comparison of the results obtained for the nonuniform trailing-edge flap deflections, with those obtained for  $\delta_f = 20^\circ/20^\circ/20^\circ$ . The data show that these three trailing edge flap settings resulted in about the same variation of  $C_L$  with  $\alpha$ , and also about the same variation of  $C_{l\beta}$  with  $C_L$ . For the trailing-edge flap conditions investigated, no effect on  $C_{n\beta}$  was observed and hence the data are not presented.

Based on the results presented in figure 12, it appears that the reduction in the effective dihedral (obtained at a constant  $C_L$ ) provided by increasing trailing-edge flap deflection, is associated with the reduction in angle of attack at which a given lift coefficient is obtained. Therefore, one possible means for further reducing the level of  $-C_{l\beta}$  is through the development of an effective high lift system which will permit the desired lift coefficient to be achieved at reduced angles of attack.

Airframe component build-up studies.— Figures 13 and 14 present the variation of the lateral-directional stability derivatives, with angle of attack, for various airframe component combinations. From the data of figure 13 it can be seen that the outboard vertical fins and the centerline vertical tail provide a stabilizing increment to the directional stability derivative,  $C_{n\beta}$ , over the normal operational angle of attack range. However, the contribution of the outboard vertical fins to  $C_{n\beta}$  is reduced for angles of attack greater than  $20^\circ$ , and the contribution of the centerline vertical tail to  $C_{n\beta}$

is reduced for angles of attack greater than 10°. The data of figure 13 also show that the centerline ventral fin has no effect on the lateral-directional stability derivatives.

Figure 14 shows the effect of the horizontal tail on the lateral-directional stability characteristics of the model. As can be seen from figure 14, at low angles of attack the addition of the horizontal tail ( $i_t = 0^\circ$ ) provided the model with a stabilizing increment to  $C_{n\beta}$  which is comparable to the increments provided by addition of either the outboard vertical fins or the centerline vertical tail. The increase in directional stability provided by the horizontal tail, for the model at low angles of attack, is probably due to the horizontal tail acting as an endplate for the vertical tail. It should be noted, however, that for angles of attack greater than about 14° the horizontal tail ( $i_t = 0^\circ$ ) is directionally destabilizing and resulted in the complete model exhibiting unstable values of  $C_{n\beta}$  for angles of attack from 16° to 22°. However, as also shown by figure 14, deflecting the horizontal tail to  $i_t = -15^\circ$  resulted in an increase in  $C_{n\beta}$  (relative to the horizontal tail-off condition) over the angle of attack range tested.

The data of figures 13 and 14 also show that the relatively high levels of  $-C_{l\beta}$ , exhibited by the wing-body combination, are only slightly influenced by other configuration components.

Effect of fuselage forebody strakes.—As shown by the data of a previous section, the maximum value of the directional stability derivative,  $C_{n\beta}$ , of the complete configuration was found to be only about 0.001. Previous studies of similar configurations (see, for example, reference 7) have indicated that increased values of  $C_{n\beta}$  may be required. Of course, increases in  $C_{n\beta}$  could be

provided by increasing the size of the vertical tail; however, this may be detrimental to the supersonic cruise performance. Therefore, to provide necessary information for future trade studies, the use of nose strakes (see figure 2(e) for geometric details) has been investigated. Figure 15 presents a comparison of the lateral-directional data obtained for the complete model with the nose strakes on and off. As can be seen, the particular nose strakes tested provided a substantial increase in the directional stability derivative,  $C_{n\beta}$ . Furthermore, the increase in  $C_{n\beta}$  is seen to be accompanied by increased values of  $C_{Y\beta}$ , indicating that the stabilizing influence originates from the forward portion of the configuration. However, as indicated in reference 8, increased values of  $C_{n\beta}$  originating from the nose may be accompanied by undesirable reductions in the damping in yaw. Therefore, additional tests are required to assess the total effect of nose strakes on the dynamic stability characteristics of the configuration.

In addition to the relatively low level of directional stability, the model was also found to exhibit large out-of-trim yawing moments. Figure 16 presents the lateral-directional characteristics obtained for the complete model at  $\beta = 0^\circ$ , for conditions with and without the previously discussed nose strakes. The data show that without nose strakes, extremely large asymmetric yawing moments occur for angles of attack greater than  $15^\circ$ . The data of figure 16 also show that when the strakes were added to the fuselage forebody, the asymmetry in yawing moment was virtually eliminated. Previous studies (see, for example, reference 9) have identified asymmetric displacement of vortex cores originating from long slender fuselage forebodies as one phenomena responsible for yawing moment asymmetries. A sketch of the flow field over the fuselage forebody, observed during smoke flow visualization

tests of the present model, is presented in figure 17. For the model without the nose strakes, the vortex cores emanating from the fuselage forebody were found to be asymmetrically disposed as sketched in figure 17(a). Addition of the nose strakes apparently provides a well defined point of separation which, in turn, resulted in the symmetric vortex formation sketched in figure 17(b). Although this phenomenon is probably Reynolds number dependent, the investigation reported in reference 10 has indicated that it may persist at full-scale Reynolds numbers.

The effect of the nose strakes on the longitudinal aerodynamic characteristics of the configuration is presented in figure 18. As can be seen, the particular strakes tested introduced an increased level of longitudinal instability for angles of attack above 5°. However, it should be noted that the strakes were solely intended to investigate potential improvements in directional characteristics. Therefore, additional study is required to define the appropriate stake geometry which will provide the beneficial increase in  $C_{n\beta}$  and eliminate the yawing moment asymmetry, without the attendant increase in longitudinal instability.

#### LATERAL CONTROL CHARACTERISTICS

Previous analytical studies of highly swept arrow-wing concepts have indicated that the lack of adequate roll control, for providing lateral trim under steady-state crosswind landing condition, may impose added low-speed operational constraints. Therefore, during the present investigation tests were conducted to determine the lateral control effectiveness provided by the ailerons and differential deflection of the trailing-edge flap segments, and

to assess the potential advantages of thrust vectoring concepts for providing increased roll control. It should be pointed out that the model used in the investigation was relatively rigid, and that the effects of elasticity have not been considered.

Aerodynamic lateral control effectiveness.- The data of figure 7 have shown that the trailing-edge flap segment  $t_5$  is relatively ineffective for providing lift; however, because of its geometric moment arm, segment  $t_5$  has been found to be relatively effective for producing roll control. For example, figure 19 shows the variation of the lateral-directional aerodynamic characteristics with angle of attack for the model using the outboard aileron ( $t_6$ ) and the combination of outboard aileron and trailing-edge flap segment  $t_5$ . As can be seen, segment  $t_5$  provides approximately one-half the rolling moment produced by deflecting the outboard aileron ( $t_6$ ) alone. Figure 20 presents the corresponding longitudinal data for the configuration with the above lateral control conditions. Also presented in figure 20 are the data obtained for the symmetric,  $\delta_f = 40^\circ/40^\circ/20^\circ$  flap condition. As can be seen from comparison of the data of figure 20, the use of segment  $t_5$  for lateral control results in only minor lift losses, indicating that segment  $t_5$  may be used more effectively as an aileron than as a trailing-edge flap.

In order to further establish the relative lateral control effectiveness of the individual trailing-edge segments, tests were conducted wherein the segments were deflected individually. The results are summarized in figure 21 for an assumed approach angle of attack of  $8^\circ$ . It is of course recognized that the incremental values of rolling moment coefficient, provided by the individual segments, will not necessarily sum to the total obtained by deflection of

various segments in combination. However, comparison of the data of figure 19 with results obtained by summation of corresponding data of figure 21 shows that good agreement does exist. Hence, the data of figure 21 may be considered to be representative of the lateral control capabilities of the present trailing-edge system.

From the data of figure 21 it can be seen that the variation of  $C_l$  with deflection angle for segment  $t_6$  is non-linear, thereby indicating that upwardly deflecting segment  $t_6$  can produce a lift loss which is greater than the lift gain produced by a corresponding downward deflection of this segment. Since previous studies have shown that such segments are ineffective at deflections greater than  $40^\circ$ , and since it is desired that no lift losses accompany the lateral control provided, the data of figure 21 indicate that the maximum lateral control produced by segment  $t_6$  would be about  $C_l = 0.01$ . The data of figure 21 also show that the maximum lateral control provided by segment  $t_5$  for  $+40^\circ$  deflection would be  $C_l = 0.006$ . Hence, for the assumed approach angle of attack of  $8^\circ$ , the lateral control provided by segments  $t_5$  and  $t_6$  would be limited to about  $C_l = 0.016$ . However, as shown by figure 21, segments  $t_1$  and  $t_3$  produce significantly higher levels of rolling moment than segments  $t_5$  and  $t_6$ , which suggests that utilizing surfaces  $t_1$  and  $t_3$  as flaperons may substantially increase the lateral control available.

Assuming that segment deflections greater than  $40^\circ$  will result in flow separation (as indicated by figures 6 and 7), then the total roll control available with minimum lift loss, using segments  $t_5$  and  $t_6$  as ailerons and segment  $t_1$  and  $t_3$  as flaperons, is as follows:

$\delta_f$ $t_1, t_3$ deg	$\delta_a$ $t_1, t_3$ deg	$C_L$ $t_1 + t_3$	$C_L$ $t_5 + t_6$	$C_L$ Total
0	± 40	0.028	0.016	0.044
10	30	0.021		0.037
20	20	0.014		0.030
30	10	0.007	↓	0.023
40	0	0	↓	0.016

If it is assumed that the lateral control available remains constant over the angle of attack range considered, then lines of constant lateral control available may be superimposed on the plot of  $C_L$  versus  $\delta_f$  as illustrated in figure 22. It should be noted that the longitudinal data presented in figure 22 are obtained from figure 6, assuming that the lift contribution of segment  $t_5$  is negligible.

The roll control required for lateral trim under crosswind conditions may be obtained from the expression

$$C_L = C_{L\beta} \beta \quad (3)$$

where the values of  $C_{L\beta}$  are a function of lift coefficient and flap deflection (see figure 12). The sideslip angle,  $\beta$ , is by definition

$$\beta = \sin^{-1} \frac{v}{V} \quad (4)$$

where  $v$  = crosswind velocity, and  $V$  is the approach speed which is assumed to be a function of  $C_L$  only.

$$V = \sqrt{W/S \cdot 2/\rho C_L} \quad (5)$$

Therefore, for a given approach lift coefficient, flap deflection and crosswind velocity, equation 3 defines the lateral control required. Superimposing the lateral control required on the plot of lateral control available, and plotting the locus of points for which the lateral control available equals the lateral

control required, results in the lateral control constraint illustrated in figure 23. From figure 23 it can be seen that for an assumed approach angle of 8°, the requirement for lateral trim in a 30 knot crosswind would limit the approach lift coefficient to values of about 0.5. Although increases in approach  $C_L$  would be provided by reducing the crosswind velocity (see figure 23), the 30 knot crosswind constraint is considered to be consistent with current design practice.

In order to more clearly demonstrate the relationship between crosswind velocity and approach lift coefficient (or approach speed) the results of figure 23 are presented as a nomogram in figure 24. From figure 24 it can be seen that desirable reductions in approach speed would be accompanied by an increasingly restrictive crosswind constraint.

It is of course recognized that the above results are for a lateral control system of outboard ailerons and differential trailing-edge flaps, and that other sources of lateral control may allow the crosswind constraint to be relaxed. One concept is to provide increased trailing-edge flap effectiveness (for example with the use of propulsive-lift concepts). Increased trailing-edge flap effectiveness would, of course, provide increased lateral control; moreover, it would permit increased lift to be obtained at a given angle of attack, which, as indicated previously, will provide reduced levels of  $-C_{l\beta}$  at a given value of  $C_L$ . The reduction in  $-C_{l\beta}$  will of course result in reduced levels of required lateral control.

Effect of thrust vectoring. - As indicated in the previous section, the development of propulsive lift concepts may allow the crosswind constraint to be relaxed. As an illustration, the 30 knot crosswind constraint calculated

for the configuration employing symmetric thrust vectoring is compared with the constraint for the basic configuration in figure 25. As can be seen from comparison of figures 25(a) and (b), the use of symmetric thrust vectoring would result in an increase in approach lift coefficient from about .5 to about 0.55. The increase in approach lift coefficient, provided by symmetric thrust vectoring is due to: (1) the previously mentioned reduction in  $-C_{l\beta}$  at a given lift coefficient, which results in a reduction in lateral control required, and (2) an increase in aileron (differential flap) deflection available, due to reduced symmetrical flap deflection required to achieve a given  $C_L$ .

In order to investigate the use of differential thrust vectoring as a possible means for providing further increased lateral control, tests were conducted wherein the outboard exhaust nozzles were deflected 20° differentially from the undeflected condition. Figure 26 presents the rolling moment coefficient produced by the differential thrust vectoring and also presents the values of rolling moment coefficient which would be directly attributable to differential inclination of the thrust produced by the outboard engines. The calculated value of rolling moment coefficient is computed from the expression

$$C_l = -\frac{\sum Y_i}{b} C_T \sin \delta N_i \quad (6)$$

As would be expected (based on the longitudinal results obtained from symmetric thrust vectoring tests) the experimental and calculated results are in relatively good agreement. However, it is interesting to note that the calculated rolling moment coefficient somewhat underestimates the experimentally determined values. This result is probably due to the upwardly deflected engine exhaust acting as a spoiler, and hence providing a slight increase in lateral control.

If it is assumed that  $\pm 20^\circ$  differential thrust vectoring of all four engines may be superimposed on  $20^\circ$  of symmetric thrust vectoring, then for  $C_T = 0.13$  an incremental rolling moment coefficient of 0.009 is computed from equation 6. The increase in lateral control, provided by differential thrust vectoring, further relaxes the lateral control constraint as illustrated in figure 27. Hence for the conditions considered (i.e.,  $\alpha = 8^\circ$  and a 30 knot crosswind) the approach lift coefficient could be increased to 0.6.

It should be noted that the particular thrust vectoring concept investigated produced only limited additional circulation lift and therefore, is seen to require substantial deflection angles to achieve the lateral control shown in figure 27. However, it may be possible to reduce these required deflections and further relax the lateral control constraint through the use of alternate propulsive-lift concepts which do produce substantial levels of additional circulation lift.

#### SUMMARY OF RESULTS

The results of low-speed wind tunnel tests of an advanced supersonic cruise arrow-wing configuration may be summarized as follows:

1. Deflection of the wing leading-edge apex flaps downward to suppress the wing apex vortices, and hence provide improved longitudinal stability, results in a reduction in directional stability.
2. For  $\alpha < 10^\circ$ , deflecting the entire plain trailing-edge flap system from  $0^\circ$  to  $30^\circ$  resulted in essentially a linear increase in  $C_L$  with  $\delta_f$ . However for  $\alpha > 10^\circ$ , or  $\delta_f > 30^\circ$ , the effectiveness of the plain trailing-edge flap system was reduced.

3. For the particular configuration tested, the increment in lift provided by thrust vectoring was essentially limited to the vector component of the thrust forces.
4. The horizontal tail tested was effective in providing longitudinal control over the angle of attack range tested. However, the horizontal tail provided only a small contribution to longitudinal stability for  $\alpha < 10^\circ$ .
5. Increasing the trailing-edge flap deflection resulted in a reduction in  $-C_{l\beta}$  at a given lift coefficient. This result is apparently due to a reduction in angle of attack at which the given lift coefficient is obtained.
6. The outboard vertical fins and the centerline vertical tail provided a stabilizing increase in  $C_{n\beta}$  over the normal operational angle of attack range. The addition of the horizontal tail provided a substantial increase in  $C_{n\beta}$  at low angles of attack.
7. The use of nose strakes was found to provide a significant increase in  $C_{n\beta}$  and to eliminate large asymmetric yawing moments at high angles of attack; however, the particular strakes tested were longitudinally destabilizing.
8. The high levels of effective dihedral, and inadequate lateral control exhibited by the model, resulted in a 30 knot crosswind landing constraint which would limit the approach lift coefficient of the configuration to about 0.5.
9. The use of symmetric and differential thrust vectoring resulted in increased lateral control which provided relaxed crosswind landing constraints and permitted increased approach lift coefficients.

## REFERENCES

1. Morris, Odell A.; and Fournier, Roger H.: Aerodynamic Characteristics at Mach Numbers 2.30, 2.60, and 2.96 of a Supersonic Transport Model Having a Fixed, Warped Wing. NASA TM X-1115, 1965.
2. Morris, Odell A.; and Patterson, James C., Jr.: Transonic Aerodynamic Characteristics of a Supersonic Transport Model with a Fixed, Warped Wing Having 74° Sweep. NASA TM X-1167, 1965.
3. Coe, Paul L., Jr.; McLemore, H. Clyde; and Shivers, James P.: Effect of Upper Surface Blowing and Thrust Vectoring on Low-Speed Aerodynamic Characteristics of a Large-Scale Supersonic Transport Model. NASA TM X-72792, 1975.
4. Parlett, Lysle P.; and Shivers, James P.: Low-Speed Wind-Tunnel Tests of a Large-Scale Blended-Arrow Advanced Supersonic Transport Having Variable Cycle Engines and Vectoring Exhaust Nozzles. NASA TM X-72809.
5. Coe, Paul L., Jr., and Fournier, Paul G.: Application of Powered-Lift Concepts for Improved Cruise Efficiency of Long-Range Aircraft Presented at LaRC Conference on Powered-Lift Aerodynamics and Acoustics, May 1976. NASA SP-406.
6. Lockwood, Vernard E.: Effect of Trailing Edge Flap Deflection on the Lateral and Longitudinal-Stability Characteristics of a Supersonic Transport Model Having a Highly-Swept Arrow Wing. NASA TM X-71936, 1974.
7. Grantham, William D.; and Deal, Perry L.: A Piloted Fixed-Base Simulator Study of Low-Speed Flight Characteristics of an Arrow-Wing Supersonic Transport. NASA TN D-4277, 1968.
8. Grafton, Sue B.; Chambers, Joseph R.; and Coe, Paul L., Jr.: Wind-Tunnel Free-Flight Investigation of a Model of a Spin-Resistant Fighter.

Configuration. NASA TN D-7716, 1974.

9. Coe, Paul L., Jr.; Chambers, Joseph R.; and Letko, William: Asymmetric Lateral-Directional Characteristics of Pointed Bodies of Revolution at High Angles of Attack. NASA TN D-7095, 1972.
10. Chapman, Gary T.; Keener, Earl R.; and Malcolm, Gerald N.: Asymmetric Aerodynamic Forces on Aircraft Forebodies at High Angles of Attack - Some Design Guides. Stall/Spin Problems of Military Aircraft. AGARD-CP-199, June 1976, paper no. 12.

TABLE I.- DIMENSIONAL CHARACTERISTICS OF MODEL

Wing (aspect ratio of 1.72):

Area, $m^2$ ( $ft^2$ ) . . . . .	2.067	(22.25)
Span, m (ft) . . . . .	1.89	(6.20)
Root chord, m (ft) . . . . .	2.515	(8.252)
Tip chord, m (ft) . . . . .	9.242	(0.794)
Mean aerodynamic chord, m (ft) . . . . .	1.557	(5.109)
Leading-edge sweep, deg -		
At body station 1.275 m (4.184 ft) . . . . .	74	
At body station 4.758 m (15.609 ft) . . . . .	70.5	
At body station 6.238 m (20.615 ft) . . . . .	60	

Vertical tail:

Area, $m^2$ ( $ft^2$ ) . . . . .	.0327	(.352)
Span, m (ft) . . . . .	.171	(.562)
Root chord, m (ft) . . . . .	.0732	(.240)
Leading-edge sweep, deg . . . . .	59	

Vertical fin (two):

Area, $m^2$ ( $ft^2$ ) . . . . .	.084	(.90558)
Span, m (ft) . . . . .	0.147	(0.484)
Root chord, m (ft) . . . . .	0.499	(1.637)
Tip chord, m (ft) . . . . .	0.071	(0.2331)
Leading-edge sweep, deg . . . . .	73.4	

Horizontal tail (aspect ratio of 1.39):

Area, $m^2$ ( $ft^2$ ) . . . . .	.140	(1.613)
Span, m (ft) . . . . .	.457	(1.499)
Root chord, m (ft) . . . . .	.540	(1.772)
Tip chord, m (ft) . . . . .	.116	(0.380)
Leading-edge sweep, deg . . . . .	43	
Dihedral, deg . . . . .	-15	

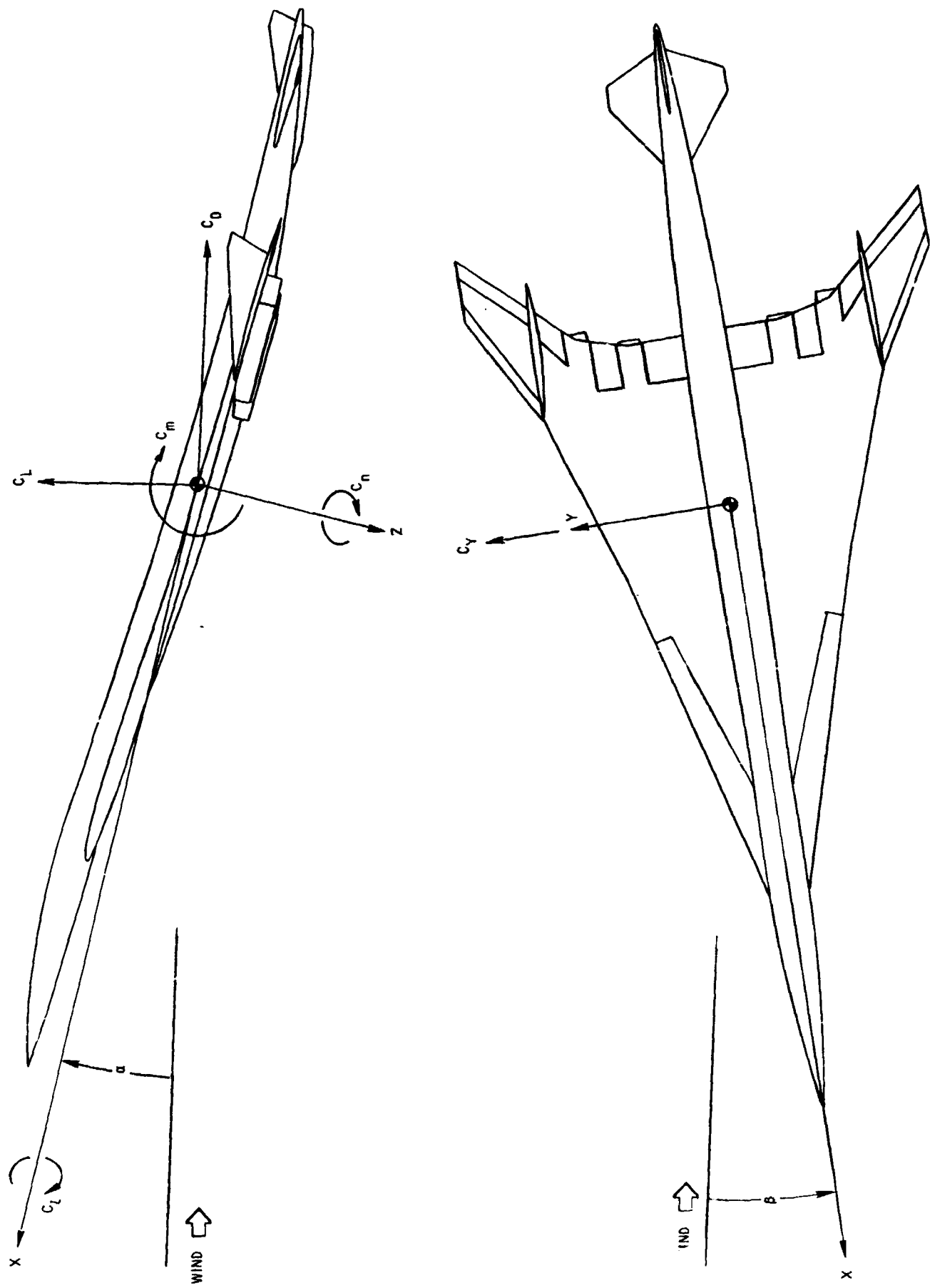
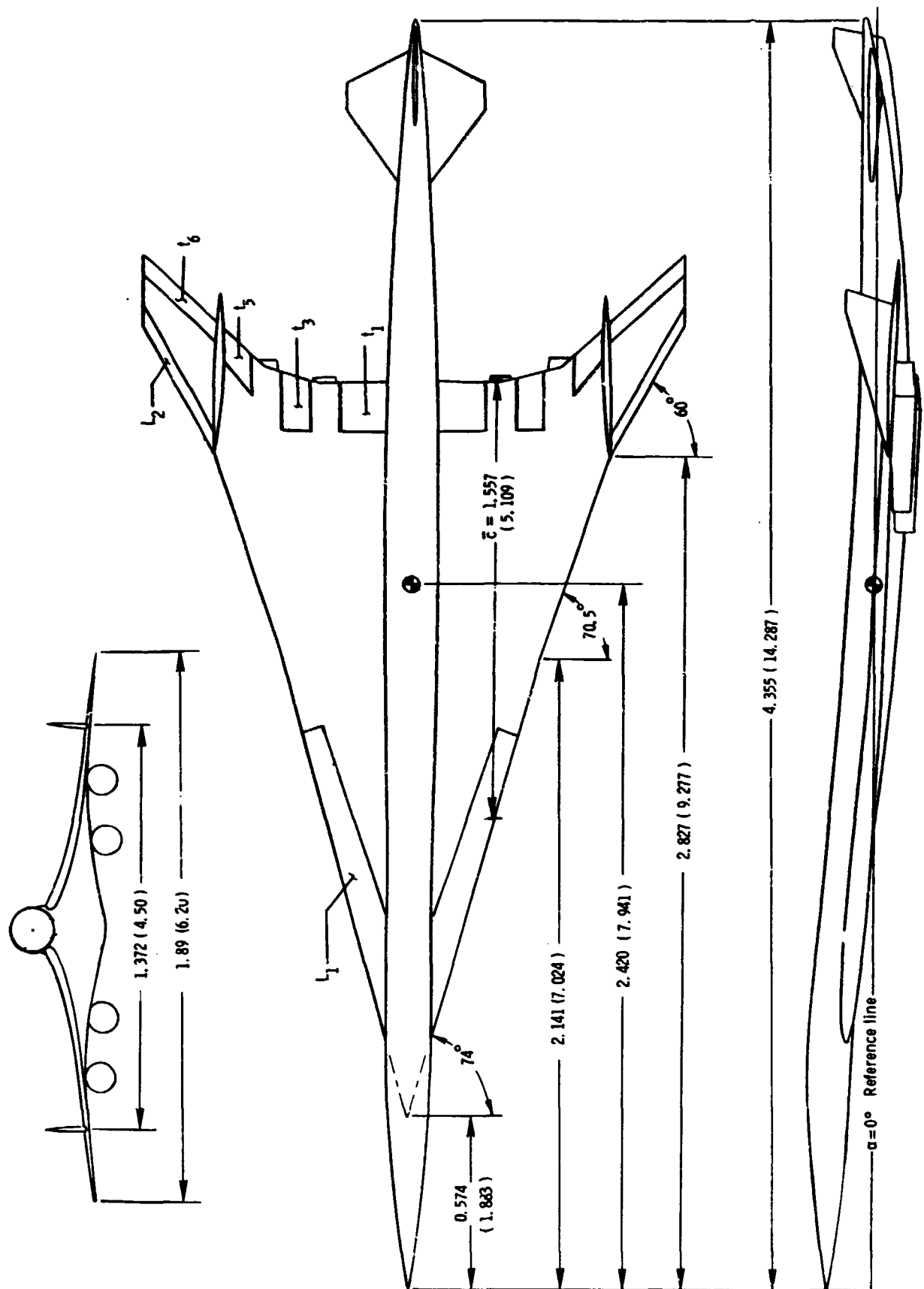
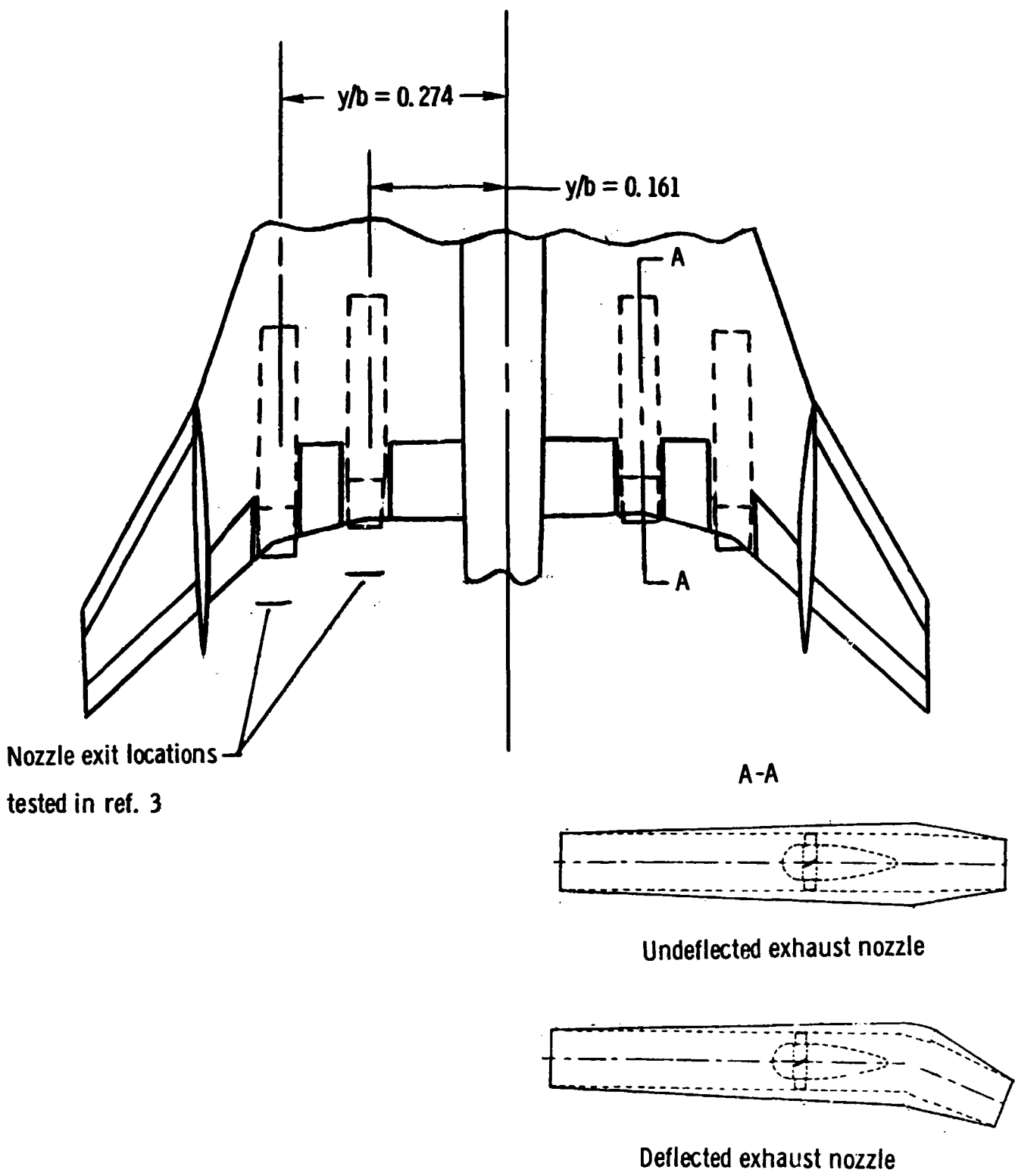


Figure 1. - The body system of axes.



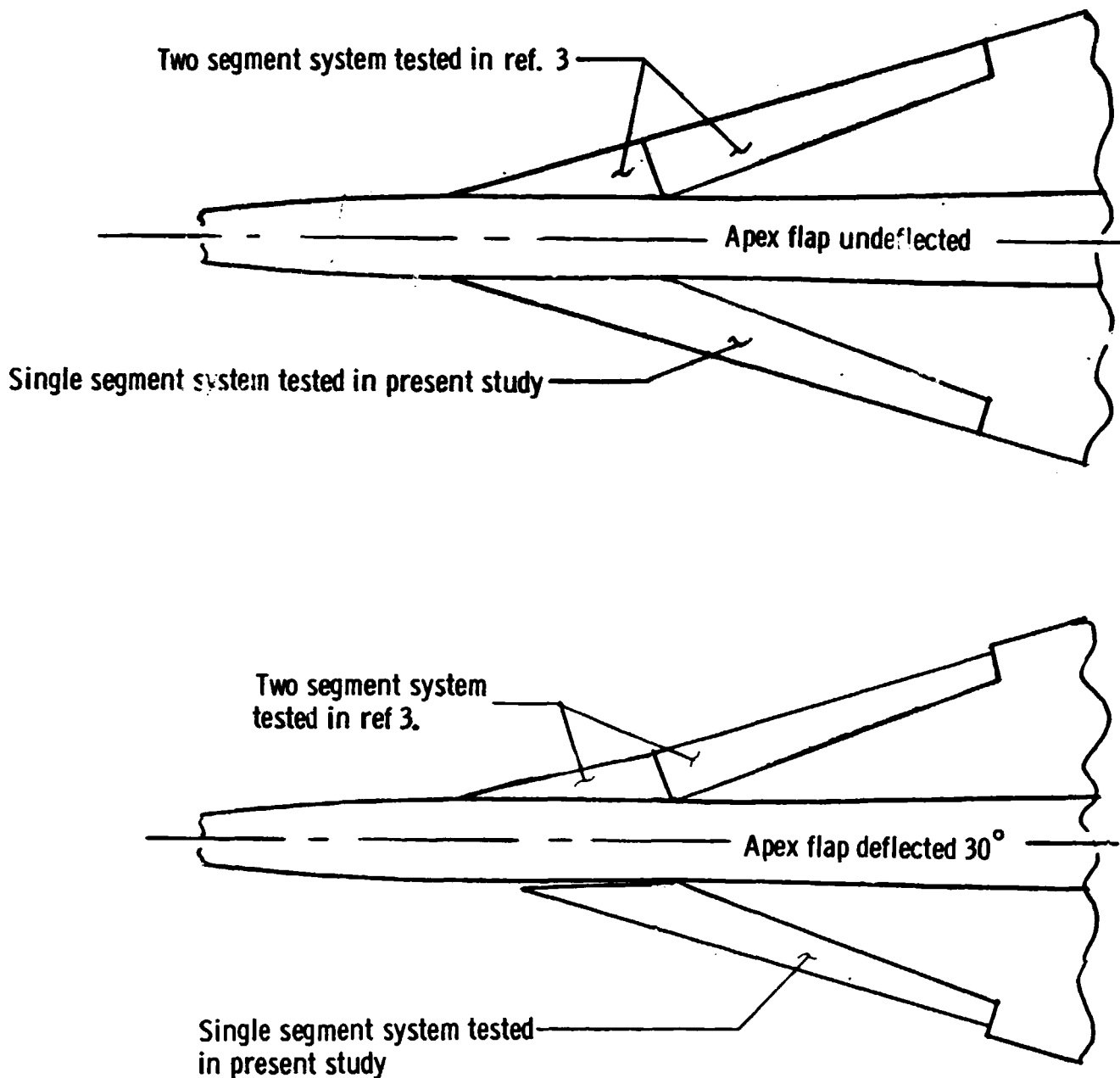
(a) Three-view sketch of model. Dimensions are given in meters and parenthetically in feet.

Figure 2. - Geometric characteristics of model.



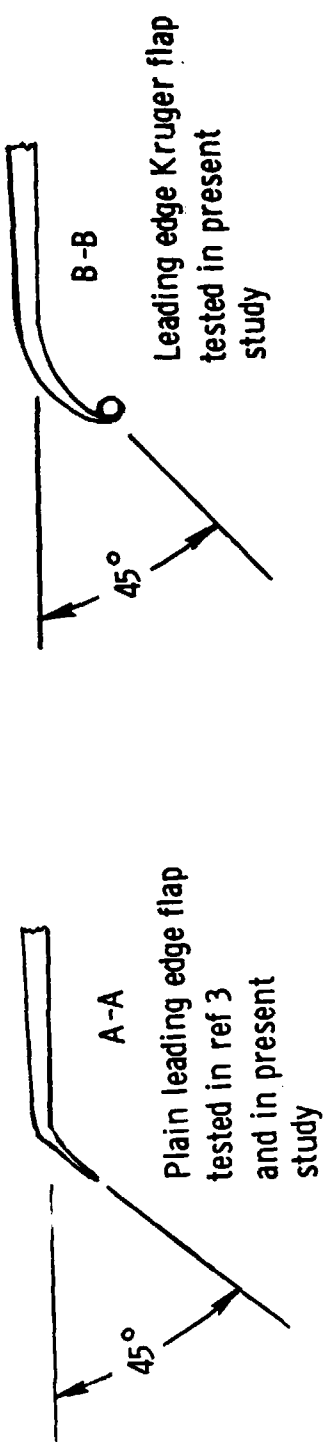
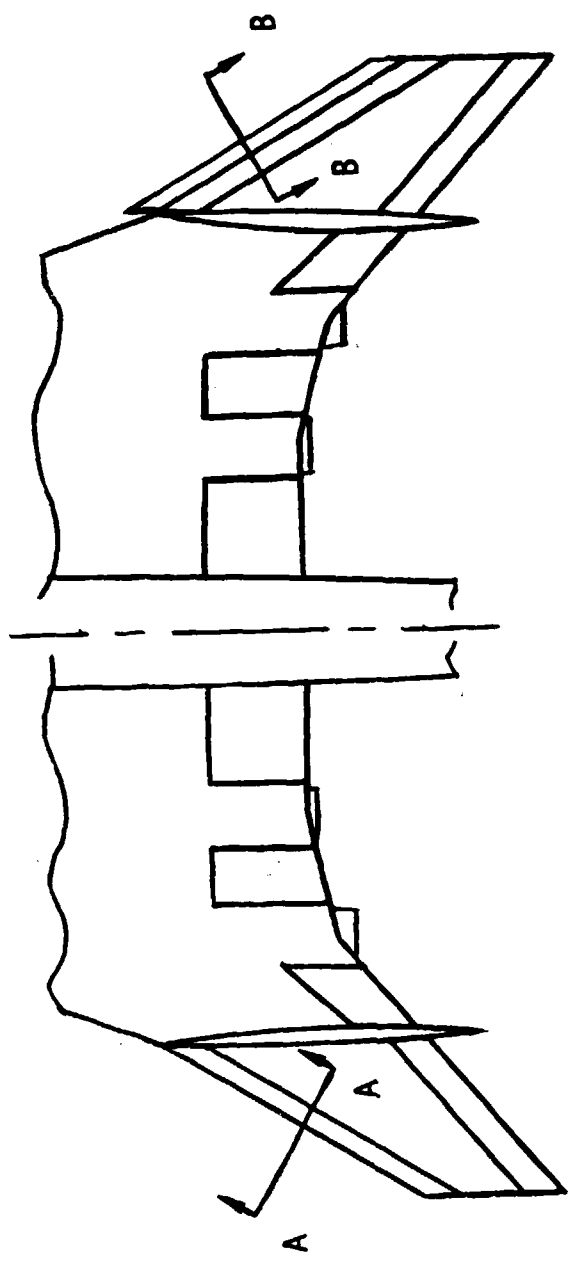
(b) Sketch of nacelles and engine simulator

Figure 2. - Continued



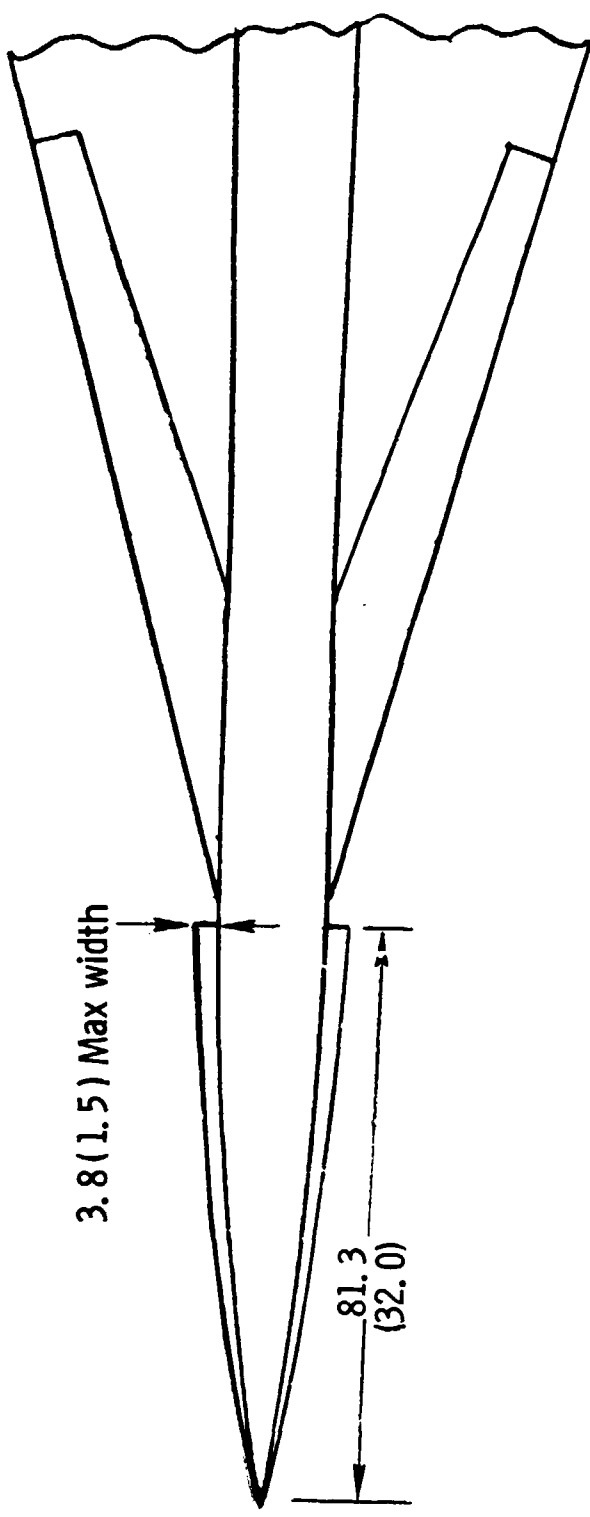
(c) Sketch of leading edge apex flap system

Figure 2 - Continued



(d) Sketch of outboard wing-panel leading edge flaps.

Figure 2. - Continued.



(e) Sketch of fuselage forebody strakes. Dimensions are in centimeters and parenthetically in inches.

Figure 2. - Concluded.

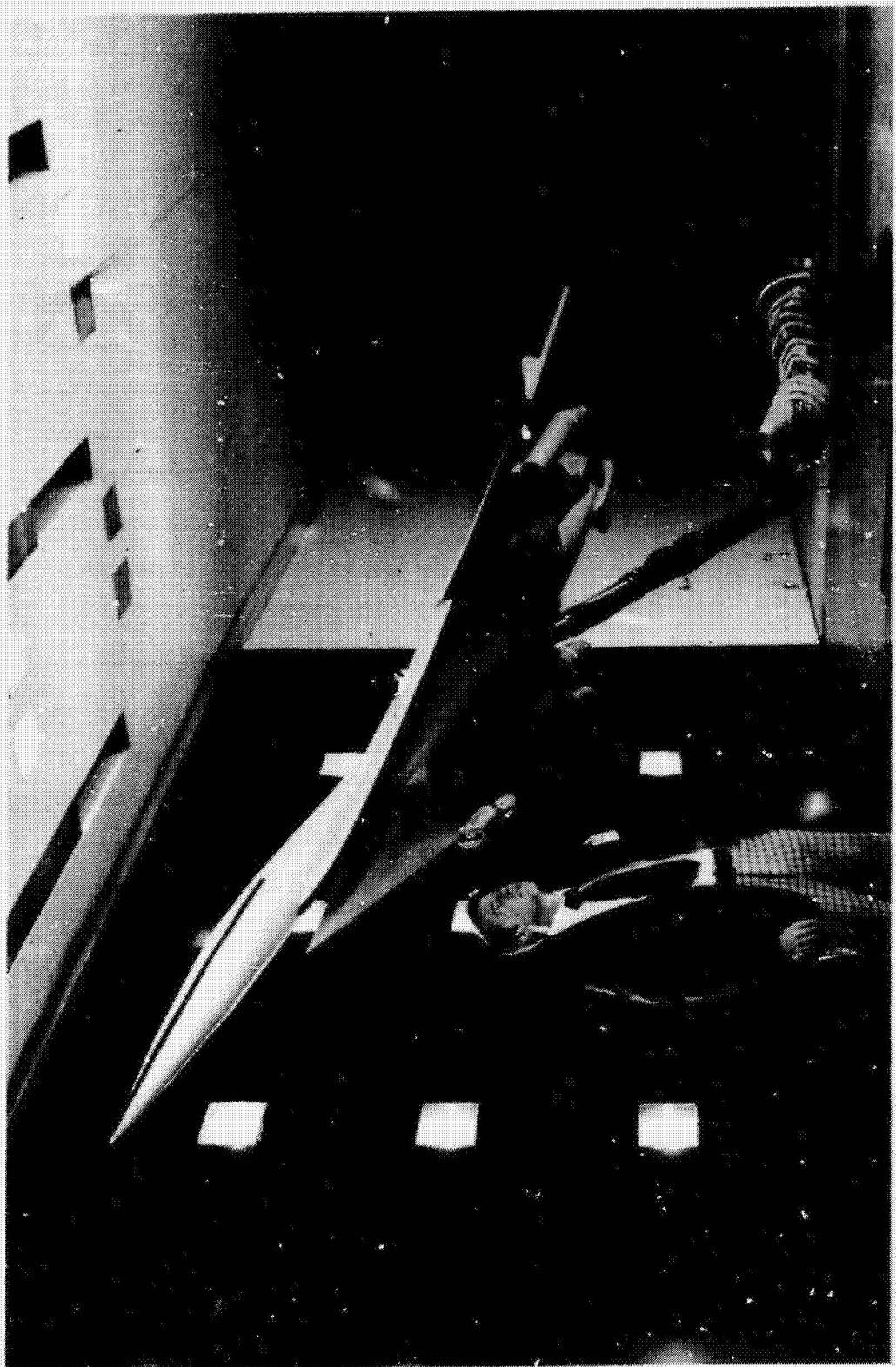


Figure 3. - Photograph of model mounted for tests in Langley V/ STOL tunnel.

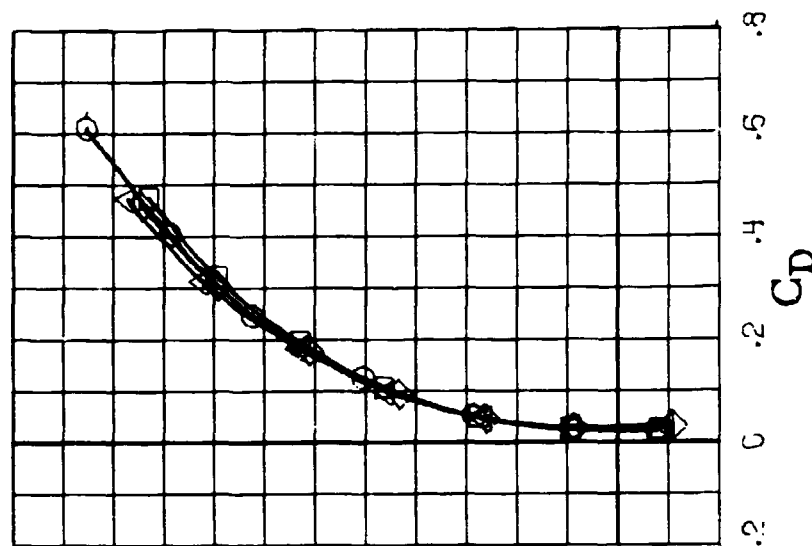
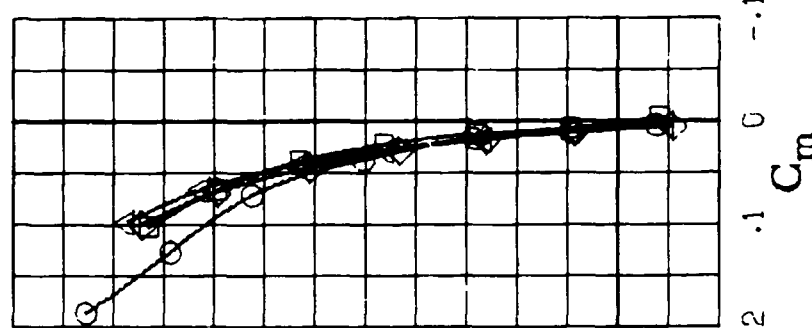
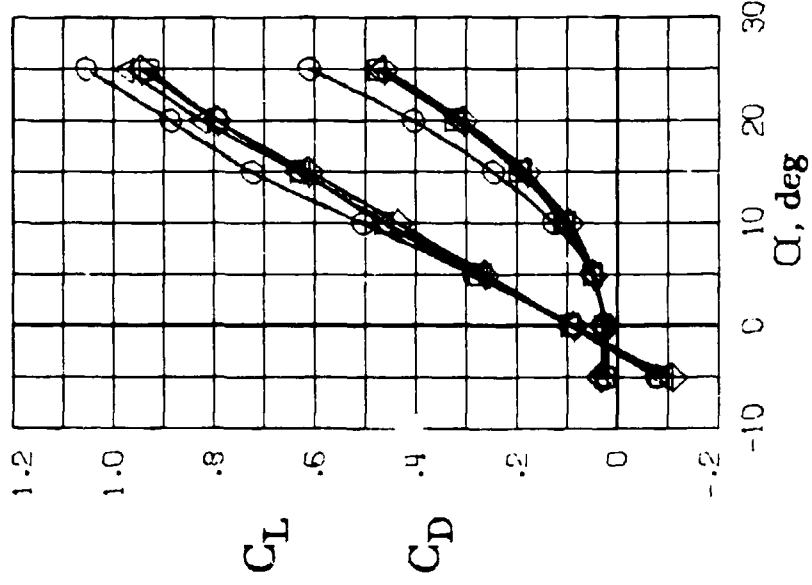
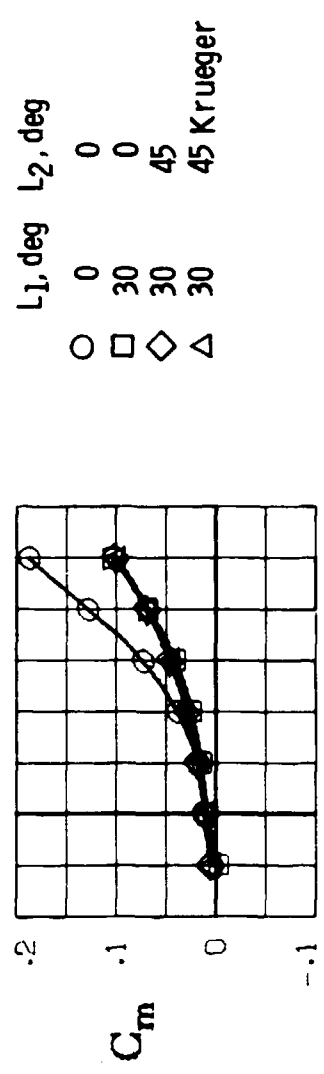


Figure 4. - Effect of wing leading edge devices on the longitudinal aerodynamic characteristics of the wing - body - outboard vertical fin combination.  
 $\delta_f = 0$ ,  $C_T = 0$ .

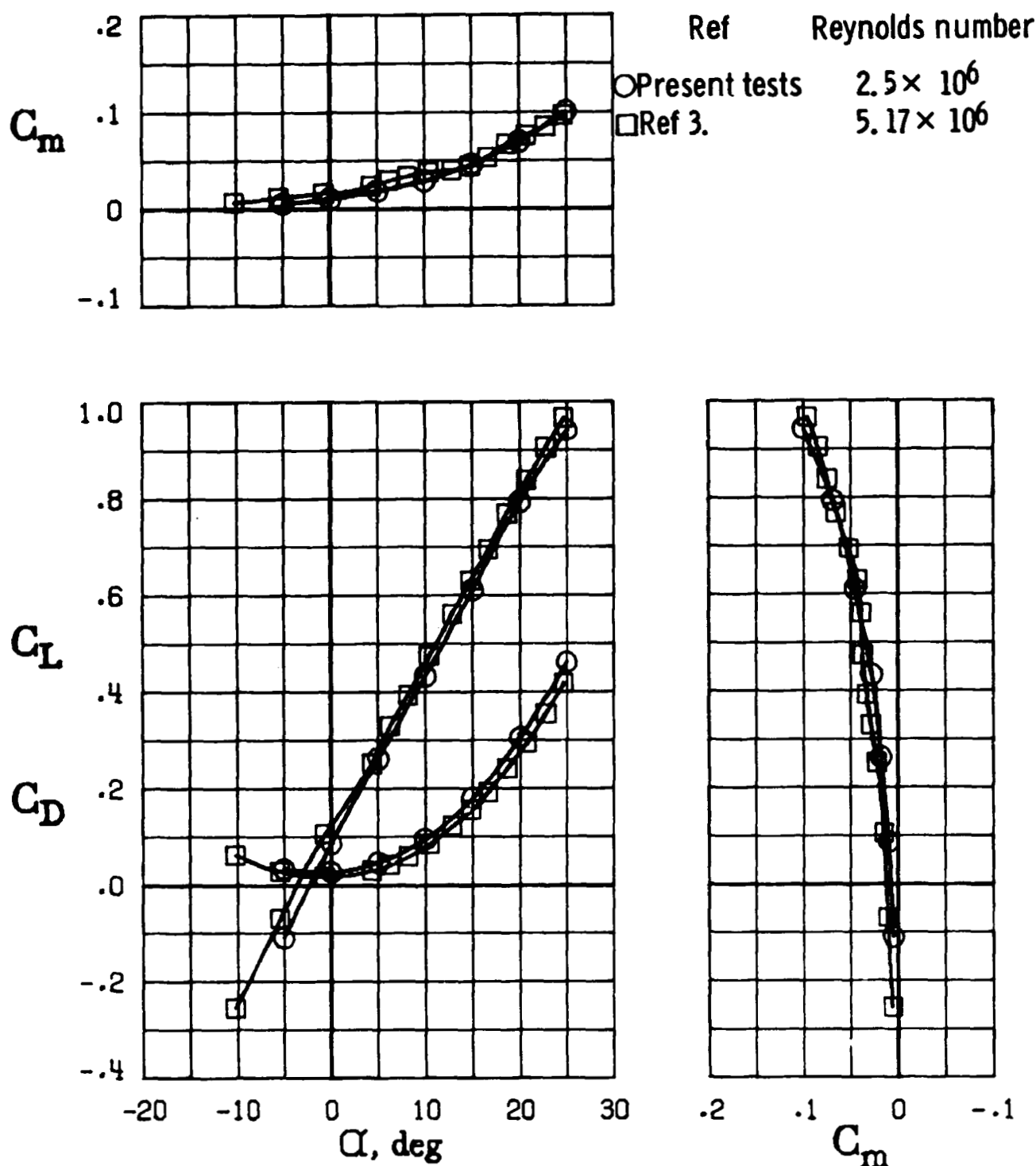


Figure 5. - Comparison of data obtained from present tests with data of ref. 3.  $L_1 = 30^\circ, L_2 = 45^\circ$ .

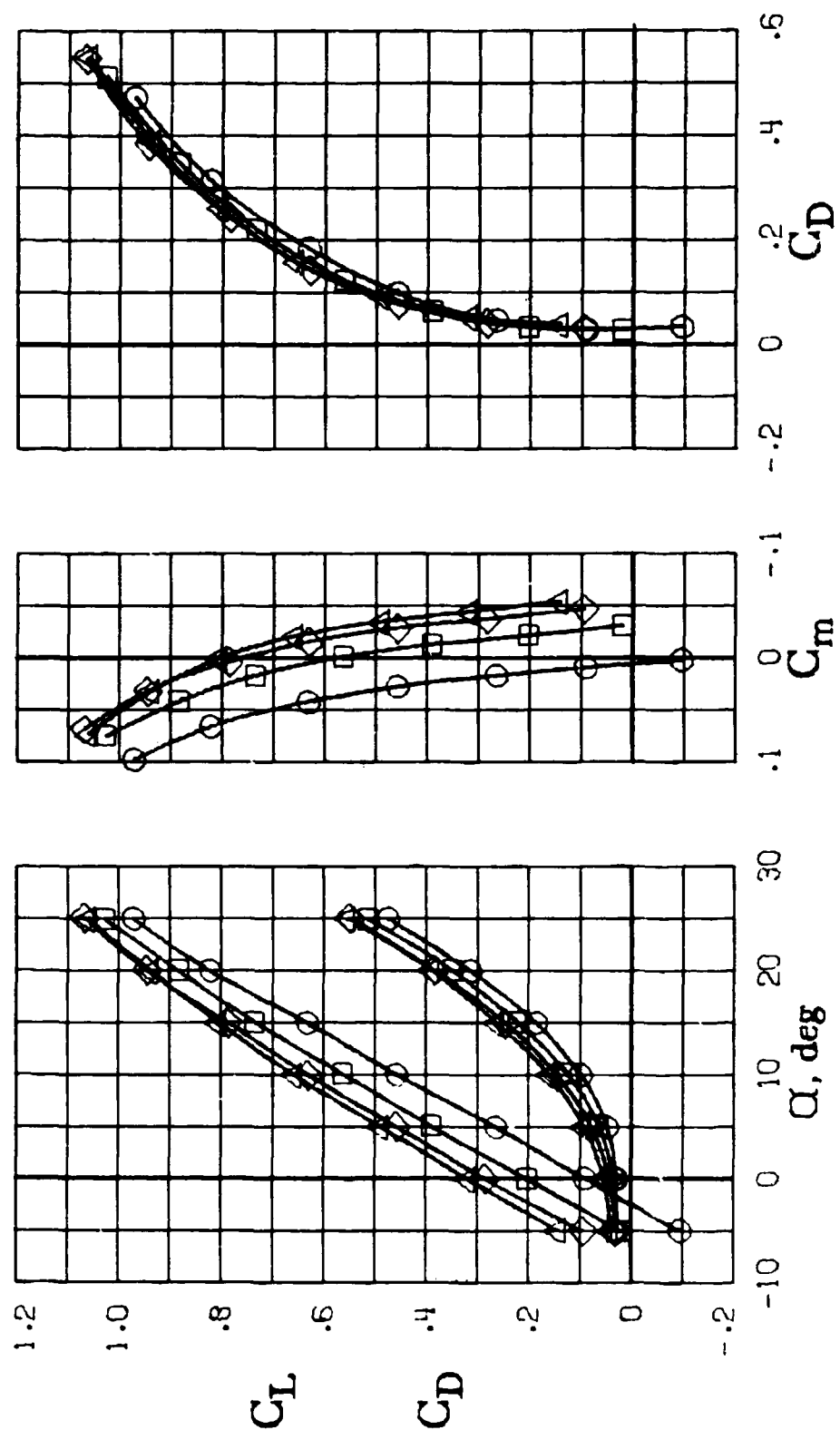
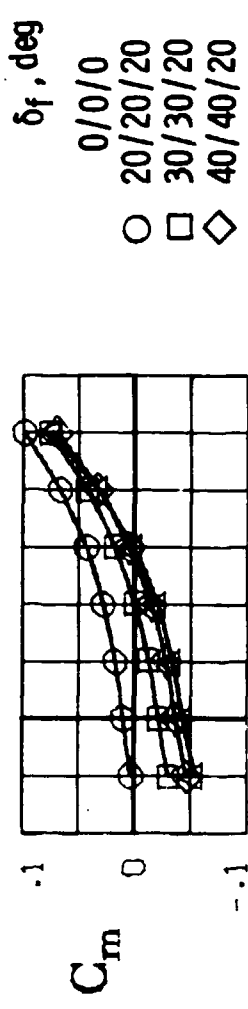


Figure 6. - Effect of trailing-edge deflection on longitudinal aerodynamic characteristics of the wing - body - outboard vertical fin combination.  
 $L_1 = 30^\circ, L_2 = 45^\circ$  Krueger,  $C_T = 0$ .

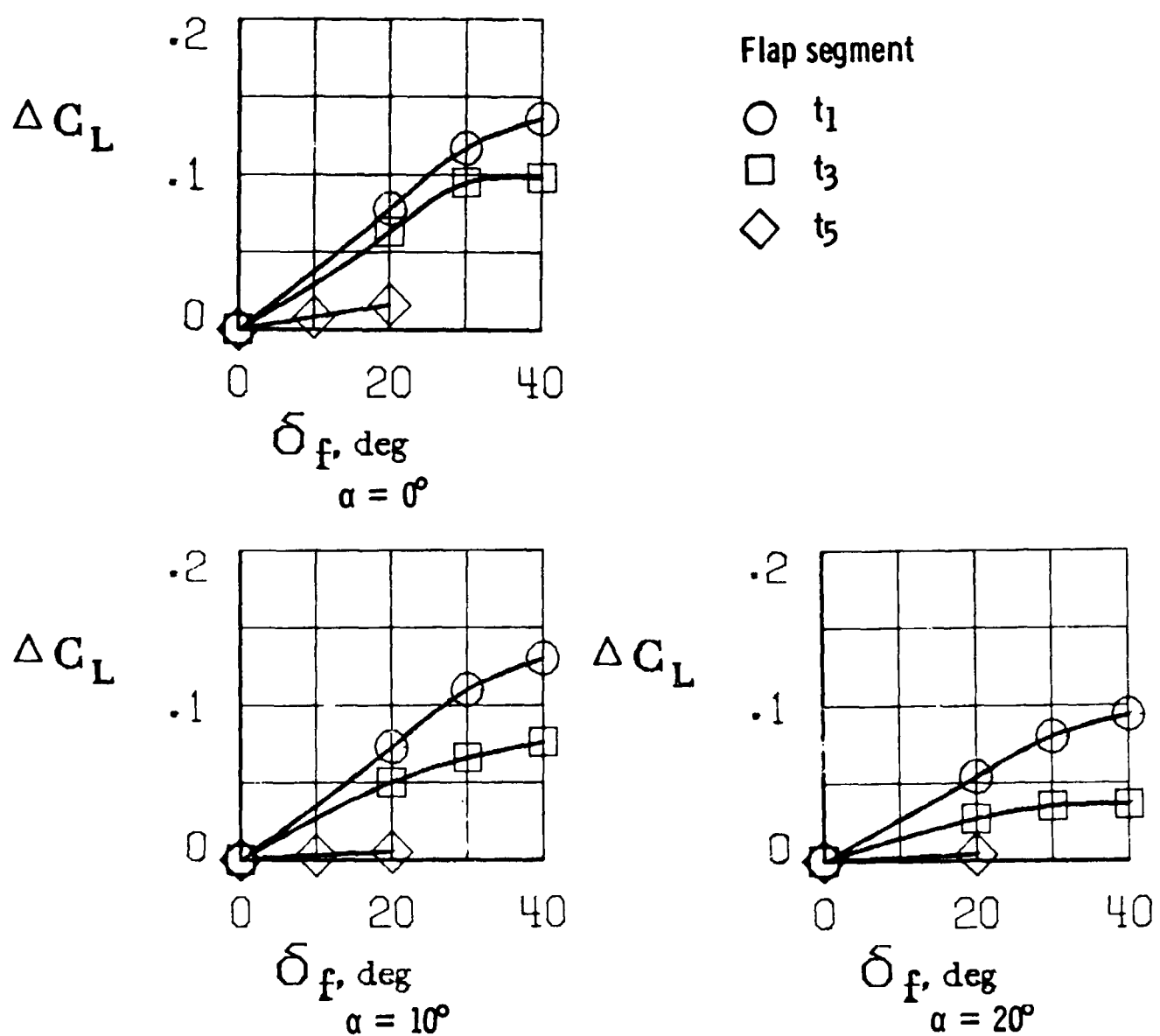
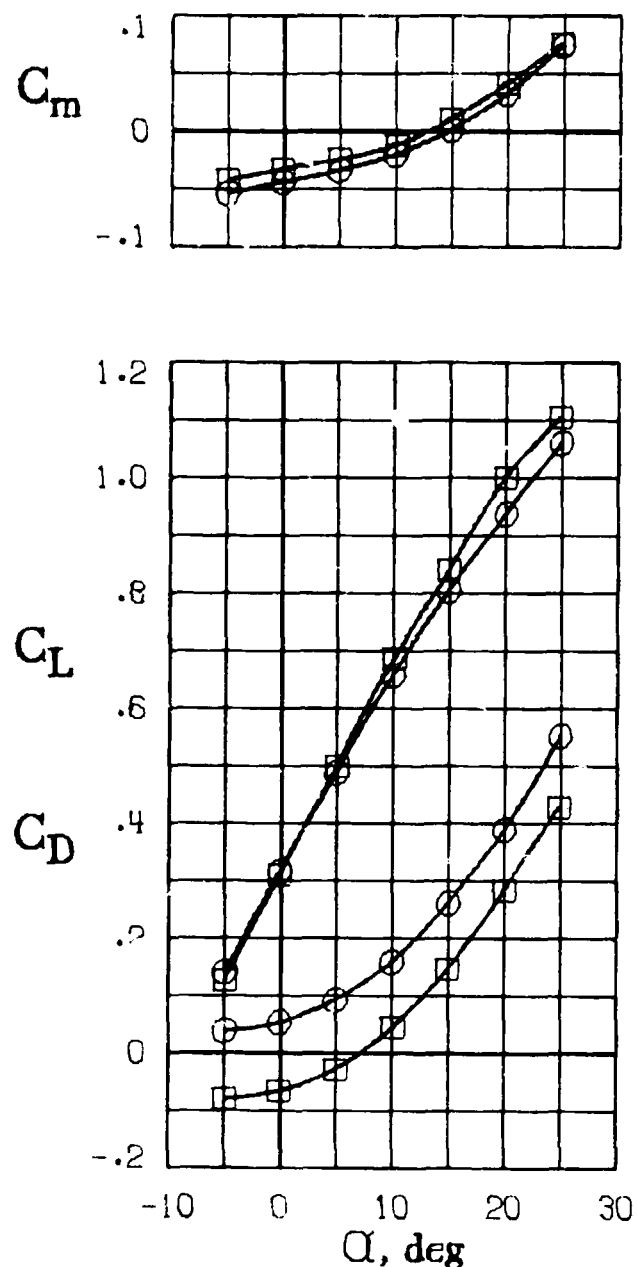
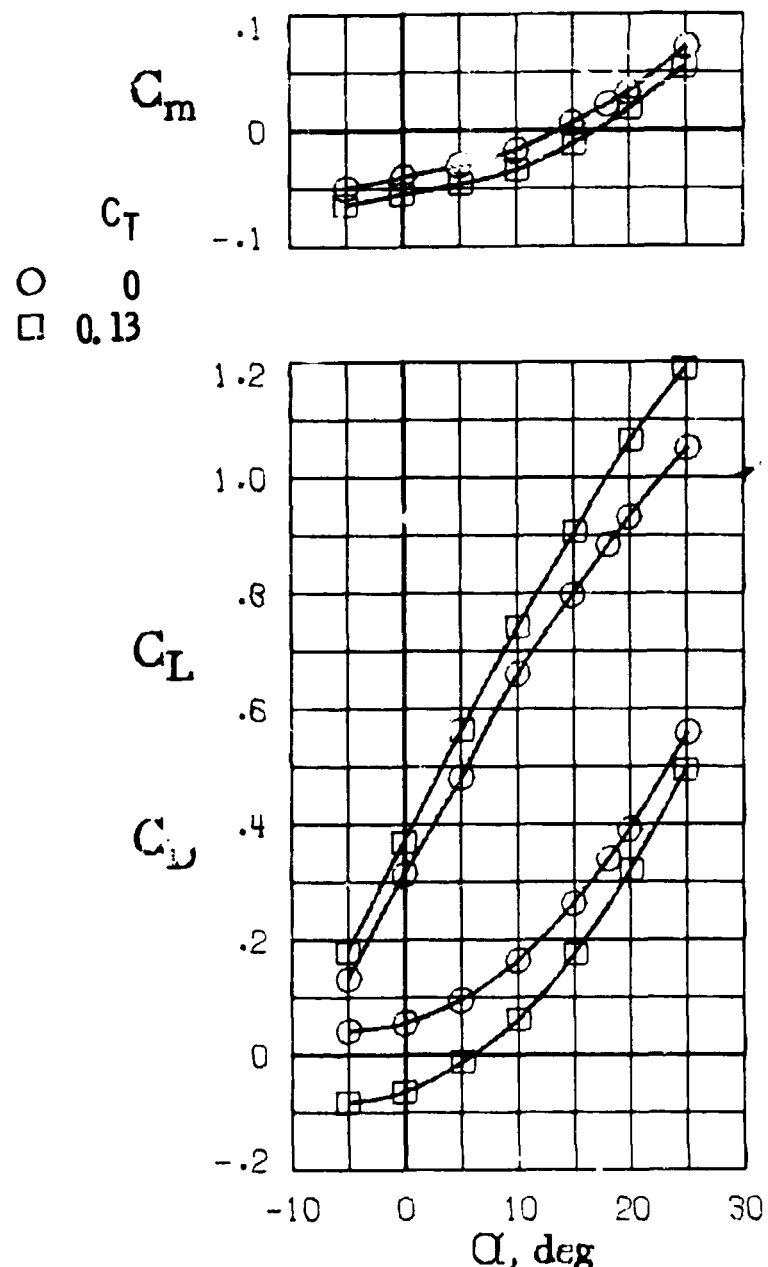


Figure 7. - Individual trailing edge flap effectiveness.



(a)  $\delta_n = 0$



(b)  $\delta_n = 20$

Figure 8. - Effect of thrust and thrust vectoring on longitudinal aerodynamic characteristics of the wing - body - outboard vertical fin combination.  
 $L_1 = 30$ ,  $L_2 = 45^\circ$  Krueger,  $\delta_f = 40^\circ/40^\circ/20^\circ$ .

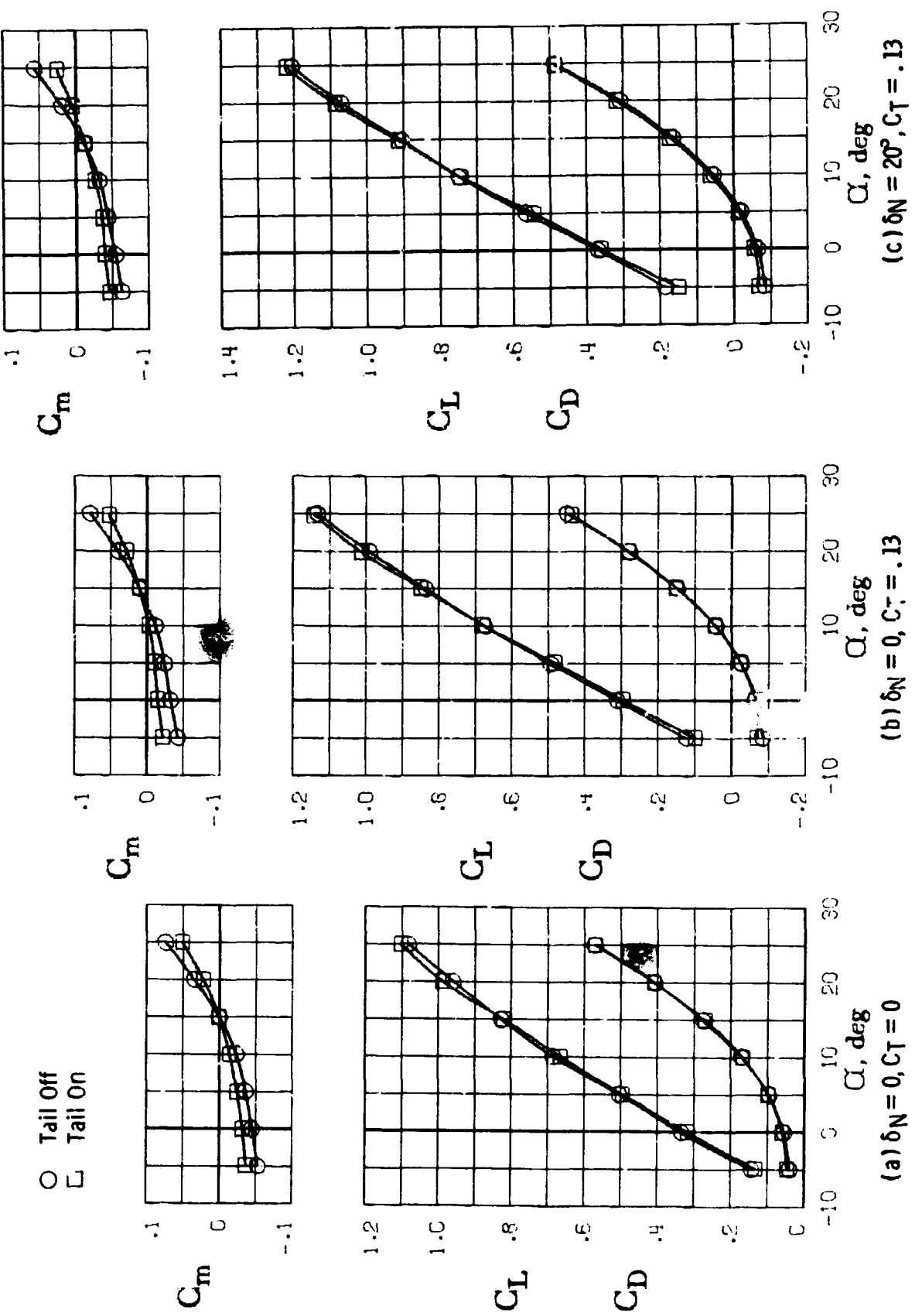
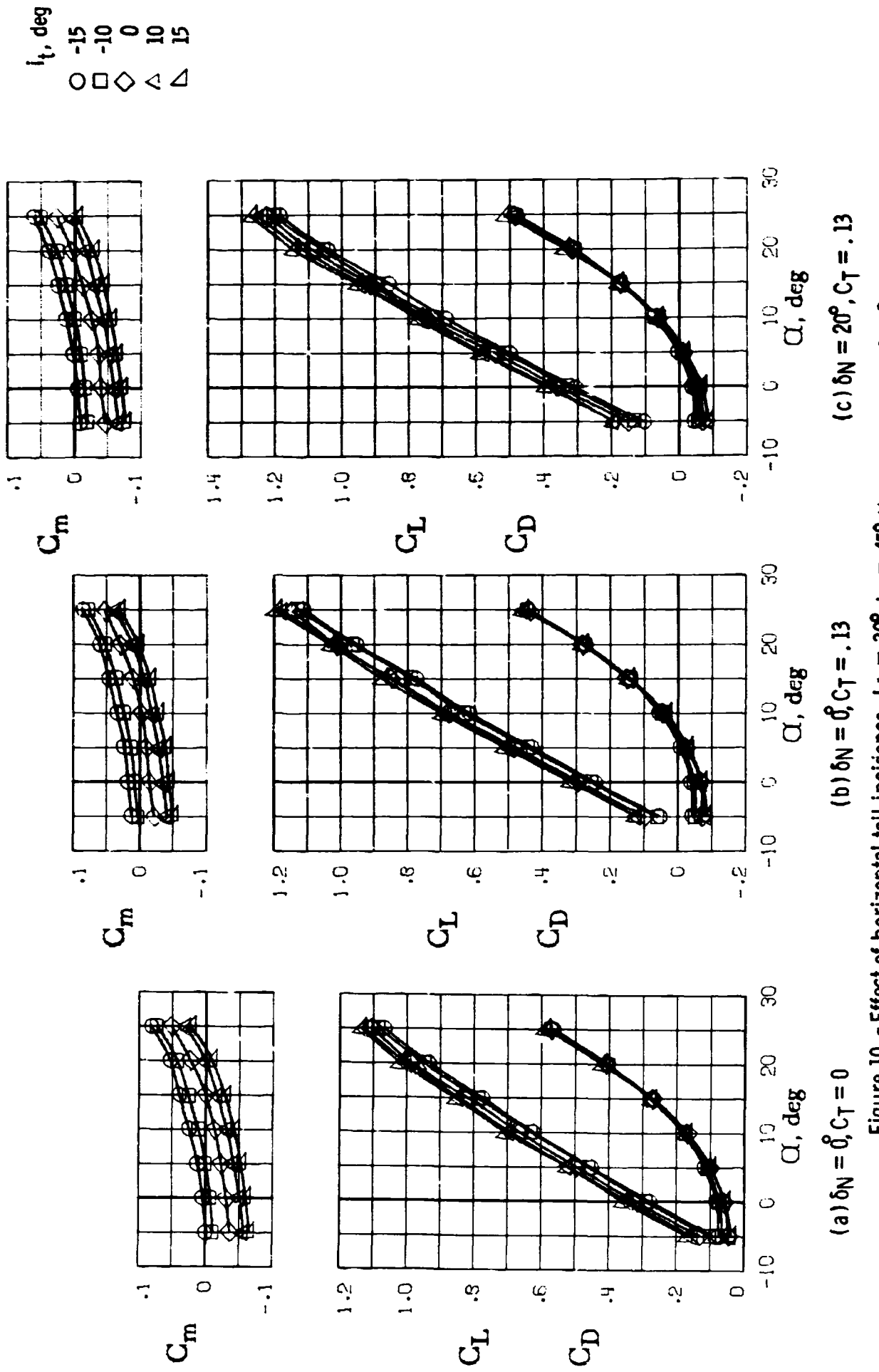


Figure 9 - Horizontal tail effectiveness and effects of thrust  
 $L_1 = 30^\circ, L_2 = 45^\circ$  Krueger,  $\delta_f = 40^\circ/40^\circ/20^\circ$ .



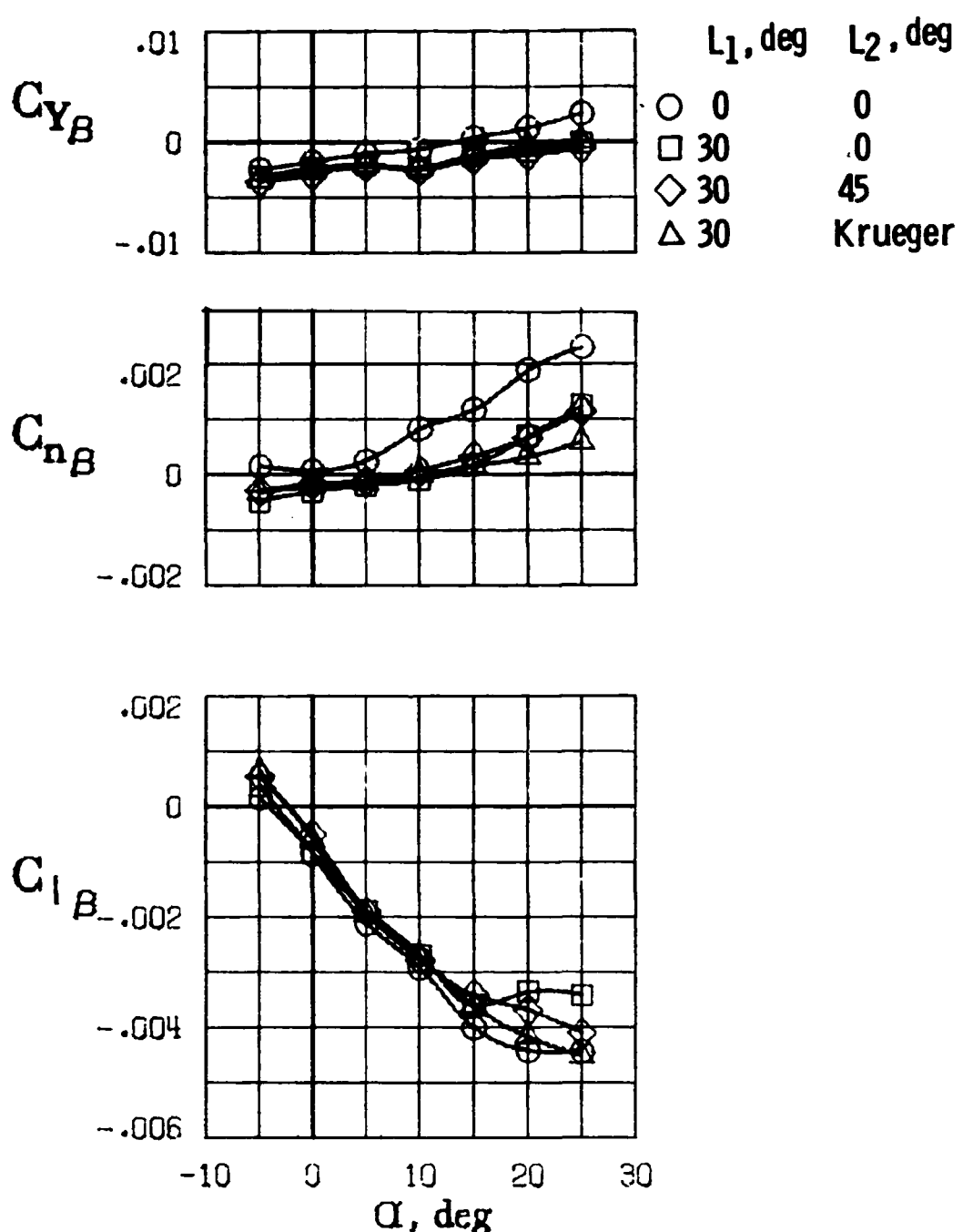
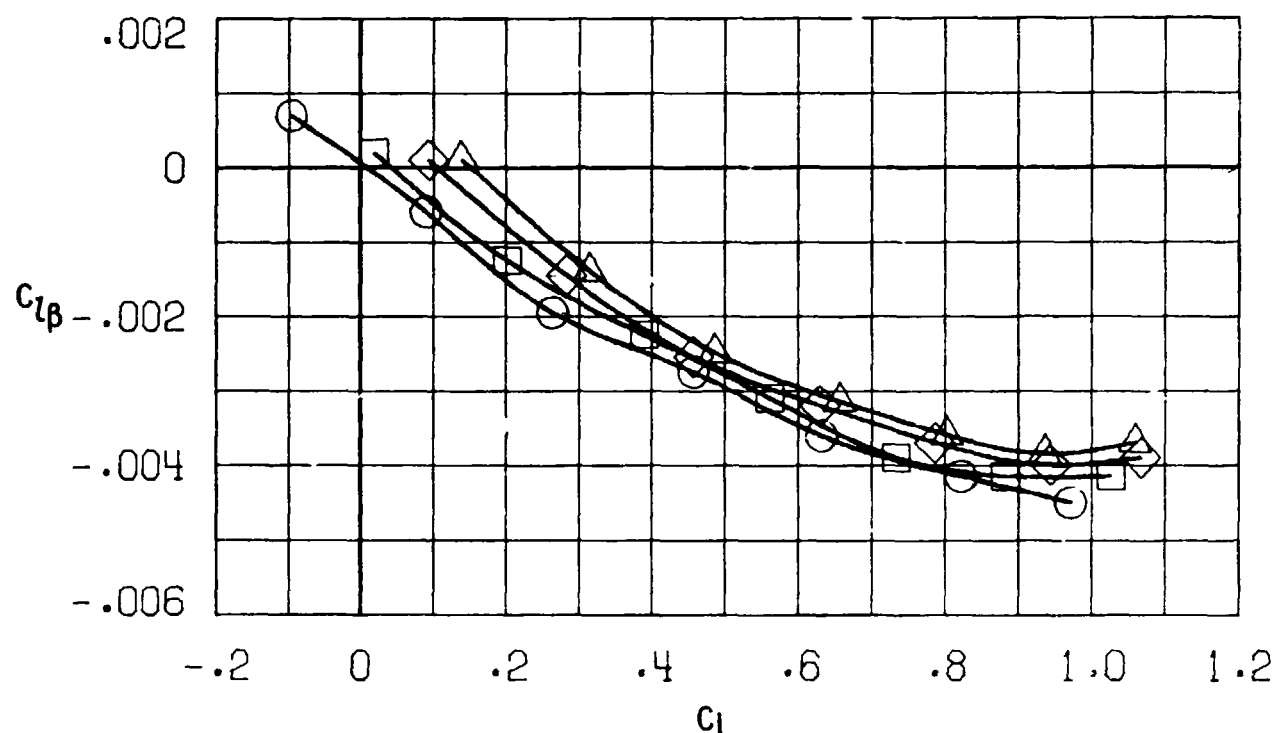
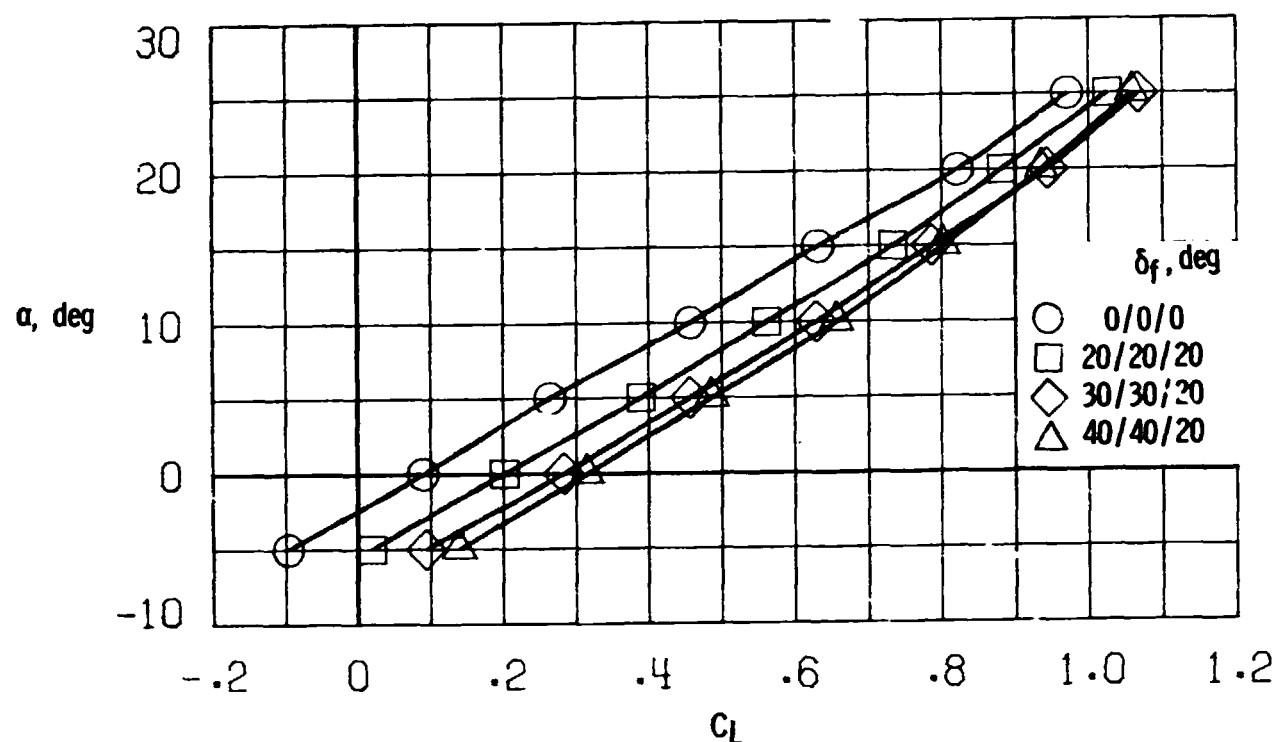
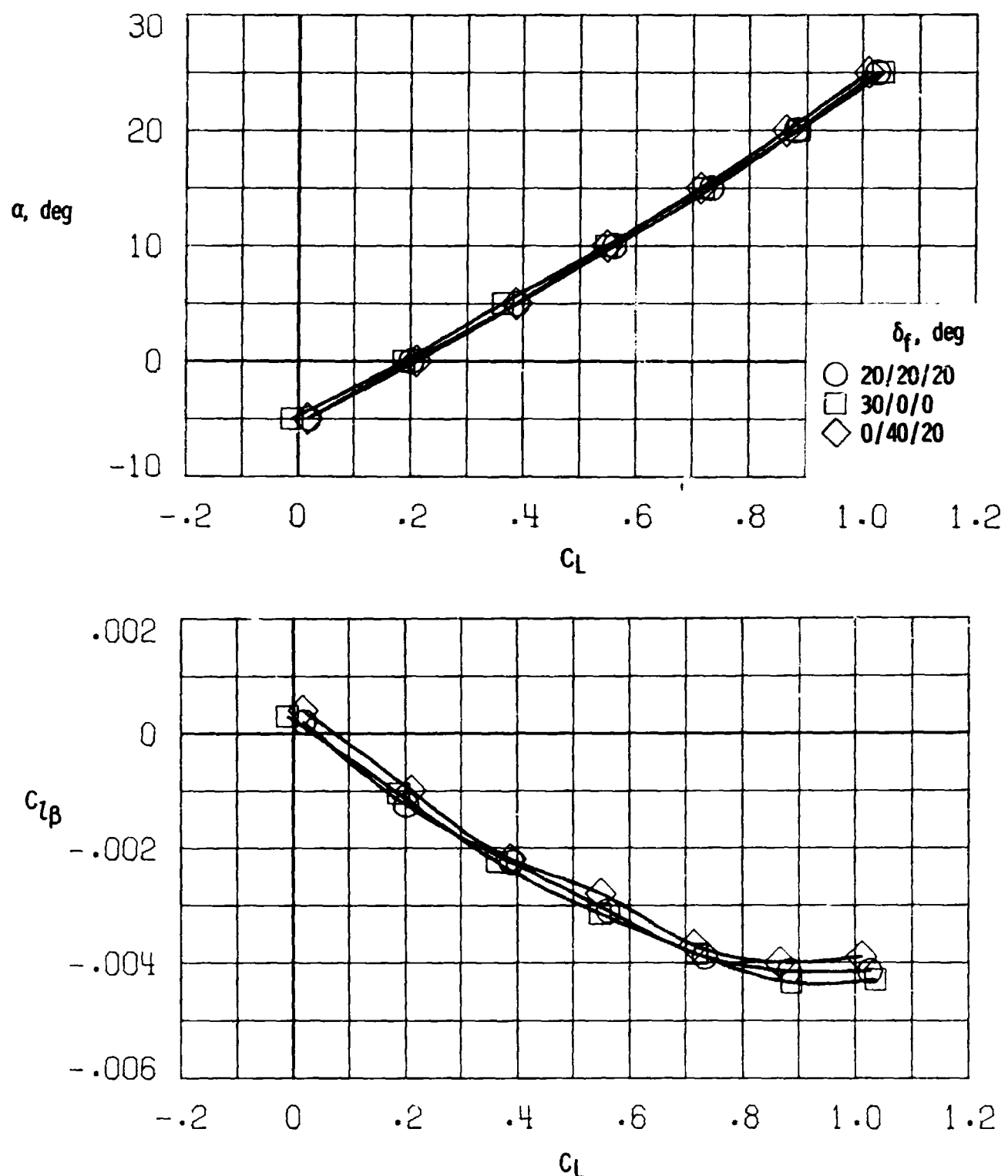


Figure 11. - Effect of wing leading edge devices on the lateral - directional aerodynamic characteristics of the wing - body outboard vertical fin combination.  $\delta_f = 0^\circ$ .



(a) Uniform trailing edge deflection

Figure 12. - Effect of trailing edge flap deflection on the effective dihedral of the wing - body outboard vertical fin combination.  $L_1 = 30^\circ$ ,  $L_2 = 45^\circ$  Krueger,  $C_T = 0$ .



(b) Non-uniform trailing edge deflections.

Figure 12. - Concluded.

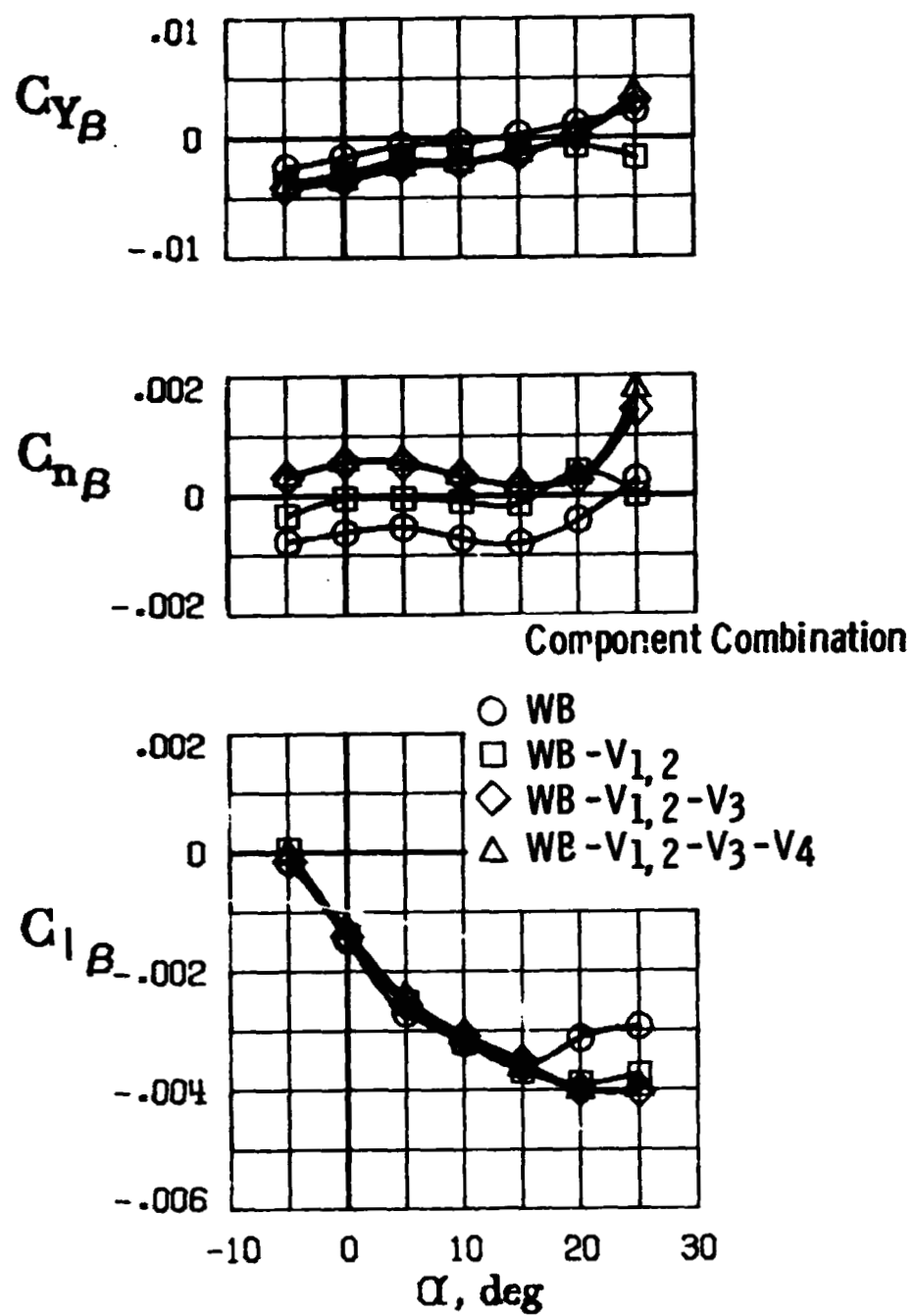


Figure 13. - Variation of lateral-directional stability derivatives with angle of attack.  $L_1 = 30^\circ$   
 $L_2 = 45^\circ$  Krueger,  $\delta_f = 40^\circ/40^\circ/20^\circ$ ,  
 $C_T = 0$ .

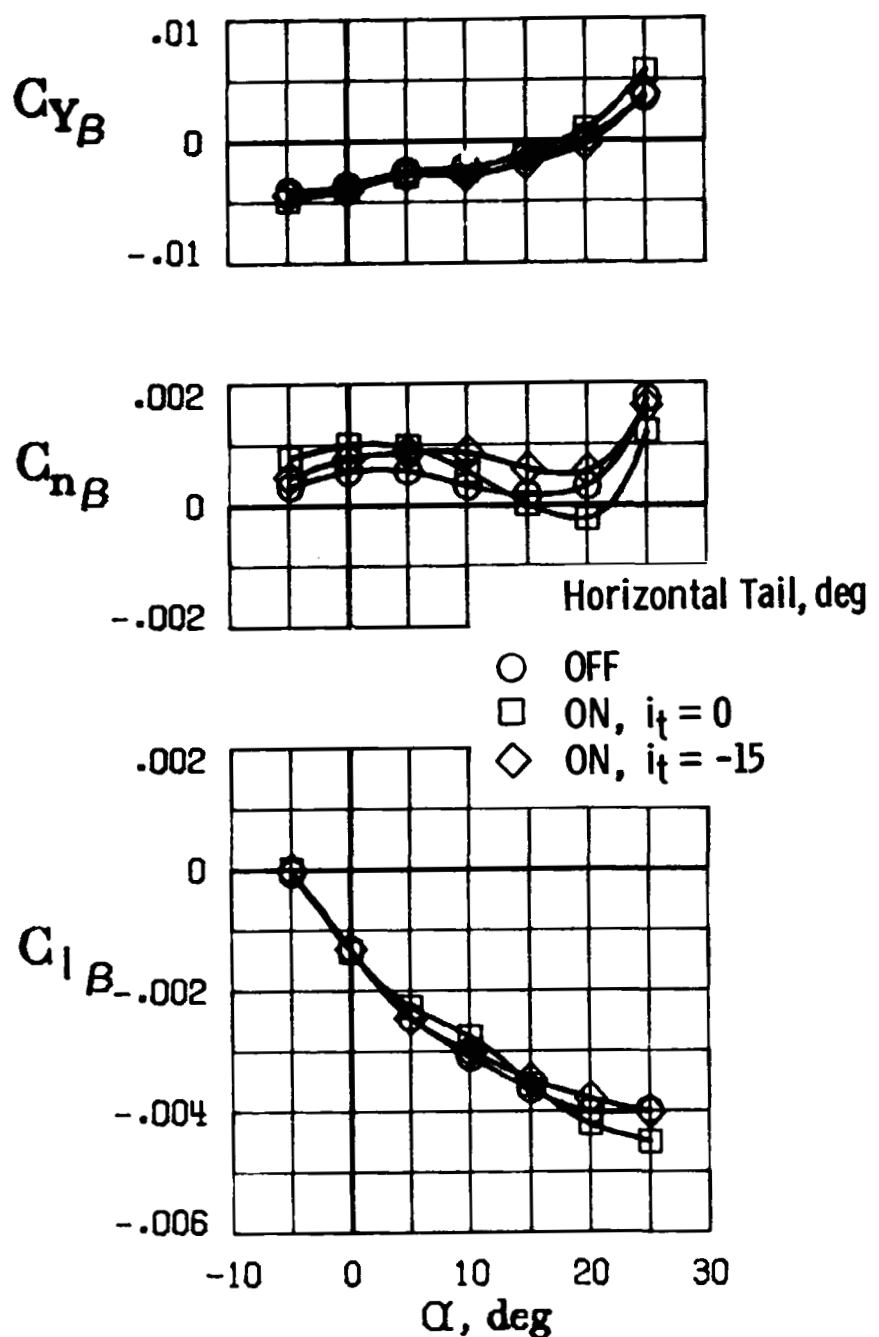


Figure 14. - Effect of horizontal tail on lateral -  
directional stability derivatives.  
 $L_1 = 30^\circ$ ,  $L_2 = 45^\circ$  Krueger,  $\delta_f = 40^\circ/40^\circ/20^\circ$ ,  
 $C_T = 0$ .

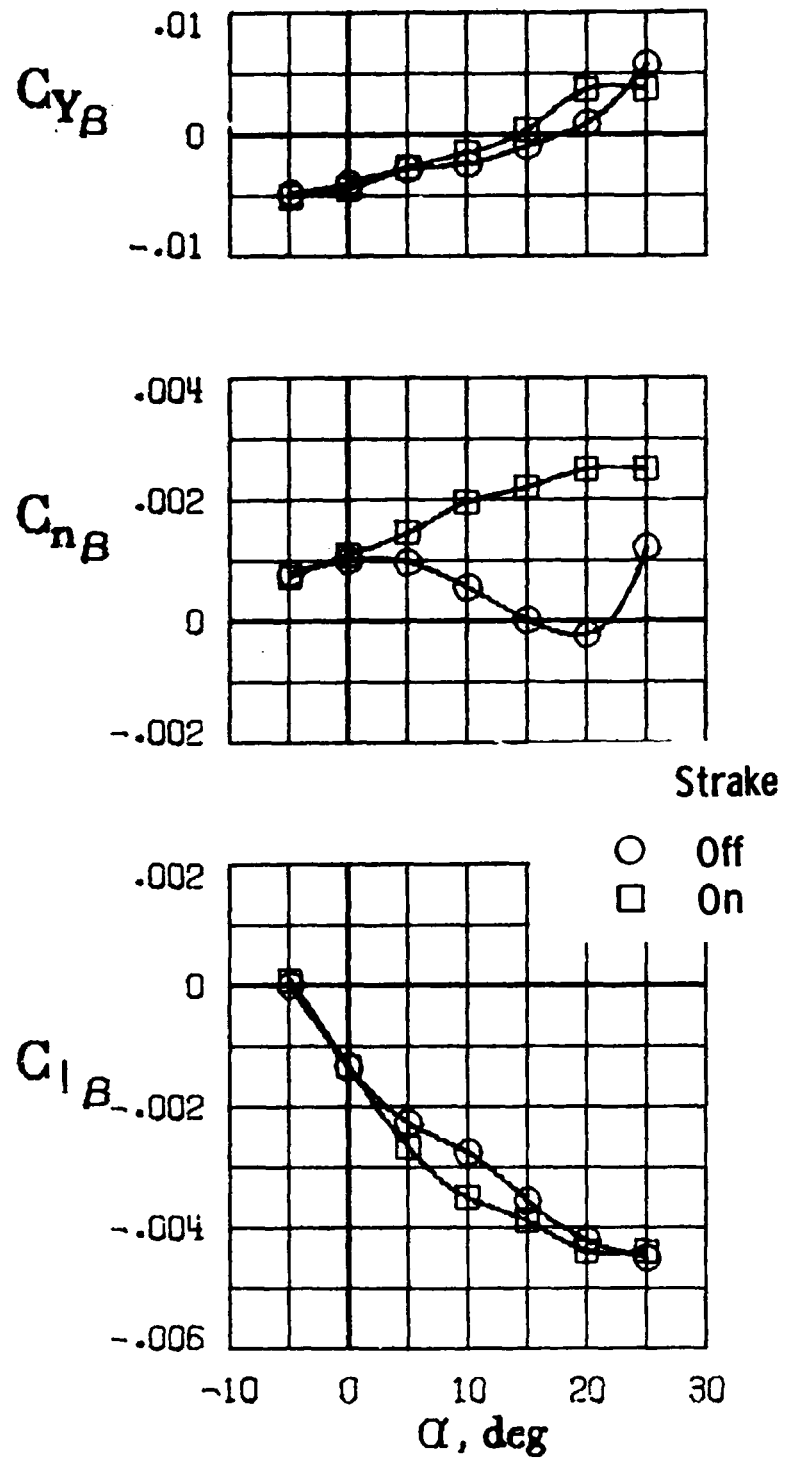


Figure 15. - Effect of nose strakes on lateral-directional stability derivatives of the complete model  
 $L_1 = 30^\circ$ ,  $L_2 = 45^\circ$  Krueger,  $\delta_f = 40^\circ/40^\circ/20^\circ$ ,  
 $C_T = 0$ .

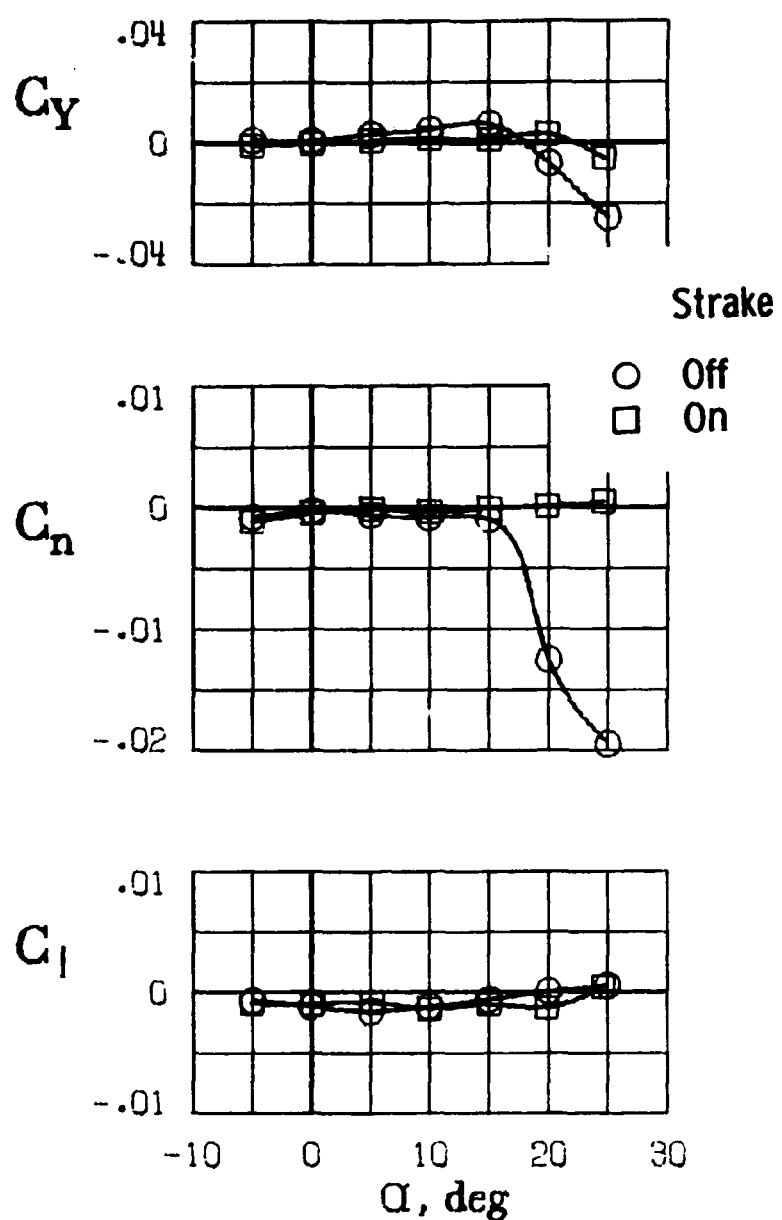
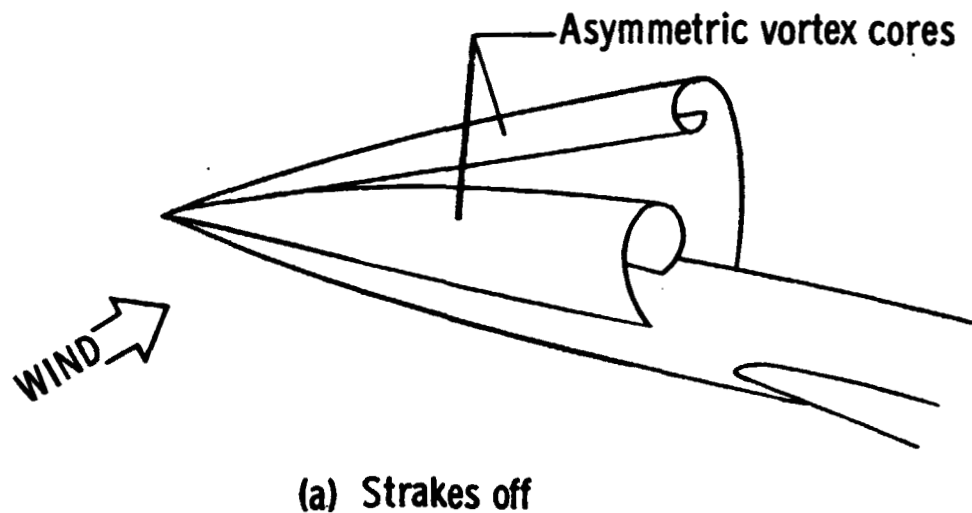
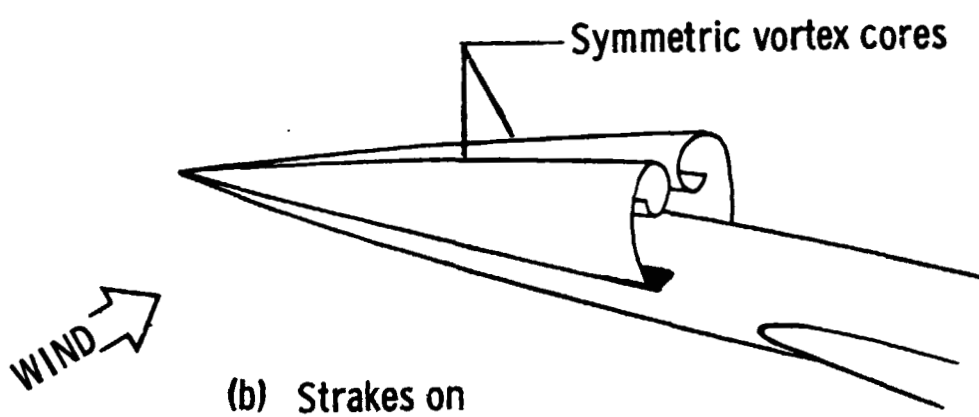


Figure 16. - Variation of the lateral -directional characteristics with angle of attack,  
 $WB - V_1, 2 - V_3 - H$ ,  $L_1 = 30^\circ$ ,  $L_2 = 45^\circ$   
Krueger,  $\delta_f = 40^\circ/40^\circ/20^\circ$ ,  $C_T = 0$ ,  $\beta = 0^\circ$ .



(a) Strakes off



(b) Strakes on

Figure 17. - Sketch of observed vortex flow.

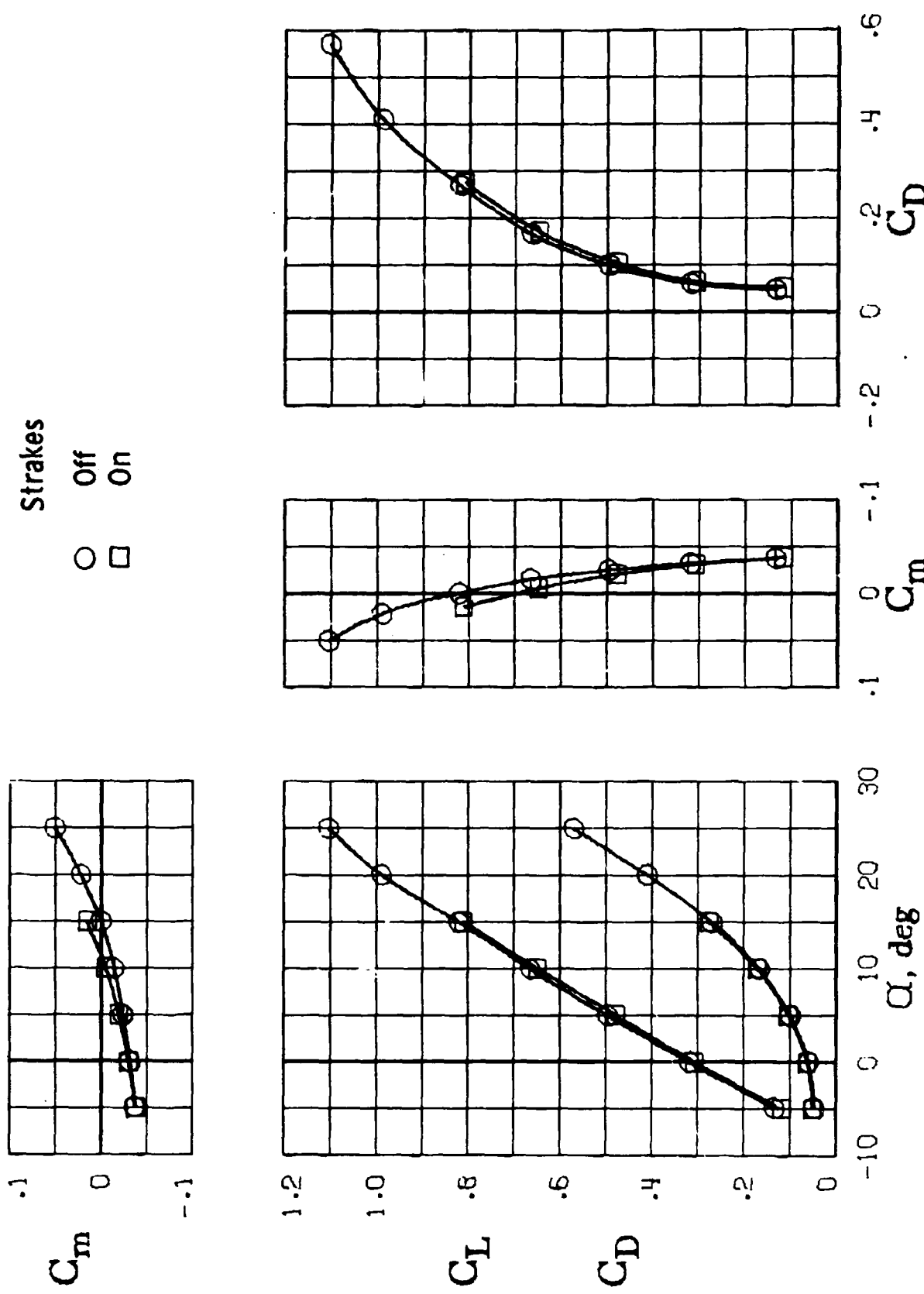


Figure 18. - Effect of strakes on longitudinal aerodynamic characteristics of the configuration.

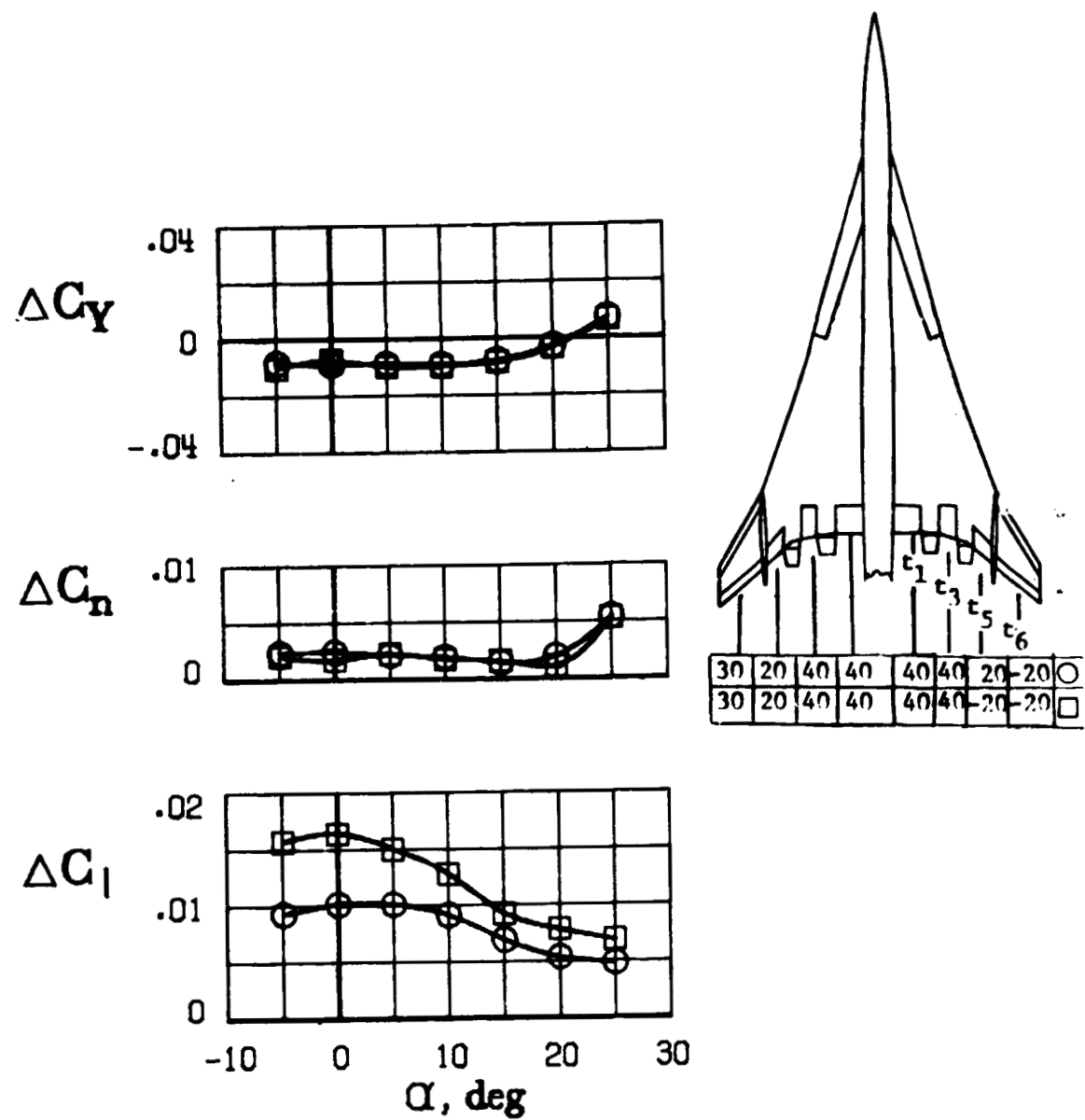


Figure 19. - Effect of lateral control surface deflection on lateral directional characteristics of complete model  $L_1 = 30^\circ$ ,  $L_2 = 45^\circ$  Krueger,  $C_T = 0$ .

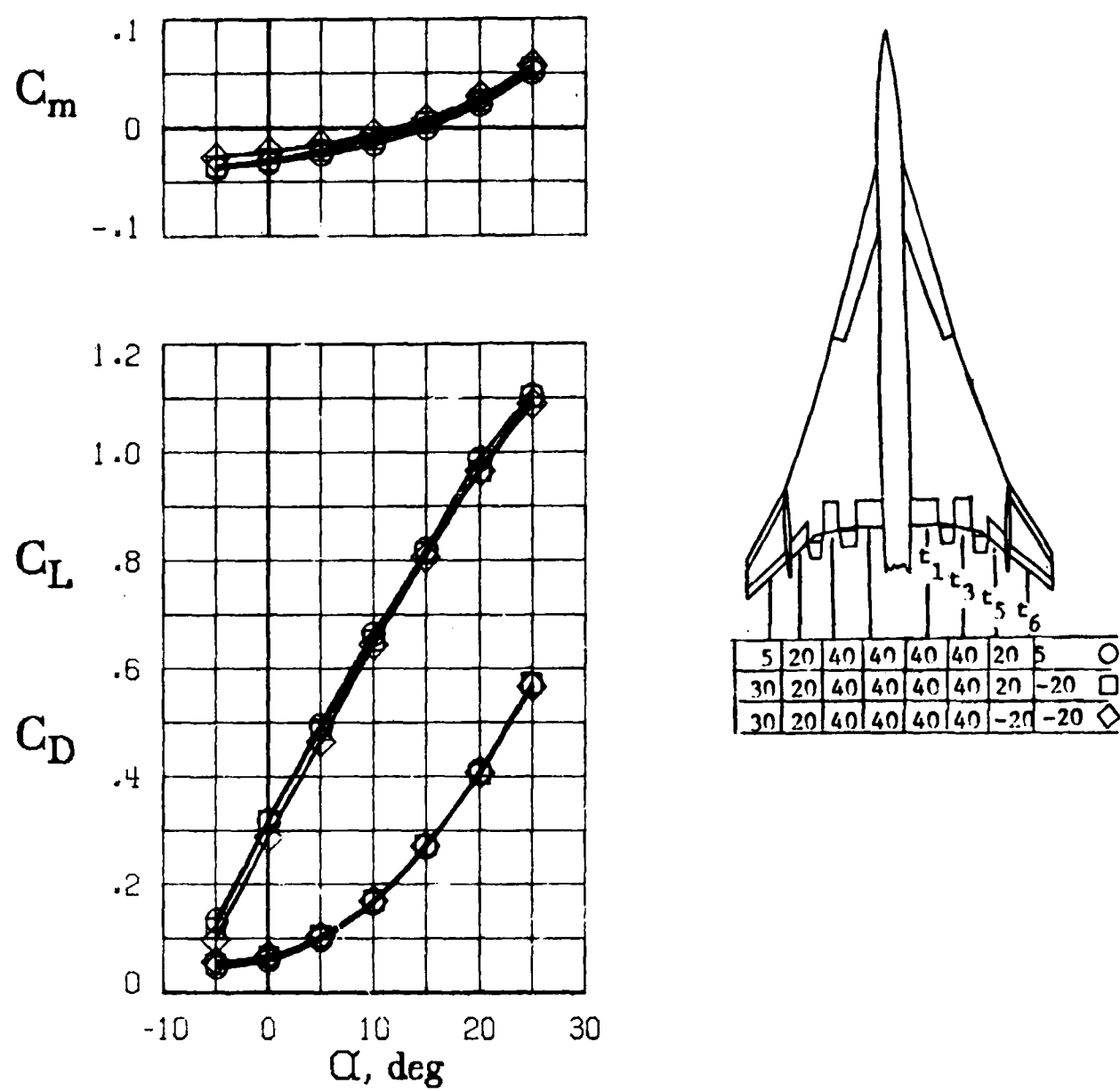


Figure 20. - Effect of lateral control surface deflection on longitudinal aerodynamic characteristics  $L_1 = 30^\circ$ ,  $L_2 = 45^\circ$  Krueger,  $C_T = 0$ .

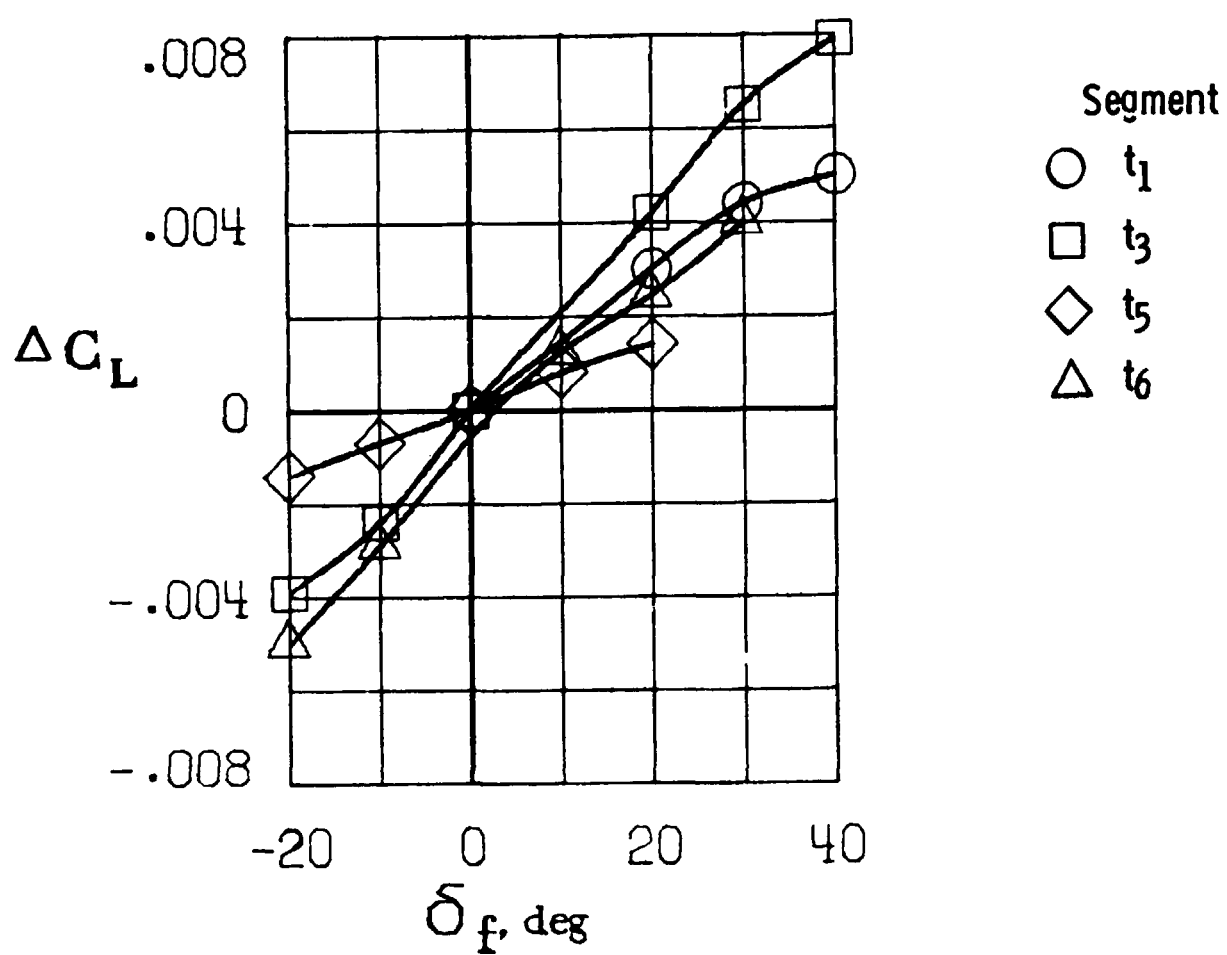


Figure 21. - Effectiveness of individual trailing-edge flap segments for roll control.  $\alpha = 8^\circ$ .

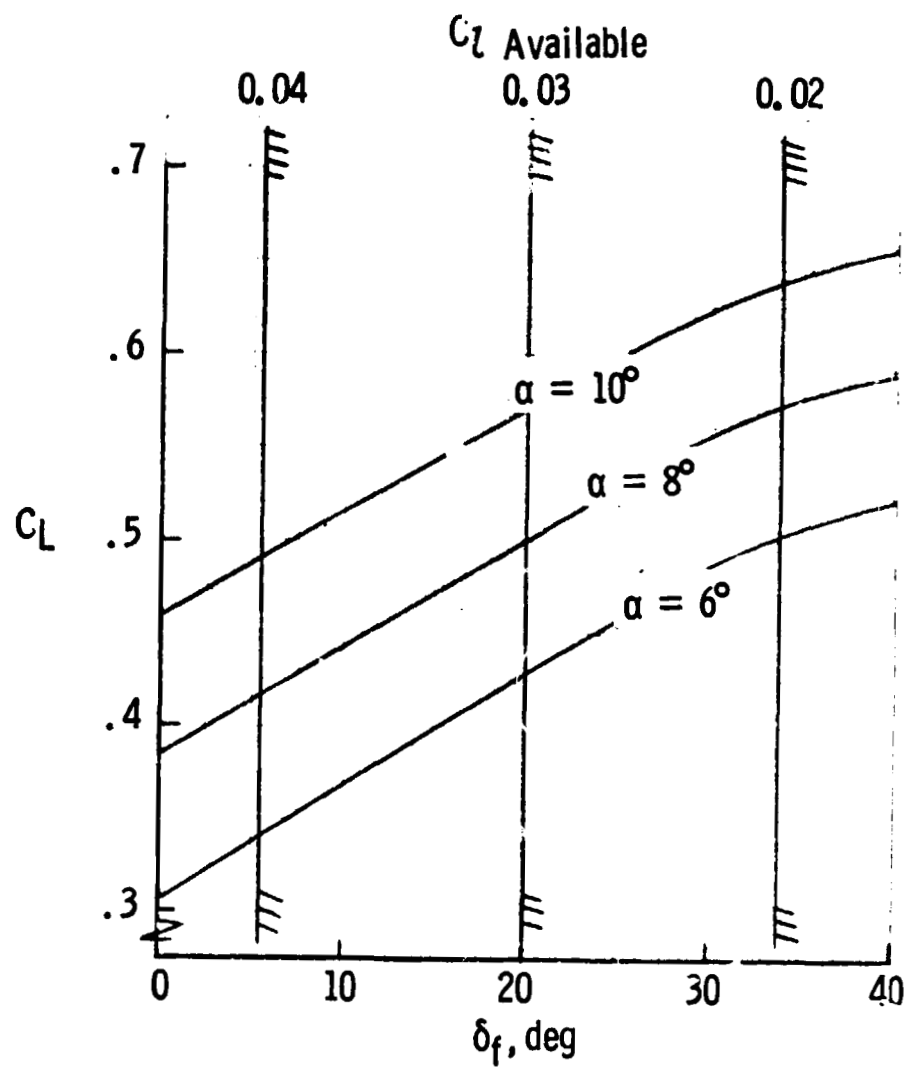


Figure 22. - Illustration of lines of constant  $C_L$  Available.

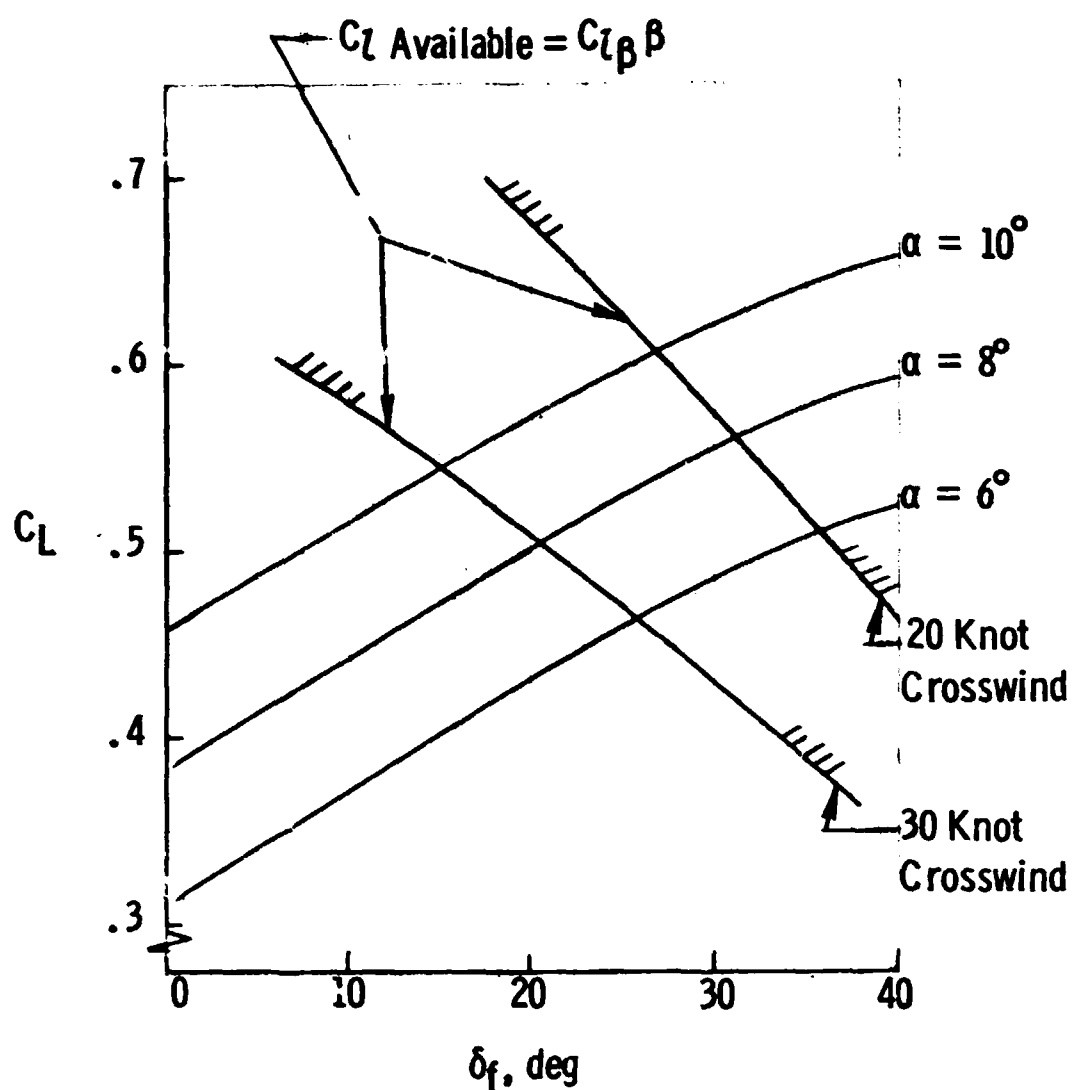


Figure 23. - Illustration of lateral control constraint.

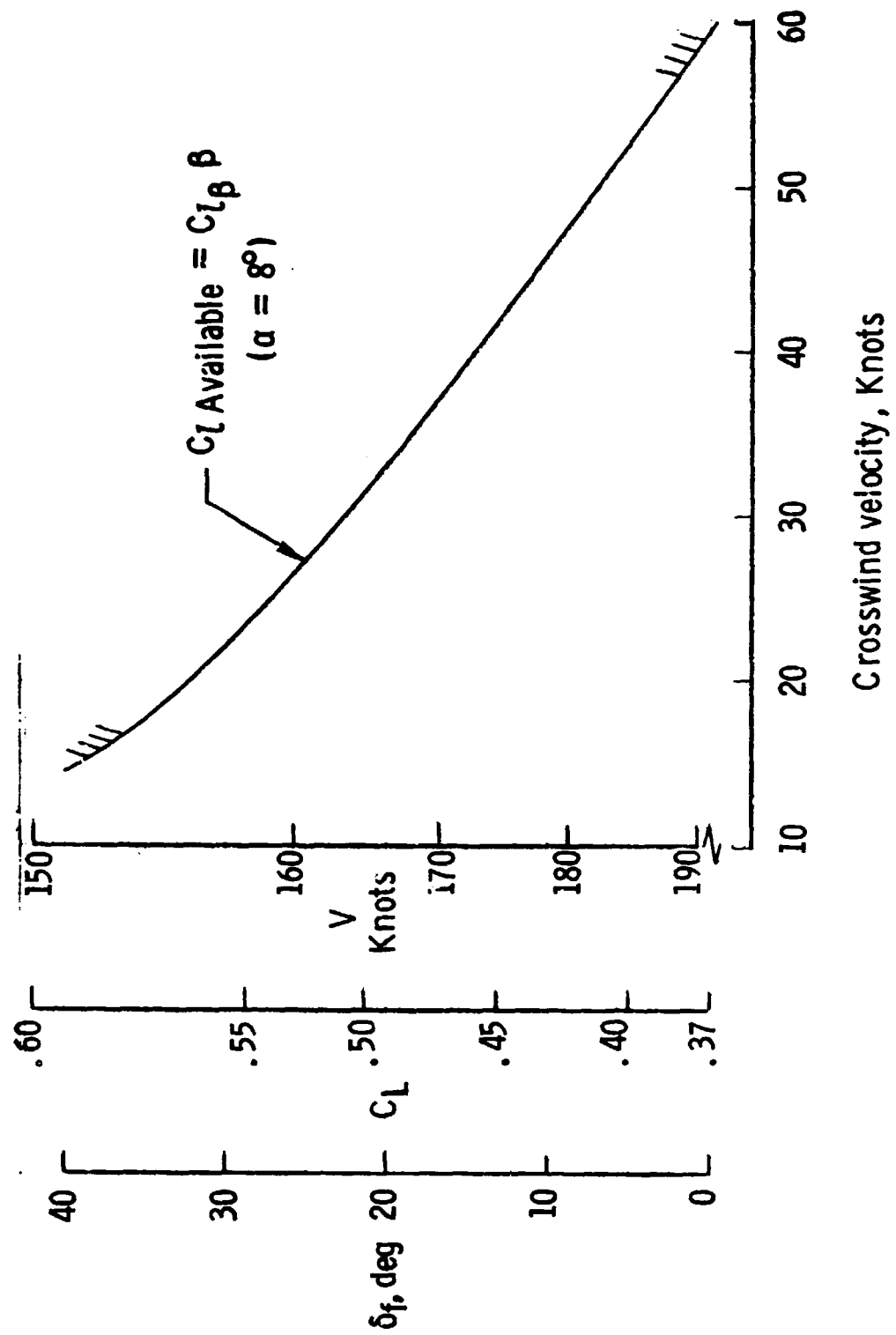


Figure 24. - Nomogram of  $\delta_f$ ,  $C_L$ , and approach speed versus crosswind velocity capability.  $\alpha = 8^\circ$ .

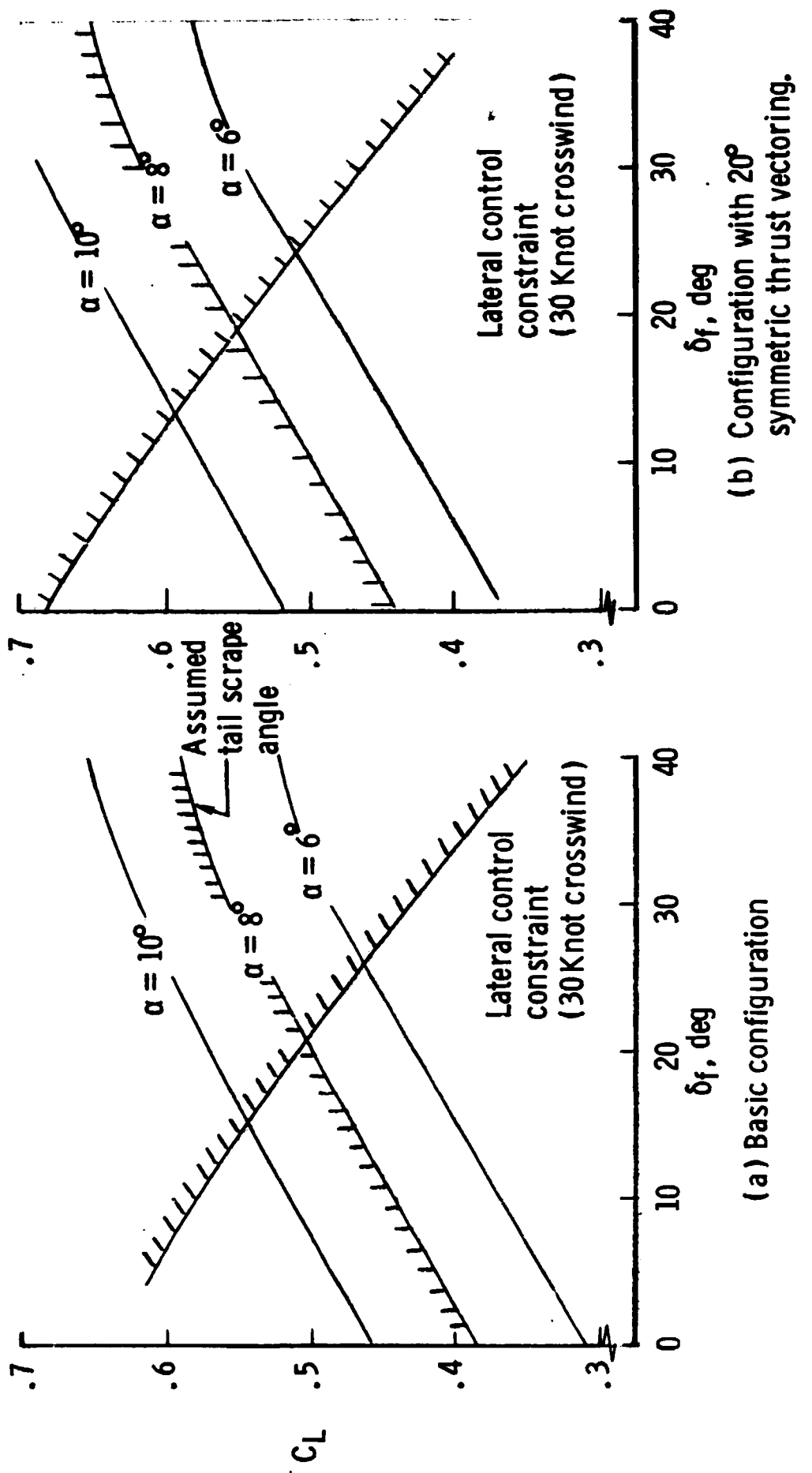


Figure 25. - Effect of thrust vectoring on lateral control constraints.  $C_T = 0.13$ .

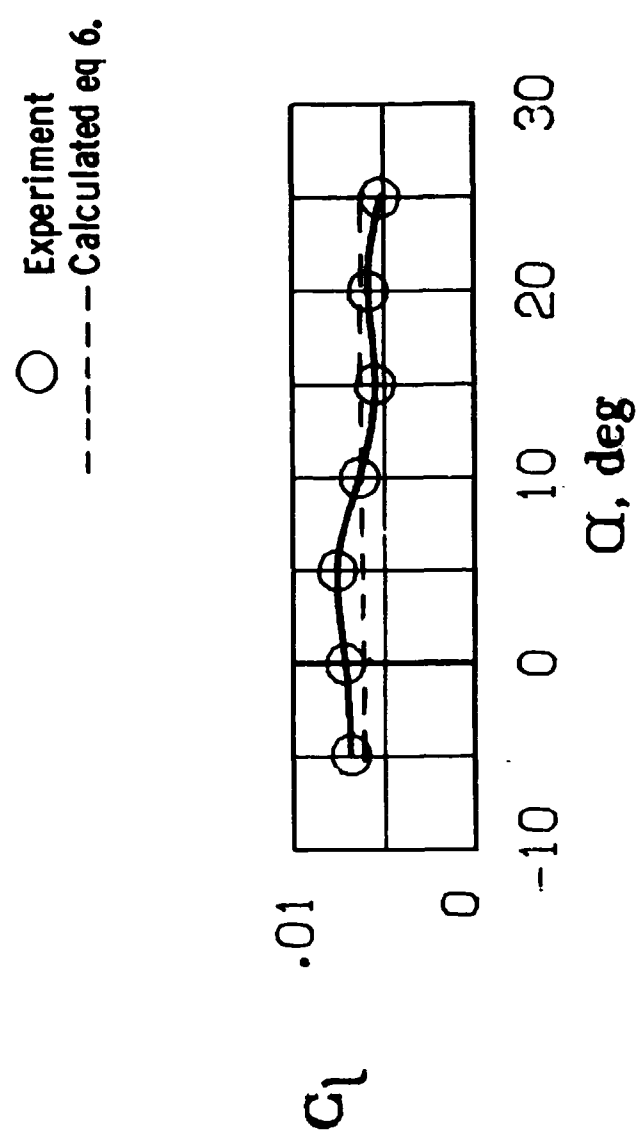


Figure 26. - Rolling moment produced by differential thrust vectoring of the outboard engines.  $\delta_f = 40^\circ / 40^\circ / 20^\circ / 20^\circ$ ,  $C_T = 0.13$ ,  $\delta_N = 20^\circ / 0^\circ / 0^\circ / -20^\circ$ .

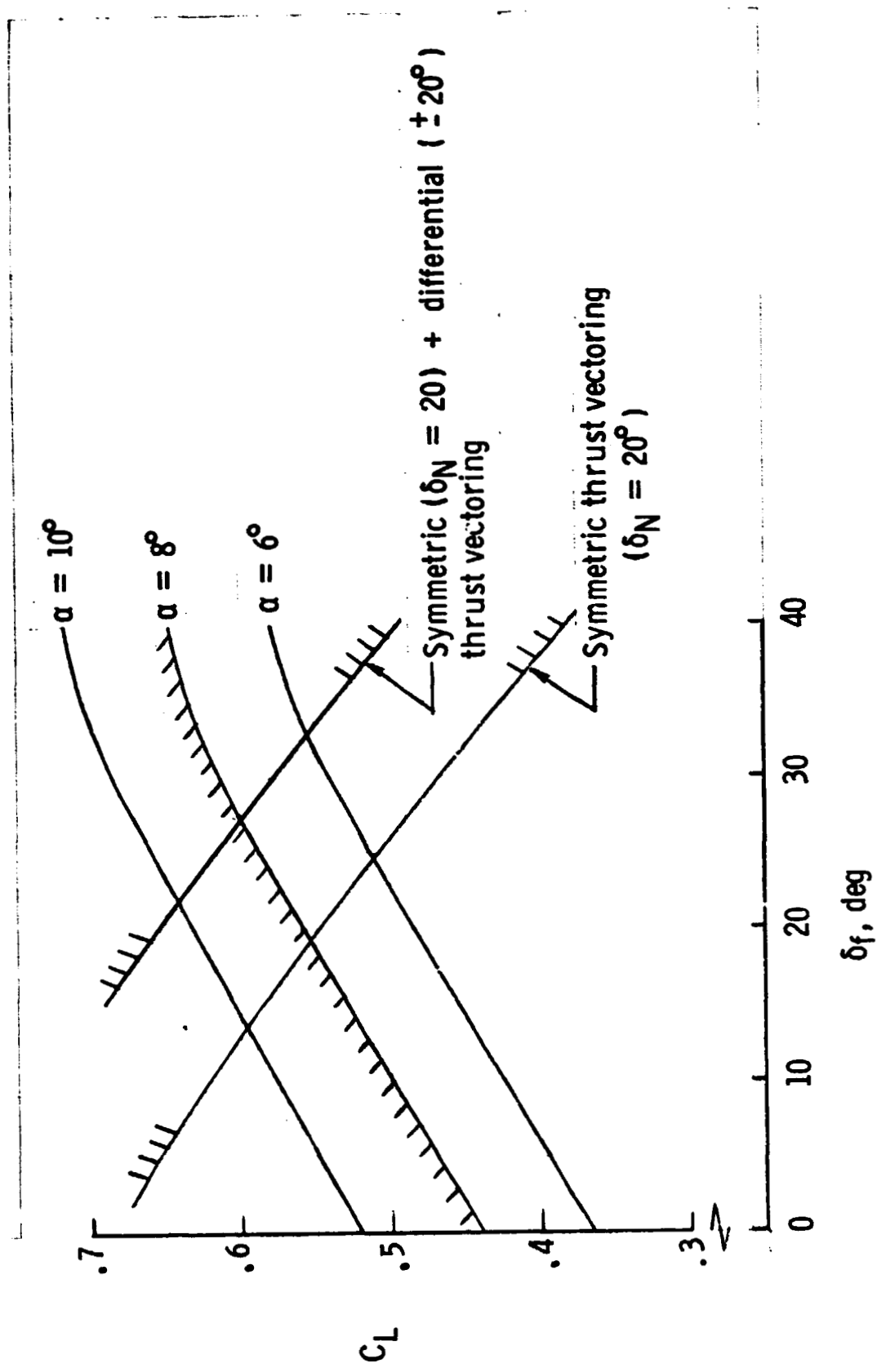


Figure 27. - Effect of differential thrust vectoring on lateral control constraint  $C_L$  = 0.13.

## APPENDIX - PRESENTATION OF TABULATED DATA

The symbols used in the data tabulation are defined as follows:

ALPHA	Angle of attack, deg
BETA	Angle of sideslip, deg
CD	Drag force coefficient; stability axis
CL	Lift force coefficient; stability axis
CPM	Pitching moment coefficient; stability axis
CRM	Rolling moment coefficient; body axis
CSF	Side force coefficient; body axis
CYM	Yawing moment coefficient; body axis
Q	Free stream dynamic pressure, ( $\text{lbf}/\text{ft}^2$ )

**TABLE A-I. - TEST PROGRAM.**

TABLE A-II. TABULATED DATA

RUN	POINT	MACH	$\alpha$	BETA	ALPHA	CL	CD	CPH	CRM	CYM	CSF
<b>RUN 1</b>											
15	.074	7.971	-5.00	-5.00	-0.0776	.0233	.0053	-0.005	-0.0007	.0126	
16	.074	8.069	-5.00	-5.00	.00930	.0254	.0132	.0046	-0.0003	.0088	
17	.074	7.963	-5.00	-5.00	.02816	.0526	.0205	.0106	-0.0012	.0071	
18	.074	7.955	-5.00	-5.00	.04882	.1243	.0417	.0138	-0.0038	.0077	
19	.074	7.987	-5.00	-5.00	.07015	.2418	.0719	.0186	-0.0026	.0082	
20	.074	8.110	-5.00	-5.00	.08847	.4071	.1257	.0193	-0.0037	.0093	
21	.074	7.946	-5.00	-5.00	1.0516	.6105	.1802	.0208	.0006	.0192	
<b>RUN 2</b>											
22	.074	8.020	0.00	0.00	-5.00	-0.0771	.0204	.0043	.0009	-0.0001	.0015
23	.074	8.020	-0.01	-0.01	.00909	.0234	.0114	.0001	-0.0002	.0026	
24	.074	8.012	-0.01	-0.01	.02852	.0506	.0173	.0002	-0.0002	.0030	
25	.074	7.938	-0.01	-0.01	.05040	.1249	.0380	.0014	.0005	.0105	
26	.074	8.045	-0.01	-0.01	.07222	.2454	.0723	.0021	.0018	.0123	
27	.074	7.946	-0.01	-0.01	.08856	.4046	.1278	.0021	.0035	.0162	
28	.074	7.979	-0.01	-0.01	24.00	1.0524	.1872	-0.019	.0093	.0325	
<b>RUN 3</b>											
29	.074	7.946	5.01	5.01	-5.06	-0.0750	.0198	.0045	.0013	.0008	
30	.074	8.028	5.01	5.01	.0936	.0218	.0107	-0.0041	.0004	-0.0091	
31	.074	8.028	5.01	5.01	.2765	.0506	.0191	.0107	.0012	-0.0036	
32	.074	8.012	5.01	5.01	.4870	.1217	.0412	.0156	.0045	.0013	
33	.074	7.963	5.01	5.01	.6902	.2385	.0750	-0.0214	.0092	.0118	
34	.074	7.971	5.01	5.01	.8867	.4069	.1259	-0.0249	.0152	.0220	
35	.074	7.979	5.01	5.01	24.00	1.0394	.1987	-0.0237	.0238	.0448	
<b>RUN 4</b>											
45	.074	7.996	-5.01	-5.01	-5.02	-0.0876	.0261	-0.053	-0.016	.0020	
46	.074	8.020	-5.01	-5.01	.01	.0960	.0265	.0070	.0044	.0013	
47	.074	8.045	-5.01	-5.01	.97	.2678	.0495	.0121	.0095	.0008	
48	.074	9.012	-5.01	-5.01	10.02	.4529	.1054	.0228	.0128	.0003	
49	.074	7.946	-5.01	-5.01	14.98	.6316	.1986	.0402	.0158	.0133	
50	.074	8.028	-5.01	-5.01	20.01	.7854	.3236	.0717	.0164	-0.0022	
51	.074	8.020	-5.01	-5.01	24.00	.9430	.4864	.1036	.0056	.0283	

TABLE A-II.- CONTINUED

RUN	POINT	MACH	Q	BETA	ALPHA	CL	CD	CPM	CRM	CYM	CSF
5	5.2	.074	8.004	-.01	-4.99	-.0624	.0239	-.0034	.0008	-.0007	.0003
	5.3	.074	8.045	-.01	-.01	.0925	.0255	.0075	.0003	-.0004	.0011
	5.4	.074	8.045	-.01	5.00	.2767	.0490	.0134	.0001	-.0002	.0011
	5.5	.074	8.037	-.01	10.02	.4631	.1065	.0233	-.0008	-.0004	.0046
	5.6	.074	8.020	-.01	15.00	.6272	.1949	.0395	-.0018	.0012	.0066
	5.7	.074	7.930	-.01	19.99	.7921	.3208	.0678	-.0005	.0003	.0030
	5.8	.074	7.945	-.01	24.96	.9279	.4751	.1032	-.0013	.0031	.0104
RUN	POINT	MACH	Q	BETA	ALPHA	CL	CD	CPM	CRM	CYM	CSF
6	5.9	.074	8.053	5.01	-5.01	-.0745	.0235	-.0032	.0025	-.0029	.0163
	6.0	.074	7.987	5.01	-.01	.0922	.0252	.0070	-.0039	-.0018	.0124
	6.1	.074	7.987	5.01	4.97	.2642	.0481	.0129	-.0094	-.0012	.0102
	6.2	.074	7.979	5.01	10.04	.4484	.1048	.0244	-.0143	-.0006	.0094
	6.3	.074	7.938	5.01	14.98	.6403	.2014	.0449	-.0203	.0031	.0013
	6.4	.074	7.979	5.01	19.98	.7890	.3250	.0767	-.0173	.0047	.0021
	6.5	.074	8.028	5.01	24.97	.9505	.4919	.1091	-.0188	.0187	.0274
RUN	POINT	MACH	Q	BETA	ALPHA	CL	CD	CPM	CRM	CYM	CSF
7	6.6	.074	7.963	-5.00	-4.98	-.0934	.0329	.0031	-.0031	.0011	.0175
	6.9	.074	8.020	-5.00	-.01	.0811	.0284	.0087	.0029	.0008	.0166
	7.0	.074	8.028	-5.00	4.99	.2482	.0467	.0158	.0094	.0003	.0123
	7.1	.074	8.028	-5.01	10.02	.4278	.0964	.0283	.0134	-.0005	.0144
	7.2	.074	8.012	-5.01	14.98	.6164	.1837	.0459	.0162	.0004	.0137
	7.3	.074	7.930	-5.01	19.97	.7739	.3019	.0692	.0189	-.0022	.0106
	7.4	.074	8.069	-5.01	24.97	.9448	.4656	.0972	.0197	.0065	.0279
RUN	POINT	MACH	Q	BETA	ALPHA	CL	CD	CPM	CRM	CYM	CSF
8	7.6	.074	7.963	.01	-5.05	-.1098	.0326	.0054	-.0002	-.0006	.0005
	7.7	.074	7.963	.01	-.00	.0865	.0271	.0104	.0006	-.0001	.0008
	7.8	.074	7.963	.01	5.00	.2618	.0468	.0183	-.0011	-.0003	.0000
	7.9	.074	7.946	.01	9.97	.4330	.0948	.0285	-.0004	-.0003	.0019
	8.0	.074	7.995	.01	14.97	.6102	.1792	.0459	-.0010	.0013	.0055
	8.1	.074	7.955	.01	19.98	.7930	.3047	.0692	.0008	.0000	.0116
	8.2	.074	7.963	.01	24.97	.9410	.4610	.1005	-.0008	.0031	.0125

TABLE A-II. - CONTINUED

RUN	POINT	MACH	$\alpha$	BETA	ALPHA	CL	CD	CPH	CRM	CYM	CSF
RUN 9											
83	.074	8.012	5.00	-4.98	-0.911	0.310	0.044	0.0025	-0.0019	-0.0164	
84	.074	8.020	5.00	*.03	0.831	0.268	*0.01	-0.0022	-0.0009	-0.0151	
85	.074	8.020	5.00	4.97	2.576	0.455	0.076	-0.0096	-0.0008	-0.0098	
86	.074	8.020	5.00	9.97	4.261	0.946	0.298	-0.0144	*0.0002	-0.0106	
87	.074	7.979	5.00	14.96	6.094	1.824	0.490	-0.0180	*0.0037	-0.0018	
88	.074	7.930	5.00	20.00	7.890	3.081	0.748	-0.0180	*0.0045	-0.0013	
89	.074	7.922	5.00	*9540	*4723	*1037	*0160	-0.0214	*0.0160	*0.0223	
RUN 10											
99	.074	8.028	-5.01	-5.00	-0.980	0.347	0.010	-0.0032	*0.011	*0.0167	
100	.074	8.028	-5.01	*.00	0.076	0.302	0.084	*0.0032	*0.009	*0.0138	
101	.074	8.028	-5.01	5.01	2.606	0.485	0.162	*0.0099	*0.007	*0.0121	
102	.074	6.045	-5.01	9.96	4.377	0.971	0.268	*0.0130	*0.000	*0.0143	
103	.074	6.045	-5.01	15.93	6.376	1.098	0.437	*0.0170	*0.011	*0.0132	
104	.074	7.946	-5.01	19.97	8.001	3.096	0.651	*0.0216	*0.003	*0.0073	
105	.074	7.971	-5.01	24.97	*9694	*4750	*0915	*0.022	*0.0096	*0.0267	
RUN 11											
106	.074	8.012	*.01	-5.00	-0.966	0.325	*0.024	*0.007	*0.0006	*0.0002	
107	.074	7.996	0.00	*.02	0.899	0.282	*0.095	*0.006	*0.0001	*0.0006	
108	.074	7.996	0.00	4.97	2.636	0.461	*0.171	*0.001	*0.0002	*0.0012	
109	.074	7.987	0.00	9.98	4.568	0.982	*0.282	*0.006	*0.0003	*0.0034	
110	.074	7.963	0.00	14.98	6.307	1.039	*0.427	*0.0006	*0.0014	*0.0076	
111	.074	7.971	0.00	19.97	8.214	3.136	*0.665	*0.0016	*0.0010	*0.0019	
112	.074	7.914	0.00	24.97	*9706	*4733	*0.981	*0.0007	*0.0040	*0.0130	
RUN 12											
113	.074	8.028	5.01	-4.98	-1.012	0.320	*0.020	*0.0034	*0.0022	*0.0012	
114	.074	8.028	5.01	*.02	0.810	0.267	*0.095	*0.0029	*0.0012	*0.0128	
115	.074	8.028	5.01	4.98	2.539	0.463	*0.172	*0.0097	*0.0007	*0.0086	
116	.074	8.028	5.01	9.97	4.386	0.958	*0.278	*0.0144	*0.0001	*0.0096	
117	.074	7.996	5.01	14.98	6.220	1.040	*0.444	*0.0193	*0.0026	*0.0005	
118	.073	7.914	5.01	19.98	8.077	3.121	*0.706	*0.0202	*0.0028	*0.0037	
119	.074	7.971	5.01	24.93	*9701	*4774	*0.985	*0.0232	*0.0155	*0.0271	

TABLE A-II. - CONTINUED

RUN	POINT	MACH	Q	BETA	ALPHA	CL	CD	CPM	CRM	CYH	CSF
25	229	.076	.076	-5.01	-5.06	.0108	.0272	.0325	-.0021	.0012	.0173
	230	*.074	*.074	-5.01	.00	*.0296	*.0340	*.0234	*.0052	*.0004	*.0155
	231	*.074	*.070	-5.01	4.96	*.0826	*.0625	*.0140	*.0102	*.0006	*.0117
	232	*.074	*.053	-5.01	9.96	*.5577	*.1234	*.0023	*.0135	*.0006	*.0120
	233	*.074	*.037	-5.01	14.96	*.7298	*.2204	*.0171	*.0170	*.0029	*.0125
	234	*.073	7.922	-5.01	20.05	*.8855	*.2553	*.0456	*.0212	*.0040	*.0007
	235	*.073	7.881	-5.01	26.99	1.0161	*.5112	*.0712	*.0204	*.0031	*.0137

RUN	26	MACH	POINT	Q	BETA	ALPHA	CL	CD	CPM	CMM	CYN	CSF
236	•075	8.234	0.00	-5.07	•0192	•0260	-•0306	-•0013	-•0006	•0007		
237	•073	7.971	0.00	•00	•2013	•0321	-•0215	-•0017	-•0002	•0016		
238	•073	7.971	0-2	5.04	•3893	•0630	-•0123	-•0016	-•0000	•0017		
239	•073	7.955	0.00	10.06	•5615	•1228	-•0004	-•0025	•0001	•0032		
240	•073	7.889	0.00	15.03	•7336	•2204	•0173	-•0015	•0012	•0057		
241	•073	7.848	0.00	19.98	•8427	•4373	•0423	-•0009	•0040	•0064		
242	•073	7.663	0.00	24.93	•8260	•5127	•0757	-•0004	•0064	•0066		

RUN	POINT	MACH	$\alpha$	BETA	ALPHA	CL	CD	CPH	CAM	CYM	CSF
31											
275	•074	8.037	-5.02	-5.03	•0987	•0305	-•0474	-•0014	•0007	•0173	
276	•074	8.012	-5.02	-5.04	•2779	•0636	-•0389	•0058	-•0003	•0170	
277	•074	7.979	-5.02	5.04	•4586	•0795	-•0285	•0116	•0002	•0112	
278	•074	7.979	-5.02	10.07	•6346	•1481	-•0157	•0144	•0009	•0119	
279	•073	7.930	-5.02	15.03	•7632	•2455	•0048	•0169	•0030	•0127	
280	•073	7.848	-5.02	20.03	•9290	•3829	•0342	•0206	-•0042	•0039	
281	•073	7.807	-5.02	24.96	1.0579	•5442	•0654	•0204	•0023	•0128	

TABLE A-II. - CONTINUED

RUN 32

POINT	MACH	$\alpha$	BETA	ALPHA	CL	CD	CPM	CRM	CYM	CSF
282	*074	8.028	.01	-5.02	.0937	.0290	-0.466	-0.0010	-0.0005	-0.0009
283	*074	8.028	.01	.00	.2831	.0414	-0.373	-0.0013	-0.0004	*0.013
284	*074	7.987	.01	5.00	.4570	.0783	-0.281	-0.0018	-0.0002	*0.016
285	*074	8.061	.01	9.94	.6287	.1429	-0.149	-0.0020	*0.001	*0.021
286	*074	8.053	.01	16.98	.7862	.2461	-0.064	-0.0014	*0.013	*0.036
287	*074	8.020	.01	20.02	.9442	.3827	*0.325	-0.0009	-0.0019	-0.0026
288	*074	7.996	.02	25.02	1.0668	.5470	*0.685	-0.0007	-0.0001	*0.061

RUN 33

POINT	MACH	$\alpha$	BETA	ALPHA	CL	CD	CPM	CRM	CYM	CSF
289	*074	8.078	5.01	-5.04	.1004	.0292	-0.446	-0.0007	-0.0018	*0.0189
290	*074	8.078	5.01	.05	.2825	.0411	-0.365	-0.0088	-0.0004	-0.0144
291	*074	8.078	5.01	5.06	.4549	.0782	-0.260	-0.0145	-0.0005	*0.0085
292	*074	8.070	5.01	10.05	.6198	.1439	-0.131	-0.0176	-0.0005	-0.0062
293	*074	8.028	5.01	14.99	.7837	.2443	*0.080	-0.0206	*0.012	*0.0006
294	*073	7.946	5.01	19.95	.9198	.3757	*0.361	-0.0198	-0.0013	*0.0043
295	*074	7.996	5.01	25.01	1.0585	.5447	*0.693	-0.0186	*0.0042	*0.0016

RUN 34

POINT	MACH	$\alpha$	BETA	ALPHA	CL	CD	CPM	CRM	CYM	CSF
296	*074	8.037	-5.00	-4.98	.1393	.0404	-0.541	-0.0004	*0.008	*0.0184
299	*074	8.012	-5.00	.04	.3196	.0546	-0.444	*0.0070	-0.0004	*0.0158
300	*074	8.012	-5.00	5.04	.4895	.0939	-0.350	*0.0117	-0.0007	*0.0100
301	*074	8.020	-5.00	9.96	.6605	.1631	-0.218	*0.0153	*0.0007	*0.0115
302	*073	7.971	-5.00	14.98	.8041	.2615	*0.016	*0.0167	*0.0026	*0.0131
303	*074	7.996	-5.00	20.01	.9354	.3944	*0.368	*0.200	-0.0042	*0.0042
304	*074	7.996	-5.00	24.97	1.0468	.5485	*0.690	-0.0195	*0.0042	*0.0193

RUN 35

POINT	MACH	$\alpha$	BETA	ALPHA	CL	CD	CPM	CRM	CYM	CSF
305	*074	8.037	0.00	-6.98	.1405	.0380	-0.541	*0.003	-0.0006	-0.0004
306	*074	8.037	0.00	-0.03	.3162	.0525	-0.442	-0.0006	-0.0007	*0.0022
307	*074	8.012	0.00	4.97	.4874	.0920	-0.341	-0.0006	-0.0005	*0.0024
308	*074	8.004	0.00	9.96	.6572	.1581	-0.205	-0.0007	-0.0001	*0.0024
309	*073	7.971	0.00	14.97	.8039	.2609	*0.010	-0.0009	*0.0009	*0.0054
310	*073	7.979	0.00	19.98	.9372	.3886	*0.326	-0.0001	-0.0027	-0.0014
311	*074	8.004	0.00	24.97	1.0601	.5514	*0.690	-0.0005	-0.0004	*0.0060

TABLE A-II. - CONTINUED

RUN	POINT	MACH	$\alpha$	$\beta$	ALPHA	CL	CD	CPM	CRM	CYM	CSF
312	•074	8.061	5.01	-4.97	•1284	•0380	-•0520	•0003	-•0026	-•0185	
313	•074	7.996	5.01	•05	•3064	•0514	-•0427	-•0071	-•0008	-•0145	
314	•074	8.037	5.01	5.02	•4886	•0920	-•0330	-•0136	-•0005	-•0091	
315	•074	7.996	5.01	10.02	•6483	•1594	-•0189	-•0168	-•0003	-•0079	
316	•073	7.946	5.01	15.02	•8027	•2614	•0064	-•0202	•0012	•0014	
317	•074	8.045	5.01	19.98	•9333	•3904	•0378	-•0190	-•0002	-•0024	
318	•074	8.045	5.01	25.00	1.0499	•5405	•0728	-•0179	•0043	•0023	

RUN	POINT	MACH	$\alpha$	$\beta$	ALPHA	CL	CD	CPM	CRM	CYM	CSF
321	•074	8.111	-5.00	-4.99	•0080	•0334	-•0218	-•0011	•0015	•0187	
322	•074	8.045	-5.00	•07	•1912	•0384	-•0142	•0058	•0006	•0148	
323	•074	8.070	-5.00	5.05	•3609	•0659	-•0061	•0109	•0004	•0112	
324	•074	8.070	-5.00	10.03	•5430	•1262	•0045	•0150	•0005	•0137	
325	•073	7.946	-5.00	14.96	•7272	•2230	•0220	•0178	•0023	•0129	
326	•073	7.971	-5.00	19.96	•8849	•3565	•0494	•0228	-•0037	•0031	
327	•073	7.946	-5.00	24.95	1.0225	•5159	•0765	•0236	•0037	•0119	

RUN	POINT	MACH	$\alpha$	$\beta$	ALPHA	CL	CD	CPM	CRM	CYM	CSF
328	•073	7.979	0.00	-5.04	-•0104	•0328	-•0210	•0001	-•0006	•0010	
329	•074	8.045	-•01	•01	•1880	•0363	-•0121	•0000	-•0005	•0021	
330	•074	8.028	-•01	5.02	•3634	•0642	-•0059	-•0003	-•0002	•0028	
331	•074	8.020	-•01	9.95	•5674	•1234	•0059	-•0007	•0000	•0039	
332	•074	7.996	-•01	14.96	•7194	•2181	•0224	-•0008	•0008	•0058	
333	•073	7.997	-•01	19.94	•8866	•3504	•0470	•0021	-•0025	-•0013	
334	•073	7.979	-•01	24.98	1.0357	•5199	•0809	•0111	•0004	•0066	

RUN	POINT	MACH	$\alpha$	$\beta$	ALPHA	CL	CD	CPM	CRM	CYM	CSF
335	•073	7.971	5.01	-4.98	-•0037	•0319	-•0213	•0018	-•0012	-•0172	
336	•074	8.045	5.01	•01	•1653	•0360	-•0127	-•0050	-•0050	-•0140	
337	•074	8.045	5.01	4.97	•3631	•0636	-•0045	-•0116	-•0011	-•0092	
338	•073	7.979	5.01	9.94	•5408	•1235	•0059	-•0166	•0000	-•0078	
339	•073	7.979	5.01	14.96	•7211	•2209	•0258	-•0028	•0020	•0008	
340	•073	7.946	5.01	19.97	•8903	•3521	•0513	-•0208	•0000	-•0015	
341	•073	7.930	5.01	24.99	1.0193	•5141	•0800	-•0198	•0045	•0071	

TABLE A-II. . CONTINUED

RUN	MACH	$\alpha$	BETA	ALPHA	CL	CD	CPH	CRM	CYM	CSF
40	POINT	.074	8.028	-5.00	-4.96	.0206	.0340	-.0157	.0013	.0170
	344	.074	8.028	-5.00	.02	.0002	.0400	-.0215	.0050	.011
	345	.074	8.028	-5.00	4.98	.3732	.0676	-.0124	.0004	.0108
	346	.074	8.028	-5.00	9.99	.5478	.1265	-.014	.009	.0114
	347	.074	8.028	-5.00	14.98	.7081	.2182	-.0231	.0032	.0109
	348	.074	7.930	-5.00	19.96	.8567	.3474	-.0172	.0013	.0037
	349	.073	7.922	-5.00	24.99	.0007	.5087	-.0211	.0034	.0166
 RUN 41										
POINT	MACH	$\alpha$	BETA	ALPHA	CL	CD	CPH	CRM	CYM	CSF
	352	.074	8.037	-0.01	-5.00	.0175	.0320	-.0296	-.0007	.0004
	353	.074	8.037	-0.01	.02	.2104	.0385	-.0209	-.0001	.0005
	354	.074	8.037	-0.01	4.96	.3879	.0674	-.0111	-.0005	-.0002
	355	.074	8.028	-0.01	9.96	.5490	.1228	-.0021	.0002	.0022
	356	.073	7.979	-0.01	14.96	.7147	.2197	-.0217	-.0014	.0043
	357	.073	7.963	-0.01	19.96	.8658	.3448	-.0491	-.0014	-.0031
	358	.073	7.979	-0.01	24.99	.0109	.5104	-.0016	-.0002	.0040
 RUN 42										
POINT	MACH	$\alpha$	BETA	ALPHA	CL	CD	CPH	CRM	CYM	CSF
	359	.073	7.979	5.00	-4.95	.0210	.0313	-.0289	.0020	.0019
	360	.073	7.979	5.00	.02	.0022	.0372	-.0195	-.0052	.0186
	361	.074	8.070	5.00	4.96	.3732	.0655	-.0103	-.0116	.0157
	362	.073	7.946	5.00	9.98	.5441	.1240	-.0034	-.0145	.0101
	363	.074	8.070	5.00	15.00	.7118	.2190	-.0249	-.0023	.0078
	364	.073	7.963	5.00	19.96	.8533	.3431	-.0534	-.0203	.0011
	365	.073	7.981	5.00	24.99	.0994	.5021	-.0877	-.0190	.0019
 RUN 43										
POINT	MACH	$\alpha$	BETA	ALPHA	CL	CD	CPH	CRM	CYM	CSF
	366	.073	7.971	0.00	-5.00	-.0235	.0366	-.0125	.0062	.0054
	369	.073	7.971	0.00	-.02	.1580	.0375	-.0045	.0059	-.0065
	370	.073	7.971	0.00	5.06	.3402	.734	-.0026	.0057	-.0060
	371	.074	7.996	0.00	9.97	.5217	.1202	-.0139	.0050	-.0080
	372	.074	8.012	0.00	14.98	.6937	.2117	-.0293	.0047	-.0038
	373	.073	7.946	0.00	19.96	.8619	.3405	-.0542	.0053	-.0017
	374	.073	7.979	0.00	24.97	.10141	.5066	.0873	-.0047	-.0007

TABLE A-II. - CONTINUED

RUN 44	POINT	MACH	<i>Q</i>	<i>BETA</i>	ALPHA	CL	CD	C <sub>P</sub> H	CRM	CYN	CSF
377	.073	7.987	0.00	-5.01	-0.0539	.0344	-0.0109	.0047	-0.0005	*.0051	
378	.073	7.979	0.00	.04	.1484	.0343	-0.0025	.0048	*.0001	-0.0032	
379	.073	7.979	0.00	.96	.3255	.0562	*.0463	.0049	*.0007	-0.0063	
380	.073	7.979	0.00	.98	.5130	.1150	.0154	.0053	*.0009	-0.0036	
381	.073	7.971	0.00	15.03	.6915	.7084	.0318	.0037	*.0019	*.0005	
382	.073	7.938	0.00	19.98	.8672	.3395	.0368	.0052	-0.0007	*.0038	
383	.073	7.987	0.00	24.98	1.0154	.5045	.0890	.0037	*.0008	*.0031	
RUN 45	POINT	MACH	<i>Q</i>	<i>BETA</i>	ALPHA	CL	CD	C <sub>P</sub> H	CRM	CYN	CSF
386	.074	8.061	0.00	-4.95	-0.0627	.0319	-0.0065	.012	*.0003	*.0015	
387	.073	7.963	0.00	.04	.1227	.0307	*.0009	.0029	*.0005	*.0042	
388	.073	7.987	0.00	.97	.3108	.0536	*.0088	.0029	*.0009	*.0049	
389	.073	7.971	0.00	.00	.4908	.1082	.0193	.0027	*.0011	*.0025	
390	.073	7.971	0.00	14.98	.6696	.1984	.0348	.0027	*.0011	*.0010	
391	.073	7.971	0.00	19.95	.8494	.3283	.0587	.0039	*.0004	*.0051	
392	.074	8.053	0.00	25.01	1.0030	.4954	.0904	.0027	*.0011	*.0032	
RUN 46	POINT	MACH	<i>Q</i>	<i>BETA</i>	ALPHA	CL	CD	C <sub>P</sub> H	CRM	CYN	CSF
395	.073	7.979	0.00	-6.99	-0.0545	.0362	*.0111	.0092	*.0038	*.0001	
396	.074	8.020	0.00	.04	.1367	.0372	*.0038	.0099	*.0026	*.0027	
397	.074	8.020	0.00	.01	.3212	.0593	*.0051	.0086	*.0016	*.0050	
398	.074	8.037	0.00	.96	.4949	.1119	*.0171	.0073	*.0011	*.0009	
399	.074	8.012	0.00	15.00	.6791	.2061	*.0344	.0058	*.0006	*.0017	
400	.074	8.045	0.00	20.01	.8496	.3347	.0609	.0064	*.0017	*.0012	
401	.074	8.004	0.00	24.98	.9854	.4911	.0943	.0026	*.0012	*.0062	
RUN 47	POINT	MACH	<i>Q</i>	<i>BETA</i>	ALPHA	CL	CD	C <sub>P</sub> H	CRM	CYN	CSF
404	.073	7.938	0.00	-4.99	-0.0660	.0327	*.0092	.0076	*.0026	*.0012	
405	.074	8.078	0.00	.04	.1366	.0322	*.0010	.0080	*.0016	*.0030	
406	.074	8.053	0.00	.97	.3101	.0546	*.0071	.0069	*.0008	*.0035	
407	.074	8.029	*.01	.95	.4872	.1075	*.0186	.0059	*.0004	*.0023	
408	.074	8.012	*.01	14.99	.6666	.1947	*.0344	.0052	*.0013	*.0015	
409	.073	7.922	*.01	19.96	.8388	.3261	.0600	.0060	*.0015	*.0039	
410	.073	7.815	*.01	24.97	.9849	.4877	.0928	.0040	*.0007	*.0035	

TABLE A-II. - CONTINUED

RUN 48	POINT	MACH	$\alpha$	BETA	ALPHA	$\gamma$	CD	CPH	CRM	CYM	CSF
413	•074	8.029	0.00	-4.97	-0.03	-0.0748	•0317	-0.0050	•0055	-0.0018	-0.0005
414	•074	8.061	0.00	4.97	4.97	•1176	•0295	•0026	•0055	-0.0009	-0.0016
415	•074	8.061	0.00	9.99	4.97	•2966	•0509	•0099	•0050	-0.0002	-0.0023
416	•074	8.061	0.00	14.96	4.799	•1041	•0214	•0032	•0007	•0014	•0014
417	•074	8.029	0.00	14.96	6.603	•1941	•0373	•0029	•0029	•0007	•0036
418	•073	7.946	0.00	19.99	8.261	•3195	•0608	•0041	•0005	-0.0003	-0.0047
419	•074	8.061	0.00	24.99	9.863	•4861	•0940	•0034	•0005	•0034	•0061

RUN 49	POINT	MACH	$\alpha$	BETA	ALPHA	$\gamma$	CL	CD	CPH	CRM	CYM	CSF
422	•074	8.045	0.00	-4.99	-0.02	-0.1149	•0357	•0039	-0.0019	-0.0010	-0.0006	
423	•074	8.086	0.00	5.02	5.02	•0789	•0305	•0114	-0.0013	-0.0003	-0.0010	
424	•074	8.086	0.00	9.98	9.98	•2653	•0485	•0179	-0.0014	-0.0000	-0.0013	
425	•074	8.086	0.00	14.98	6.992	•4510	•0992	•0275	-0.0016	-0.0003	-0.0029	
426	•073	7.938	0.00	14.98	6.392	•1879	•0426	•0126	-0.0013	•0010	•0054	
427	•074	8.045	0.00	19.98	8.169	•3140	•0655	•0003	-0.0004	•0015	•0015	
428	•073	7.930	0.00	24.98	9.646	•4728	•0974	-0.0000	-0.0002	•0065	•0065	

RUN 50	POINT	MACH	$\alpha$	BETA	ALPHA	$\gamma$	CL	CD	CPH	CRM	CYM	CSF
431	•074	8.061	0.00	-4.99	•02	-0.1075	•0340	•0029	-0.0019	-0.0006	-0.0016	
432	•073	7.971	0.00	4.95	4.95	•0863	•0293	•0101	-0.0002	-0.0002	-0.0019	
433	•073	7.971	0.00	10.05	10.05	•2652	•0675	•0172	-0.0011	-0.0002	-0.0001	
434	•073	7.971	0.00	14.99	6.551	•4551	•0999	•0274	-0.0009	-0.0001	-0.0022	
435	•073	7.946	0.00	19.98	6.336	•1860	•0412	•0050	•0012	•0050	•0050	
436	•073	7.905	0.00	24.98	8.112	•3121	•0652	•0013	-0.0006	-0.0003	-0.0064	
437	•074	8.029	0.00	-	-	•4728	•0962	-0.0001	•0003	•0013	•0061	

RUN 51	POINT	MACH	$\alpha$	$\beta^2 T_A$	ALPHA	$\gamma$	CL	CD	CPH	CRM	CYM	CSF
440	•074	6.070	0.00	-4.99	-0.01	-0.1053	•0335	-0.0000	•0015	-0.0015	-0.0004	
441	•074	6.111	0.00	4.97	4.97	•0944	•0293	•0077	•0013	-0.0008	•0009	
442	•074	6.111	0.00	9.97	9.97	•2701	•0483	•0148	•0009	-0.0004	-0.0010	
443	•074	6.094	0.00	14.99	4.573	•4573	•0997	•0259	•0001	-0.0019	•0019	
444	•074	6.078	0.00	19.99	6.376	•1876	•0405	•0001	•0013	-0.0005	•0053	
445	•073	7.487	0.00	19.99	8.180	•3146	•0634	•0024	-0.0002	-0.0005	-0.0061	
446	•073	7.979	0.00	24.95	9.706	•4752	•0957	•0013	•0004	•0004	•0061	

TABLE A-II. - CONTINUED

RUN 52

POINT	MACH	$\alpha$	BETA	ALPHA	CL	CD	CPM	CRM	CYM	CSF
449	.074	8.029	0.00	-4.96	-0.0869	0.0312	-0.0009	0.0030	-0.0012	.0002
450	.074	8.029	0.00	-4.96	.0979	.0284	.0067	.0025	-0.0009	.0006
451	.074	8.029	0.00	5.02	.2766	.0481	.0143	.0017	-0.0006	-.0002
452	.074	8.020	0.00	9.96	.4593	.0940	.0245	.0012	-0.0002	.0023
453	.073	7.971	0.00	14.99	.6484	.1898	.0403	.0012	-.0011	.0045
454	.074	8.012	0.00	20.01	.8338	.3205	.0641	.0012	-0.0002	-.0003
455	.073	7.963	0.00	24.99	.9730	.4767	.0948	.0019	.0001	.0066

RUN 58

POINT	MACH	$\alpha$	BETA	ALPHA	CL	CD	CPM	CRM	CYM	CSF
511	.073	7.979	0.00	-5.03	-0.1416	.0386	.0058	-0.0040	-0.0009	.0010
512	.074	8.053	0.00	-4.91	.0525	.0320	.0134	.0041	-0.0009	.0027
513	.074	8.061	0.00	4.97	.2328	.0475	.0204	.0041	-0.0006	.0027
514	.074	8.061	0.00	9.97	.4152	.0959	.0302	.0045	-0.0007	.0046
515	.074	8.053	0.00	14.99	.5862	.1781	.0468	.0078	.0001	.0107
516	.073	7.971	0.00	20.01	.7790	.3043	.0690	-.0028	-.0024	.0016
517	.072	7.766	0.00	25.00	.9390	.4621	.0987	-.0021	-.0016	.0059

RUN 59

POINT	MACH	$\alpha$	BETA	ALPHA	CL	CD	CPM	CRM	CYM	CSF
520	.074	8.078	0.00	-5.01	-0.1222	.0356	.0034	-.0020	-0.0003	.0005
521	.074	8.135	0.00	-4.92	.0616	.0302	.0108	-.0023	-0.0004	.0005
522	.074	8.094	0.00	5.02	.2459	.0472	.0163	-.0028	-.0002	.0013
523	.074	8.061	0.00	6.94	.4287	.0661	.0283	-.0030	-.0004	.0032
524	.074	8.037	0.00	14.99	.6644	.1794	.0436	-.0045	.0013	.0066
525	.073	7.671	0.00	14.99	.7754	.2033	.0667	-.0011	-.0014	-.0016
526	.073	7.423	0.00	24.96	.9461	.4634	.0977	-.0009	-.0001	.0035

RUN 62

POINT	MACH	$\alpha$	BETA	ALPHA	CL	CD	CPM	CRM	CYM	CSF
603	.074	8.135	0.00	-5.06	-0.1094	.0345	.0014	-.0054	-.0016	.0033
602	.074	8.135	0.00	4.97	.0744	.0288	.0139	-.0057	-.0019	.0052
610	.074	8.127	0.00	4.97	.2532	.0502	.0176	-.0050	-.0016	.0036
511	.074	8.102	0.00	10.04	.4402	.1065	.0276	-.0052	-.0014	.0060
612	.074	8.078	0.00	14.99	.6069	.1931	.0436	-.0057	-.0003	.0083
613	.074	8.029	0.00	19.99	.7721	.3184	.0734	-.0033	-.0026	-.0016
614	.073	7.864	0.00	25.01	.9136	.4730	.1096	-.0032	-.0035	-.0021

TABLE A-II - CONTINUED

RUN	POINT	MACH	$\alpha$	BETA	ALPHA	CL	CD	CPH	CRM	CYM	CSF
RUN 69					-5.01	-0.1011	-0.0273	-0.0006	-0.0036	-0.0011	0.0018
	517	0.074	8.078	0.00	0.08	0.0848	0.0279	0.0119	-0.0037	-0.0110	0.0032
	618	0.074	8.078	0.00	5.06	0.2606	0.0499	0.0159	-0.0032	-0.0010	0.0029
	619	0.074	8.053	0.00	10.04	0.4407	0.1052	0.0246	-0.0035	-0.0009	0.0054
	620	0.074	8.053	0.00	15.04	0.6195	0.1967	0.0432	-0.0034	-0.0005	0.0070
	621	0.074	8.020	0.00	19.98	0.7754	0.3168	0.0718	-0.0025	-0.0022	-0.0009
	622	0.073	7.946	0.00	25.01	0.9193	0.4756	0.1091	-0.0024	-0.0024	-0.0023
	623	0.073	7.840	0.00							
RUN 70	POINT	MACH	$\alpha$	BETA	ALPHA	CL	CD	CPH	CRM	CYM	CSF
	626	0.074	8.070	0.00	-5.03	-0.0911	0.0252	-0.0050	0.0008	-0.0003	-0.0012
	627	0.074	8.070	0.00	0.77	0.0896	0.0267	0.0064	0.0006	-0.0001	0.0000
	628	0.074	8.070	0.00	4.37	0.2714	0.0497	0.0112	0.0011	-0.0002	-0.0007
	629	0.074	8.070	0.00	10.01	0.4498	0.1052	0.0201	0.0005	-0.0003	0.0026
	630	0.074	8.053	0.00	14.99	0.6232	0.1965	0.0392	-0.0011	0.0007	0.0056
	631	0.074	7.996	0.00	15.99	0.7613	0.3208	0.0692	-0.0023	-0.0023	-0.0023
	632	0.073	7.443	0.00	24.46	0.9245	0.4767	0.1955	-0.0001	-0.0041	-0.0036
RUN 71	POINT	MACH	$\alpha$	BETA	ALPHA	CL	CD	CPH	CRM	CYM	CSF
	635	0.073	7.546	0.00	-5.02	-0.0760	0.0241	-0.0075	0.0030	0.0001	-0.0014
	636	0.074	8.011	0.00	0.04	0.0910	0.0262	0.0029	0.0027	-0.0003	-0.0016
	637	0.074	8.119	0.00	4.97	0.2745	0.0503	0.0055	0.0032	-0.0002	-0.0016
	638	0.074	8.045	0.00	10.04	0.4617	0.1079	0.0183	0.0026	-0.0005	0.0011
	639	0.074	8.020	0.00	15.06	0.6296	0.1991	0.0373	0.0013	0.0005	0.0049
	640	0.073	7.571	0.00	19.98	0.7818	0.3205	0.0664	0.0024	-0.0023	-0.0018
	641	0.073	7.799	0.00	24.99	0.9257	0.4785	0.1040	0.0016	-0.0045	-0.0033
RUN 72	POINT	MACH	$\alpha$	BETA	ALPHA	CL	CD	CPH	CRM	CYM	CSF
	644	0.074	8.078	0.00	-5.00	-0.0766	0.0245	-0.0093	0.0044	-0.0007	-0.0029
	645	0.074	8.078	0.00	0.02	0.0945	0.0265	0.0017	0.0055	-0.0004	-0.0022
	646	0.074	8.061	0.00	4.97	0.2816	0.0503	0.0063	0.0053	-0.0007	-0.0021
	647	0.074	7.996	0.00	9.96	0.4602	0.1072	0.0162	0.0040	-0.0010	0.0013
	648	0.073	7.971	0.00	14.96	0.6316	0.1986	0.0359	0.0019	0.0001	0.0047
	649	0.073	7.963	0.00	20.01	0.7948	0.3269	0.0674	0.0033	-0.0031	-0.0039
	650	0.073	7.971	0.00	24.98	0.9208	0.4810	0.1041	0.0016	-0.0043	-0.0024

TABLE A - II - CONTINUED

RUN	POINT	MACH	$\alpha$	BETA	ALPHA	CL	CD	CPH	CRM	CYM	CSF
76	685	.074	8.037	-5.00	-4.97	.1441	.0413	-.0534	-.0004	.0027	.0126
	686	.074	8.029	-5.00	.05	.3207	.0562	-.0446	.0064	.0025	.0087
	687	.074	8.012	-5.00	5.04	.5034	.0981	-.0350	.0126	.0026	.0045
	688	.073	7.971	-4.98	10.04	.6721	.1719	-.0214	.0147	.0033	.0054
	689	.073	7.971	-4.98	15.03	.8206	.2769	-.0078	.0169	.0050	.0059
	690	.073	7.938	-4.98	19.97	.9786	.4220	-.0419	.0172	-.0011	-.0099
	691	.073	7.938	-4.98	25.00	1.0902	.5843	-.0813	.0174	.0056	.0003
77	692	.074	8.061	-.01	-4.97	.1472	.0389	-.0536	-.0011	-.0013	.0002
	693	.074	8.037	-.01	-.00	.3277	.0541	-.0438	-.0013	-.0009	.0021
	694	.073	7.979	-.01	5.06	.5049	.0972	-.0335	-.0003	-.0003	.0023
	695	.073	7.963	-.01	10.04	.6707	.1697	-.0180	-.0011	-.0005	.0033
	696	.074	8.045	-.01	15.02	.8163	.2748	-.0049	-.0008	.0007	.0059
	697	.073	7.963	-.01	19.86	.9564	.4053	-.0363	-.0015	-.0033	-.0033
	698	.074	7.996	-.01	24.94	1.1096	.5854	-.0781	.0019	-.0019	-.0040
78	699	.073	7.987	4.99	-4.98	.1466	.0387	-.0512	-.0017	-.0051	-.0119
	700	.073	7.971	4.99	.01	.3198	.0531	-.0418	-.0083	-.0037	-.0074
	701	.073	7.963	4.99	4.99	.4930	.0949	-.0350	-.0144	-.0027	-.0021
	702	.073	7.971	4.99	10.05	.6748	.1708	-.0175	-.0173	-.0040	-.0013
	703	.074	7.996	4.99	15.03	.8229	.2779	-.0116	-.0190	-.0029	-.0086
	704	.073	7.955	4.99	19.97	.9626	.4121	-.0427	-.0141	-.0053	-.0018
	705	.073	7.946	4.99	24.93	1.1329	.5948	-.0827	-.0119	.0082	.0231
80	722	.073	7.979	.01	BETA	ALPHA	CL	CD	CPH	CRM	CSF
	723	.074	7.996	.01		-4.98	.1471	.0395	-.0562	-.0009	-.0012
	724	.074	8.020	.01		.04	.3383	.0554	-.0453	-.0010	-.005
	725	.073	7.987	.02		5.06	.5079	.1004	-.0318	-.0009	-.0005
	726	.073	7.987	.02		10.01	.6720	-.1732	-.0115	-.0014	-.0012
	727	.073	7.930	.02		14.99	.8241	.2819	-.0149	-.0010	-.0010
	728	.073	7.971	.02		19.87	.9703	.4163	-.0528	-.0013	-.0001
						24.62	1.1420	.6043	.1025	.0004	.0005

TABLE A-II. - CONTINUED

RUN	POINT	MACH	$\alpha$	BETA	ALPHA	CL	CD	CPH	CRM	CYM	CSF
82	746	.073	7.955	-6.99	-6.96	1444	0.418	-0.0540	-0.0004	-0.0024	0.0212
	747	.074	8.061	-6.99	-6.04	3230	0.560	-0.0437	0.0056	-0.0032	0.0187
	748	.073	7.946	-6.99	5.01	5032	0.974	-0.349	0.112	-0.0030	0.0132
	749	.073	7.979	-6.99	9.98	6782	1691	-0.0235	0.0142	-0.0025	0.0146
	750	.073	7.979	-6.99	16.98	8220	2697	0.021	0.0156	-0.0010	0.0149
	751	.073	7.987	-6.99	20.01	9605	4087	0.0347	0.0206	-0.0093	-0.0045
	752	.073	7.946	-6.99	24.98	1.0605	5605	0.0713	0.0201	-0.0155	-0.0233

RUN 83

POINT	MACH	$\alpha$	BETA	ALPHA	CL	CD	CPH	CRM	CYM	CSF
753	.074	8.029	0.00	-6.95	1556	0.397	-0.0334	-0.0007	-0.0008	-0.0008
754	.074	7.996	*0.01	0.00	3347	0.559	-0.0441	-0.0012	-0.0003	-0.0006
755	.073	7.987	*0.01	5.01	5065	0.968	-0.346	0.016	-0.0006	0.027
756	.073	7.971	*0.01	9.97	6766	1649	-0.0228	-0.0012	-0.0009	-0.0043
757	.073	7.971	*0.01	14.98	8285	2729	0.000	-0.0006	-0.0010	-0.0061
758	.073	7.979	*0.01	19.97	9614	4027	0.0312	0.0000	-0.0126	-0.0069
759	.073	7.930	*0.01	24.96	1.0808	5670	0.0729	0.0005	-0.0195	-0.0246

POINT	MACH	$\alpha$	BETA	ALPHA	CL	CD	CPH	CRM	CYM	CSF
760	.073	7.938	5.00	-6.98	1470	0.405	-0.0326	-0.0017	0.0005	-0.0204
761	.074	8.020	5.00	*0.03	3284	0.551	-0.0433	-0.0085	0.0024	-0.0163
762	.074	8.020	5.00	5.06	5064	0.969	-0.338	-0.0143	0.0023	-0.0104
763	.074	8.020	5.00	9.98	6712	1666	-0.0208	-0.0167	0.0007	-0.0062
764	.073	7.979	*0.00	14.96	8172	2687	0.0116	-0.0196	0.0006	-0.0068
765	.073	7.979	5.00	19.95	9459	4003	0.0356	-0.0194	-0.0066	-0.032
766	.073	7.905	5.00	24.95	1.0607	5591	0.0711	-0.0201	-0.0013	-0.0081

RUN 84

POINT	MACH	$\alpha$	BETA	ALPHA	CL	CD	CPH	CRM	CYM	CSF
777	.074	8.029	-5.01	-6.99	1415	0.411	-0.0324	-0.0012	-0.0023	0.0207
778	.074	8.029	-5.01	*0.04	3207	0.555	-0.0440	0.0061	-0.0032	0.0185
779	.074	8.029	-5.01	5.02	4995	0.973	-0.366	0.125	-0.0040	0.0144
780	.074	8.020	-5.01	10.01	6802	1704	-0.0248	0.0159	-0.0040	0.0163
781	.073	7.987	-5.02	15.04	8205	2729	0.011	0.0165	-0.0035	0.0181
782	.073	7.897	-5.02	19.98	9485	4074	0.0359	0.0194	-0.0123	-0.0003
783	.073	7.963	-5.02	24.97	1.0727	5713	0.0758	-0.0200	-0.00191	-0.0214

RUN 85

TABLE A-II. - CONTINUED

RUN	POINT	MACH	$\alpha$	$\delta\eta\alpha$	'ALPHA	CL	CD	CPH	CRM	CYH	CSF
86	784	.074	.012	.01	-4.98	.01431	.0400	-.0535	-.0017	-.0012	.0009
	785	.074	7.996	.01	-.01	.03339	.0553	-.0450	-.0001	-.0008	.0012
	786	.073	7.971	.01	5.00	.05043	.0970	-.0361	*.001	-.0014	.0034
	787	.073	7.971	.01	10.04	.06844	.1688	-.0241	*.0011	-.0032	.0067
	788	.073	7.963	.01	14.97	.08256	.2754	-.0001	*.001	-.0036	.0100
	789	.073	7.987	.01	20.00	.09587	.4076	*.0342	-.0014	-.0156	*.0006
	790	.073	7.987	.01	24.96	1.0C816	.5723	.0740	-.0008	-.0232	-.0205
87	POINT	MACH	$\alpha$	BETA	ALPHA	CL	CD	CPH	CRM	CYH	CSF
	791	.074	.012	4.99	-4.95	.01458	.0399	-.0520	*.0016	*.0007	-.0203
	792	.074	8.020	4.99	-.01	.02669	.0552	-.0440	-.0072	*.0024	-.0178
	793	.074	8.037	4.99	5.04	.05076	.0977	-.0360	*.0120	*.0016	-.0103
	794	.074	8.029	4.99	9.96	.06739	.1688	-.0226	*.0151	-.0009	-.0055
	795	.073	7.971	4.99	15.01	.08214	.2749	*.0030	-.0200	*.0016	*.0050
	796	.073	7.971	4.99	20.02	.09449	.4052	*.0365	*.0208	*.0092	*.0016
	797	.073	7.897	4.99	24.98	1.0E653	.5671	.0733	-.0208	-.0025	.0141
88	POINT	MACH	$\alpha$	BETA	ALPHA	CL	CD	CPH	CRM	CYH	CSF
	807	.074	7.996	-5.00	-4.97	.01179	.0474	-.0365	*.0016	*.0044	*.0236
	808	.074	8.029	-5.00	-.02	.02999	.0582	-.0324	*.0053	*.0053	*.0203
	809	.073	7.987	-5.00	4.94	.04843	.0975	-.0270	*.0108	*.0055	*.0153
	810	.073	7.979	-5.00	9.99	.06562	.1670	-.0164	*.0126	*.0046	*.0172
	811	.073	7.930	-5.00	14.99	.08094	.2663	*.0016	*.0151	*.0011	*.0149
	812	.073	7.971	-5.00	19.98	.09670	.4067	*.0247	*.0206	*.0084	*.0049
	813	.073	7.873	-5.00	24.95	1.0I33	.5702	.0472	*.0222	-.0127	-.0303
89	POINT	MACH	$\alpha$	BETA	ALPHA	CL	CD	CPH	CRM	CYH	CSF
	814	.074	8.029	0.00	-4.90	.01327	.0467	-.0372	*.0010	*.0006	-.0001
	815	.074	8.029	0.00	-.00	.03174	.0597	-.0320	-.0015	-.0001	-.0002
	816	.074	8.029	-.01	4.97	.04953	.0991	-.0245	-.0017	-.0000	*.0010
	817	.074	8.029	-.01	9.99	.06641	.1656	-.0147	*.0016	*.0000	*.0026
	818	.073	7.987	-.01	14.98	.08205	.2695	-.0000	*.0004	*.0001	*.0049
	819	.073	7.971	-.01	20.01	.09879	.4100	*.0216	*.0111	*.0133	-.0072
	820	.073	7.938	-.01	24.96	1.0J37	.5701	.0506	*.0014	-.0190	-.0263

TABLE A-II.- CONTINUED

RUN	POINT	MACH	$\alpha$	BETA	ALPHA	CL	CD	CPM	CRM	CYM	CSF
RUN 90	F-1	•073	7.971	5.00	-4.97	•1316	•0460	-•0359	-•0014	•0034	-•0249
	822	•073	7.971	5.00	-•01	•3146	•0589	-•0326	-•0082	•0047	-•0199
	823	•074	8.004	5.00	5.06	•4962	•1006	-•0281	-•0119	•0041	-•0129
	824	•074	8.004	5.00	10.05	•6704	•1725	-•0171	-•0151	•0039	-•0069
	825	•073	7.971	5.00	15.02	•8250	•2777	-•0024	-•0206	-•0009	•0054
	826	•073	7.955	5.00	19.99	•4087	•0256	-•0216	-•0107	•0042	-•0267
	827	•073	7.971	5.00	24.67	1.1119	•5742	-•0229	-•0006		
RUN 96	POINT	MACH	$\alpha$	BETA	ALPHA	CL	CD	CPM	CRM	CYM	CSF
	880	•074	8.053	-5.00	-4.99	•0823	•0704	-•0026	-•0014	-•0029	•0231
	881	•074	8.111	-5.00	•04	•2625	•0781	•0007	•0050	-•0043	•0224
	882	•074	8.111	-5.00	5.01	•4413	•1115	•0056	•0103	-•0044	•0159
	883	•074	8.094	-5.00	9.97	•6105	•1758	•0166	•0126	-•0039	•0174
	884	•074	8.053	-5.00	15.03	•7655	•2717	•0346	•0149	-•0005	•0145
	885	•073	7.955	-5.00	19.97	•9137	•3995	•0530	•0187	-•0037	•0040
	886	•073	7.897	-5.00	24.93	1.0432	•5505	•0715	•0211	-•0116	-•0282
RUN 97	POINT	MACH	$\alpha$	BETA	ALPHA	CL	CD	CPM	CRM	CYM	CSF
	887	•074	8.086	0.00	-5.00	•0841	•0704	-•0016	-•0012	-•0007	•0001
	888	•074	8.070	0.00	•03	•2630	•0789	•0015	-•0017	-•0003	•0022
	889	•074	8.045	0.00	5.02	•4450	•1134	•0083	-•0019	-•0002	•0025
	890	•074	8.020	0.00	9.91	•6073	•1734	•0189	-•0029	-•0007	•0029
	891	•074	7.996	0.00	14.97	•7626	•2706	•0322	-•0026	•0011	•0054
	892	•074	8.094	0.00	19.98	•9399	•4035	•0487	-•0004	-•0095	-•0092
	893	•073	7.930	0.00	24.92	1.0503	•5522	•0745	•0009	-•0153	-•0303
RUN 98	POINT	MACH	$\alpha$	BETA	ALPHA	CL	CD	CPM	CRM	CYM	CSF
	894	•074	8.094	5.00	-5.06	•0839	•0701	-•0023	-•0011	•0015	-•0212
	895	•074	8.094	5.00	•05	•2619	•0781	•0017	-•0084	•0035	-•0161
	896	•074	8.086	5.00	4.99	•4393	•1110	•0073	-•0143	•0043	-•0120
	897	•074	8.061	5.00	10.03	•6119	•1761	•0174	-•0175	•0047	-•0107
	898	•074	8.037	4.99	14.99	•7668	•2714	•0333	-•0198	•0055	-•0039
	899	•073	7.946	4.99	19.93	•9096	•3945	•0507	-•0193	-•0025	-•0072
	900	•073	7.799	4.99	24.93	1.0485	•5530	•0734	-•0160	•0046	-•0103

TABLE A-II. - CONTINUED

RUN 102	POINT	MACH	$\alpha$	BETA	ALPHA	CL	CD	CPH	CRM	CYH	CSF
94.0	•074	8.053	-5.00	-4.99	•1177	•0489	-•0356	-•0016	-•0043	•0256	
94.1	•074	8.078	-5.01	•03	•2992	•0606	•0297	•0061	•0057	•0223	
94.2	•074	8.086	-5.01	5.01	•4732	•1001	•0198	•0119	•0076	•0151	
94.3	•074	8.070	-5.01	9.94	•6411	•1689	-•0066	•0152	-•0099	•0102	
94.4	•074	8.012	-5.01	15.05	•8076	•2748	•0167	•0175	-•0108	•0001	
94.5	•073	7.914	-5.01	19.98	•9546	•4094	•0411	•0211	-•0116	-•0156	
RUN 103	POINT	MACH	$\alpha$	BETA	ALPHA	CL	CD	CPH	CRM	CYH	CSF
94.7	•074	8.152	•01	-5.02	•1169	•0507	•0382	-•0008	-•0006	•0007	
94.8	•074	8.143	•01	-•04	•3055	•0626	-•0309	-•0010	-•0001	•0006	
94.9	•074	8.143	•01	4.97	•4776	•1032	-•0201	-•0016	-•0000	•0015	
95.0	•074	8.111	•01	9.98	•471	•1703	-•0023	•0000	•0021	•0021	
95.1	•074	8.078	•01	14.98	•8100	•2758	•0148	-•0018	•0008	•0026	
RUN 104	POINT	MACH	$\alpha$	BETA	ALPHA	CL	CD	CPH	CRM	CYH	CSF
95.3	•074	8.152	4.99	-5.03	•1162	•0503	-•0377	-•0005	•0029	-•0258	
95.4	•074	8.152	4.99	•05	•2975	•0674	-•0309	-•0074	•0052	-•0216	
95.5	•074	8.152	4.99	4.95	•4707	•1014	-•0203	-•0147	•0070	-•0123	
95.6	•074	8.135	4.99	9.99	•6475	•1720	-•0073	-•0199	•0097	-•0047	
95.7	•074	8.111	4.99	15.03	•8019	•2739	•0135	-•0215	•0112	•0041	
95.8	•074	8.029	4.99	20.00	•9516	•4104	•0419	-•0229	•0134	•0217	
RUN 120	POINT	MACH	$\alpha$	BETA	ALPHA	CL	CD	CPH	CRM	CYH	CSF
110.8	•074	7.996	0.00	-5.03	•1190	•0525	-•0352	•0082	•0017	-•0085	
110.9	•074	7.996	0.00	•04	•3173	•0659	-•0296	•0087	•0024	-•0091	
111.0	•074	8.012	0.00	4.97	•4877	•1045	-•0207	•0084	•0021	-•0077	
111.1	•074	8.012	0.00	9.97	•6525	•1695	-•0098	•0075	•0019	-•0065	
111.2	•074	8.029	0.00	14.94	•8142	•2739	•0047	•0066	•0014	-•0028	
111.3	•073	7.971	0.00	19.97	•9652	•4047	•0244	•0065	-•0113	-•0099	
111.4	•073	7.955	0.00	24.95	1.1020	•5722	•0537	•0062	-•0136	-•0191	

TABLE A - II. - CONTINUED

RUN 121											
POINT	MACH	0	BETA	ALPHA	CL	CD	CPM	CRM	CYH	CYH	CSF
11117	.074	8.029	0.00	-5.00	0.0969	0.0574	-0.0272	0.0147	.0014	-.0102	
11118	.074	8.029	0.00	.01	2874	0.6882	-0.0211	0.0150	.0016	-.0077	
11119	.073	7.971	0.00	4.98	4647	0.1046	-0.0152	0.0133	.0022	-.0087	
11120	.073	7.979	0.00	10.00	6444	0.1694	-0.0053	0.0112	.0017	-.0071	
11121	.073	7.979	0.00	14.90	8060	0.2708	-0.0080	0.0089	.0016	-.0034	
11122	.073	7.987	0.00	20.07	9658	0.4070	-0.0289	0.0089	.0016	-.0124	
11123	.073	7.979	0.00	24.99	5669	0.0571	-0.0682	0.0137	.0010	-.0199	
RUN 123											
POINT	MACH	0	BETA	ALPHA	CL	CD	CPM	CRM	CYH	CYH	CSF
11135	.074	8.029	0.00	-5.01	1664	0.0398	-0.0660	0.0010	.0002	-.0027	
11136	.074	7.996	0.00	.05	3570	0.0570	-0.0604	0.0016	.0005	-.0012	
11137	.073	7.971	0.00	4.99	5231	0.0995	-0.0527	0.0022	.0005	-.0010	
11138	.074	8.012	0.00	9.92	7040	0.1695	-0.0431	0.0021	.0005	-.0002	
11139	.074	8.004	0.00	14.85	8523	0.2750	-0.0301	0.0021	.0011	-.0022	
11140	.073	7.979	0.00	20.02	1.0206	0.4217	-0.0098	0.0011	.0019	-.0079	
11141	.074	7.996	0.00	25.01	1.1365	0.5894	-0.0224	0.0003	.0003	-.0130	
RUN 124											
POINT	MACH	0	BETA	ALPHA	CL	CD	CPM	CRM	CYH	CYH	CSF
11144	.074	8.012	0.00	-5.04	1508	0.0399	-0.0572	0.0006	-.0002	-.0006	
11145	.074	8.004	0.00	.08	3417	0.0566	-0.0508	0.0019	-.0001	-.0011	
11146	.074	7.996	0.00	5.09	5229	0.0997	-0.0420	0.0022	.0002	-.0009	
11147	.073	7.979	0.00	10.04	6929	0.1684	-0.0329	0.0016	.0004	-.0013	
11148	.073	7.987	0.00	14.96	8457	0.2736	-0.0183	0.0024	.0005	-.0045	
11149	.074	8.012	0.00	19.93	1.0013	0.4110	-0.0005	0.0001	-.0113	-.0045	
11150	.073	7.950	0.00	24.98	1.1292	0.5823	-0.0293	0.0005	-.0005	-.0125	
RUN 125											
POINT	MACH	0	BETA	ALPHA	CL	CD	CPM	CRM	CYH	CYH	CSF
11153	.074	8.029	0.00	-5.02	1011	0.0640	-0.0114	0.0011	-.0005	-.0011	
11154	.074	8.045	0.00	-.02	2878	0.0731	-0.0079	0.0020	-.0001	-.0001	
11155	.074	8.025	0.00	4.95	4601	0.1088	-0.0001	0.0022	-.0000	-.0007	
11156	.074	8.012	0.00	9.97	6289	0.1721	-0.0102	0.0019	-.0004	-.0015	
11157	.073	7.971	0.00	14.84	7876	0.2710	-0.0247	0.0018	.0016	-.0026	
11158	.073	7.971	0.00	19.92	9468	0.4019	-0.0418	0.0005	-.0101	-.0064	
11159	.073	7.971	0.00	24.99	1.0865	0.5716	-0.0732	0.0003	-.0101	-.0140	

TABLE A-II. - CONTINUED

RUN 126	POINT	MACH	<i>q</i>	BETA	ALPHA	CL	Cn	CPH	CRM	CYM	CSF
	1162	.074	8.029	0.00	-5.03	.0861	.0742	-.0002	-.0012	-.0007	-.0002
	1163	.074	8.037	0.00	.07	.02769	.0822	.0041	-.0019	-.0002	.0007
	1164	.074	8.037	0.00	4.96	.04518	.01171	.0117	-.0014	-.0000	.0005
	1165	.074	8.029	0.00	10.06	.06238	.01610	.0236	-.0016	-.0007	.0007
	1166	.074	7.973	0.00	14.98	.07754	.02753	.0386	-.0018	-.0013	.0028
	1167	.074	8.045	0.00	19.98	.09329	.04049	.0530	-.002	-.0097	-.0061
	1168	.073	7.987	0.00	24.96	1.0677	.06664	.0807	-.001	-.0100	-.0139
RUN 182	POINT	MACH	<i>q</i>	BETA	ALPHA	CL	CD	CPH	CRM	CYM	CSF
	1709	.074	8.094	1.02	-4.98	.1318	.0411	-.0502	-.0004	-.0000	-.0027
	1710	.074	8.143	1.02	.02	.03138	.00554	-.0406	-.0005	-.0002	-.0011
	1711	.074	7.996	1.02	5.00	.04810	.00951	-.0303	-.0007	-.0004	-.0003
	1712	.074	8.152	1.02	10.00	.06604	.01644	-.0174	-.0021	-.0003	.0019
	1713	.074	8.028	1.02	14.92	.07970	.02627	.0058	-.0014	-.0012	.0030
	1714	.073	7.997	1.02	18.07	.08640	.03399	.0221	-.0000	-.0022	-.0051
	1715	.073	7.930	1.02	19.90	.09319	.03913	.0326	-.0003	-.0048	-.0079
	1716	.072	7.758	1.02	25.08	1.0506	.05587	.0716	-.0009	-.0066	-.0087
RUN 219	POINT	MACH	<i>q</i>	BETA	ALPHA	CL	CD	CPH	CRM	CYM	CSF
	1984	.062	5.607	0.00	-5.05	.1792	-.0029	-.0645	-.0002	-.0009	-.0050
	1985	.062	5.574	0.00	.06	.03686	-.0644	-.0553	-.0002	-.0009	-.0040
	1986	.062	5.656	0.00	5.05	.05632	-.0124	-.0465	-.0003	-.0008	-.0026
	1987	.062	5.664	0.00	10.02	.07421	.0618	-.0345	-.0002	-.0010	-.0023
	1988	.062	5.664	0.00	15.05	.09054	.01759	-.0120	-.0000	-.0020	-.0029
	1989	.062	5.648	0.00	20.05	1.0641	.03222	.0184	-.0020	-.0063	-.0136
	1990	.062	5.705	0.00	24.88	1.1875	.04933	.0542	-.0013	-.0068	-.0156
RUN 229	POINT	MACH	<i>q</i>	BETA	ALPHA	C <sub>-</sub>	Cn	CPH	CRM	CYM	CSF
	2084	.062	5.689	.02	-4.98	.1876	-.0022	-.0625	-.0064	-.0149	-.0179
	2085	.062	5.689	.01	.04	.03699	-.0643	-.0543	-.0064	.0155	-.0187
	2086	.062	5.689	.01	5.00	.05671	-.0192	-.0439	-.0047	.0155	-.0158
	2087	.062	5.672	.01	9.96	.07480	.0541	-.0329	-.0056	.0163	-.0178
	2088	.062	5.672	.01	14.96	.09050	.01641	-.0110	-.0057	.0160	-.0194
	2089	.062	5.590	.01	19.97	1.0686	.03085	.0185	-.0082	.0056	-.0266
	2090	.062	5.623	.01	24.92	1.2059	.04874	.0563	-.0074	-.0069	-.0308

TABLE A-II. - CONTINUED

RUN 235	POINT	MACH	$\alpha$	BETA	ALPHA	CL	CD	CPH	CRM	CYM	CSF
2144	•062	5.713	0.00	-5.05	•1509	-•0677	-•0461	-•0002	•0019	-•0033	
2145	•062	5.598	0.00	•10	•3610	-•0551	-•0393	•0004	•0025	-•0034	
2146	•062	5.598	0.00	4.95	•5442	-•0126	-•0360	-•0017	•0026	-•0022	
2147	•062	5.615	0.00	9.93	•7435	•0623	-•0124	-•0007	•0026	•0007	
2148	•062	5.615	0.00	14.95	•9138	•1736	-•0122	-•0006	•0020	-•0006	
2149	•062	5.615	0.00	19.93	•10870	•3187	•0043	•0009	-•0109	-•0055	
2150	•062	5.598	0.00	24.77	1.2210	•4859	•0253	-•0006	-•0089	-•0086	

RUN 237	POINT	MACH	$\alpha$	BETA	ALPHA	CL	CD	CPH	CRM	CYM	CSF
2160	•062	5.664	•01	-4.99	•1926	-•0836	-•0756	-•0003	•0014	-•0022	
2161	•062	5.615	•01	•06	•3933	-•0646	-•0710	-•0005	•0021	-•0049	
2162	•062	5.639	•01	4.93	•5876	-•0151	-•0641	-•0010	•0026	-•0049	
2163	•062	5.639	•01	9.95	•7722	•0614	-•0557	-•0008	•0022	-•0019	
2164	•062	5.607	•01	15.05	•9539	•1802	-•0437	-•0003	•0015	-•0020	
2165	•062	5.623	•01	20.04	•11441	•3402	-•0280	•0010	-•0117	-•0068	
2166	•062	5.598	•01	24.90	1.2685	•5136	-•0044	•0013	-•0085	-•0121	

RUN 238	POINT	MACH	$\alpha$	BETA	ALPHA	CL	CD	CPH	CRM	CYM	CSF
2170	•062	5.598	0.00	-5.04	•1926	-•0864	-•0665	•0000	•0016	-•0063	
2171	•062	5.623	0.00	•07	•3773	-•0635	-•0599	•0001	•0021	-•0039	
2172	•062	5.623	0.00	4.95	•5762	-•0191	-•0527	-•0008	•0022	-•0032	
2173	•052	5.623	•00	9.93	•7707	•0547	-•0439	-•0006	•0021	-•0008	
2174	•062	5.623	0.00	15.05	•9395	•1723	-•0299	•0003	•0013	-•0013	
2175	•062	5.590	0.00	20.05	1.1169	•3237	-•0168	•0007	-•0115	-•0064	
2176	•062	5.582	0.00	24.73	1.2476	•4904	•0036	•0014	-•0088	-•0113	

RUN 239	POINT	MACH	$\alpha$	BETA	ALPHA	CL	CD	CPH	CRM	CYM	CSF
2179	•062	5.664	0.00	-4.93	•1332	-•0568	-•0190	•0000	•0017	-•0059	
2180	•062	5.648	0.00	•09	•3299	-•0459	-•0152	•0000	•0022	-•0056	
2181	•062	5.623	0.00	4.93	•5163	-•0079	-•0102	•0003	•0020	-•0040	
2182	•062	5.623	0.00	10.05	•7218	•0667	-•0008	-•0005	•0024	-•0030	
2183	•062	5.631	0.00	14.97	•8954	•1749	•0123	-•0009	•0013	-•0017	
2184	•062	5.671	0.00	19.93	•10542	•3100	•0254	•0010	-•0102	-•0096	
2185	•062	5.717	0.00	24.82	1.2037	•4829	•0498	•0008	-•0075	-•0143	

TABLE A-II. - CONTINUED

RUN	POINT	MACH	$\alpha$	BETA	ALPHA	CL	CD	CPH	CRM	CYM	CSF
240	2188	*063	5.754	0.00	-5.04	*1034	-0.0450	-0.0088	-0.0004	*0012	-0.0021
	2189	*062	5.631	0.00	-6.11	*3051	-0.0386	-0.0047	-0.0001	*0019	-0.0036
	2190	*062	5.697	0.00	4.99	*5003	*0039	*0022	-0.0002	*0018	-0.0026
	2191	*062	5.697	0.00	10.03	*6892	*0126	*0125	*0000	*0020	-0.0016
	2192	*062	5.699	0.00	15.03	*8601	*1762	*0244	-0.0001	*0007	-0.0013
	2193	*062	5.590	0.00	19.99	1.0408	*3151	*0386	*0008	-0.0112	-0.0058
	2194	*062	5.590	0.00	24.95	1.1846	*4844	*0608	*0012	-0.0075	-0.0095
266	POINT	MACH	$\alpha$	BETA	ALPHA	CL	CD	CPH	CRM	CYM	CSF
	2443	*062	5.681	0.00	-4.96	*1236	*0512	-0.0312	*0025	*0028	-0.0116
	2444	*062	5.689	0.00	*09	*3024	*0665	-0.0246	*0014	*0029	-0.0089
	2445	*062	5.689	0.00	4.95	*4699	*1039	-0.0174	*0006	*0032	-0.0066
	2446	*062	5.697	0.00	10.00	*6475	*1708	-0.0079	-0.0009	*0029	-0.0055
	2447	*062	5.664	0.00	14.88	*8019	*2692	*0054	-0.0011	*0020	-0.0046
	2448	*062	5.631	0.00	19.98	*9545	*4009	*0278	-0.0007	-0.0111	-0.0055
	2449	*062	5.593	0.00	24.97	1.0833	*5592	*0500	*0010	-0.0175	-0.0353
267	POINT	MACH	$\alpha$	BETA	ALPHA	CL	CD	CPH	CRM	CYM	CSF
	2450	*062	5.631	0.00	-6.97	*0893	-0.0652	-0.0180	*0093	*0035	-0.0115
	2451	*062	5.713	0.00	-6.07	*2859	-0.0495	-0.0132	*0085	*0039	-0.0091
	2452	*062	5.722	0.00	4.98	*4706	-0.0184	-0.0173	*0082	*0044	-0.0108
	2453	*062	5.722	0.00	9.91	*6629	*0496	-0.0016	*0054	*0038	-0.0081
	2454	*062	5.722	0.00	15.06	*8478	*1572	*0107	*0043	*0017	-0.0931
	2455	*062	5.672	0.00	20.03	1.0096	*2899	*0294	*0051	-0.0105	-0.0090
	2456	*062	5.592	0.00	25.18	1.1497	*4557	*0538	*0062	-0.0078	-0.0136
274	POINT	MACH	$\alpha$	BETA	ALPHA	CL	CD	CPH	CRM	CYM	CSF
	2521	*062	5.689	0.00	-4.98	*0909	-0.0687	-0.0223	*0014	*0006	-0.0015
	2522	*062	5.607	*01	*08	*2952	-0.0665	-0.0152	-0.0017	*0010	-0.0012
	2523	*062	5.639	*01	5.08	*4825	-0.0245	-0.0107	-0.0024	*0010	*0001
	2524	*062	5.639	*01	10.10	*6764	*0451	-0.0027	-0.0026	*0013	*0011
	2525	*062	5.631	*01	15.08	*8492	*1509	*0109	-0.0017	*0005	*0017
	2526	*062	5.639	*01	19.90	1.0123	*2820	*0287	*0000	-0.0110	-0.0033
	2527	*061	5.566	.01	24.79	1.1479	*4369	*0521	*0001	-0.0043	-0.0082

TABLE A-II. - CONTINUED

POINT	MACH	$\alpha$	BETA	ALPHA	CL	CD	CPM	CRM	CYM	CSF
2551	.062	5.713	-.01	-6.95	.1242	-.0038	-.0425	-.0013	.0004	-.0030
2552	.062	5.713	-.01	-.03	.3108	-.0648	-.0324	-.0017	.0006	-.0017
2553	.062	5.713	-.01	4.98	.4942	-.0260	-.0240	-.0014	.0007	-.0010
2554	.062	5.697	-.01	9.95	.6722	-.0415	-.0124	-.0025	.0008	-.0014
2555	.062	5.672	-.01	14.96	.8352	-.1475	-.0103	-.0015	.0008	-.0013
2556	.062	5.590	-.01	19.93	.9890	-.2782	-.0399	-.0002	-.0092	-.0054
2557	.061	5.566	-.01	24.99	1.1335	.4508	.0793	-.0004	-.0080	-.0080
<hr/>										
2613	.062	5.615	.01	-6.97	.1264	-.0799	-.0427	-.0008	.0003	-.0020
2614	.062	5.615	.01	-.07	.3096	-.0661	-.0327	-.0012	.0005	-.0014
2615	.062	5.631	.01	5.00	.4978	-.0289	-.0246	-.0020	.0005	-.0002
2616	.062	5.672	.01	10.05	.6861	-.0442	-.0123	-.0020	.0004	-.0024
2617	.062	5.672	.01	14.95	.8399	-.1453	-.0098	-.0030	.0007	-.0017
2618	.062	5.607	.01	19.97	1.0002	.2830	.0413	-.0006	-.0057	-.0084
2619	.061	5.566	.01	24.84	1.1042	.4283	.0756	-.0003	-.0066	-.0075
<hr/>										
2891	.063	5.812	0.00	-4.92	.1250	-.0806	-.0500	-.0002	.0010	-.0035
2892	.062	5.705	0.0	-.06	.3180	-.0683	-.0438	-.0008	.0016	-.0039
2893	.062	5.631	-.01	5.07	.5126	-.0294	-.0386	-.0016	.0016	-.0038
2894	.062	5.598	-.01	9.98	.6948	-.0346	-.0283	-.0022	.0014	-.0025
2895	.062	5.557	-.01	15.02	.8752	-.1460	-.0156	-.0018	.0017	-.0014
2896	.062	5.566	-.01	19.54	1.0308	.2827	.0024	-.0068	.0210	.0260
2897	.061	5.475	-.01	24.92	1.1935	.4586	.0303	-.0071	.0211	.0250
<hr/>										
2914	.062	5.590	-.01	-.04	.1234	-.0857	-.0411	-.0005	.0009	-.0015
2915	.062	5.590	-.01	0.6	.3046	-.0700	-.0352	-.0016	.0013	-.0001
2916	.062	5.582	-.01	4.93	.4935	-.0327	-.0287	-.0024	.0011	.0009
2917	.062	5.607	-.01	9.96	.6821	-.0385	-.0189	-.0025	.0011	-.0025
2918	.062	5.631	-.01	14.93	.8497	-.1432	-.0067	-.0025	.0013	-.0035
2919	.062	5.598	-.01	20.02	1.0210	.2844	.0117	-.0066	.0229	-.0115
2920	.061	5.500	-.01	24.93	1.1746	.4554	.0360	-.0079	.0257	-.0161

TABLE A-II. - CONCLUDED

RUN 311

POINT	MACH	$\alpha$	BETA	ALPHA	CL	CD	CPM	CRM	CYN	CSF
2937	.062	5.697	0.00	-5.08	.0595	-.0507	.0032	-.0008	.0002	.0022
2938	.062	5.681	0.00	-.01	.2568	-.0482	.0084	-.0014	.0010	.0015
2939	.062	5.681	0.00	4.98	.4427	-.0163	.0134	-.0021	.0012	.0030
2940	.062	5.681	0.00	10.01	.6312	-.0464	.0236	-.0028	.0006	.0041
2941	.062	5.664	0.00	15.04	.7912	-.1415	.0357	-.0031	.0012	.0068
2942	.062	5.582	0.00	19.97	.9640	-.2764	.0518	-.0069	.0022	.0034
2943	.062	5.557	0.00	24.49	1.1279	-.4471	.0774	-.0076	.0268	.0691

RUN 314

POINT	MACH	$\alpha$	BETA	ALPHA	CL	CD	CPM	CRM	CYN	CSF
360	.063	5.763	0.00	-4.92	.0544	-.0430	.0126	-.0009	-.0001	.0018
361	.062	5.697	-.19	-.01	.2444	-.0395	.0180	-.0010	-.0006	.0016
2962	.062	5.681	0.00	5.10	.4305	-.0079	.0233	-.0022	-.0006	.0027
2963	.062	5.631	0.00	10.36	.6156	-.0541	.0337	-.0020	-.0004	.0056
2964	.062	5.623	0.00	14.99	.7736	-.1461	.0469	-.0022	-.0012	.0079
2965	.062	5.566	0.00	19.94	.9520	-.2756	.0607	-.0066	-.0232	.0350
2966	.062	5.590	0.00	25.02	1.1128	-.4461	.0851	-.0074	-.0074	.0698

1. Report No. NASA TM 74043	2. Government Accession No.	3. Recipient's Catalog No.	
4. Title and Subtitle <b>Low-Speed Wind Tunnel Investigation of an Advanced Supersonic Cruise Arrow-Wing Configuration</b>		5. Report Date	
		6. Performing Organization Code 3840	
7. Author(s) Paul L. Coe, Jr., Paul M. Smith, and Lyle P. Parlett		8. Performing Organization Report No.	
9. Performing Organization Name and Address NASA Langley Research Center Hampton, VA 23665		10. Work Unit No. 743-04-12-02	
12. Sponsoring Agency Name and Address National Aeronautics and Space Administration  Washington, D.C. 20546		11. Contract or Grant No.	
		13. Type of Report and Period Covered Technical Memorandum	
		14. Sponsoring Agency Code	
15. Supplementary Notes Paul M. Smith Vought Corporation Hampton Technical Center Hampton, VA 23664			
16. Abstract A low-speed wind tunnel investigation has been conducted in the Langley V/STOL tunnel to provide a preliminary assessment of possible means for improving the low-speed aerodynamic characteristics of advanced supersonic cruise arrow-wing configurations and to extend the existing data base of such configurations. Principle configuration variables included; wind leading-and trailing-edge flap deflection, fuselage nose strakes, and engine exhaust nozzle deflection.			
The tests were conducted at a Reynolds number (based on the mean aerodynamic chord) of about $2.5 \times 10^6$ for an angle-of-attack range from -5 to 25° and an angle-of-sideslip of ±5°.			
17. Key Words (Suggested by Author(s)) Arrow-wing Supersonic Cruise Vehicle Low-Speed Performance Stability and Control	18. Distribution Statement UNCLASSIFIED - UNLIMITED		
19. Security Classif. (of this report) UNCLASSIFIED	20. Security Classif. (of this page) UNCLASSIFIED	<. No. of Pages 32	22. Price* \$5.00

\* For sale by the National Technical Information Service, Springfield, Virginia 22161